Aus der Medizinischen Klinik für Gastroenterologie, Infektiologie und Rheumatologie (einschließlich Arbeitsbereich Ernährungsmedizin) der Medizinischen Fakultät Charité – Universitätsmedizin Berlin

DISSERTATION

The Role of Stromal Hedgehog Signaling in Intestinal Fibrosis of Mice

Die Rolle des stromalen Hedgehog-Signalweges bei der intestinalen Fibrose der Maus

zur Erlangung des akademischen Grades
Doctor medicinae (Dr. med.)

vorgelegt der Medizinischen Fakultät
Charité – Universitätsmedizin Berlin

von

Benjamin Englert

aus Gießen

Datum der Promotion: 25.11.2022

Preface

The results presented in this thesis were partly published in:

Gerling M, Buller NV, Kirn LM, Joost S, Frings O, Englert B, Bergstrom A, Kuiper RV, Blaas L, Wielenga MC, Almer S, Kuhl AA, Fredlund E, van den Brink GR, Toftgard R. Stromal Hedgehog signalling is downregulated in colon cancer and its restoration restrains tumour growth. Nature Communications, 2016;7:12321.

1. Table of Contents and Abstract

1.1 Table of Contents

1.2 Abbreviations

ANOVA	analysis of variance
AOM	Azoxymethane
CD	cluster of differentiation (in conjunction with number)
cDNA	complementary deoxyribonucleic acid
Cre	cyclization recombinase
CT	cycle threshold
Dhh	Desert Hedgehog
DMSO	dimethyl sulfoxide
DNA	deoxyribonucleic acid
dNTP	deoxynucleotide
DSS	dextran sodium sulphate
DYRK1B	dual specificity tyrosine-phosphorylation-regulated kinase 1B
ECM	extracellular matrix
EMT	epithelial-to-mesenchymal transition
FDR	false discovery rate
FFPE	formalin-fixed, paraffin-embedded
fl	floxed
H&E	Hematoxylin and Eosin stain
Hh	Hedgehog
i.p.	intraperitoneally
IBD	inflammatory bowel disease
IGF	insulin-like growth factor
IL	interleukin
ILC	innate lymphoid cells
KRAS	Kirsten rat sarcoma viral oncogene homolog
LacZ	bacterial gene, encoding for β-galactosidase
MIM	Mendelian Inheritance in Man
min.	minute(s)
MMP	matrix metalloproteinases
mRNA	messenger ribonucleic acid
n	number
NK-cells	natural killer cells
Notch	neurogenic locus notch protein homolog

NTC	non-template control
PBS	phosphate-buffered saline
PCR	polymerase chain reaction
PDGF	platelet-derived growth factor
PDGFRα	platelet-derived growth factor receptor alpha
PFA	paraformaldehyde
RNA	ribonucleic acid
RT	reverse transcriptase
RT-PCR	reverse transcription polymerase chain reaction
SEM	standard error of the mean
Shh	Sonic Hedgehog
Smad	mothers against decapentaplegic homolog
t-test	Student's *t*-test
TGF-β	transforming growth factor beta 1
Th	T helper cell
TNBS	trinitrobenzenesulfonic acid
TNF-α	tumor necrosis factor alpha
UC	ulcerative colitis
US	ultrasound
Wnt	Wingless and Int
WT	wildtype

1.2.1 Symbols for genes and proteins

Symbol	**Gene name human (HGNC)**	**Gene name mouse (MGI)**	**Protein (Uniprot)**
COL1A1/Col1a1/COL1A1	collagen type I alpha 1 chain	collagen, type I, alpha 1	Collagen alpha-1(I) chain (human); collagen alpha-1(I) chain (mouse)
COL3A1/Col3a1/COL3A1	collagen type III alpha 1 chain	collagen, type III, alpha 1	Collagen alpha-1(III) chain (human); collagen alpha-1(III) chain (mouse)
GLI1/Gli1/GLI1	GLI family zinc finger 1	GLI-Kruppel family member GLI1	Zinc finger protein GLI1 (human); zinc finger protein GLI1 (mouse)
IHH/Ihh/IHH	Indian hedgehog signaling molecule	Indian Hedgehog	Indian hedgehog protein
PTCH1/Ptch1/PTCH1	patched 1	patched 1	Protein patched homolog 1 (human); protein patched homolog 1 (mouse)
SHH/Shh/SHH	sonic hedgehog signaling molecule	sonic hedgehog	Sonic hedgehog protein (human); sonic hedgehog protein (mouse)
SMO/Smo/SMO	smoothened, frizzled class receptor	smoothened, frizzled class receptor	Smoothened homolog (human); smoothened (mouse)
TGF-β/Tgf-β/ TGF-β	transforming growth factor beta 1	transforming growth factor, beta 1	Transforming growth factor beta-1 proprotein
α-SMA/α-Sma/α-SMA	actin alpha 2, smooth muscle	actin, alpha 2, smooth muscle, aorta	Actin, aortic smooth muscle (human); actin, aortic smooth muscle (mouse)

1.3 Tables

1.4 Figures

1.5 Abstract/Zusammenfassung

The Hedgehog (Hh) signaling pathway plays a crucial role in development and homeostasis of various organs. However, disrupted Hh signaling can cause disease in mammals. Activating Hh mutations can act as oncogenic drivers, e.g. in basal cell carcinomas and medulloblastomas. In the colon, Hh participates in the development of tissue polarity and maintenance of colonic stem cells as well as playing a role in the homeostasis of mesenchymal cells.

In this study, we sought to investigate the role of Hh in tissue fibrosis in inflammatory bowel disease (IBD). IBD, with Crohn's disease and ulcerative colitis being the most prominent entities, affects various areas of the gastrointestinal tract. Besides the symptoms of inflammation, patients may also suffer from fibrosis as an important complication resulting in intestinal stenosis or the formation of fistulae, two common IBD complications, particularly in Crohn’s disease.

A promoting role of Hh signaling on fibrosis has previously been shown in human liver cirrhosis and systemic sclerosis as well as in animal models of lung- or kidney fibrosis. In the colon, Hh ligand released by enterocytes activates downstream Hh signaling in mesenchymal cells (fibroblasts, leiomyocytes) in the stroma. Therefore, we focused on alterations of stromal Hh signaling in the context of a murine colitis model.

Acute or chronic colitis was induced chemically in mice. By applying histological and *in vivo* imaging (animal ultrasound) methods, we evaluated and compared the extent of colonic fibrosis between mice with genetic Hh activation or pharmaceutical Hh inhibition. The thickness of the colonic wall as assessed by ultrasound, the diameter of *muscularis mucosae* evaluated by microscopy, and histochemical staining of collagen fibers were used as readouts for fibrosis. In acute colitis, the expression of Hh- and fibrosis-related genes was determined by PCR. To further elucidate the impact of stromal Hh signaling, we made use of transgenic mouse models with up- or downregulated Hh activity as well as pharmacological interventions.

Histology confirmed the induction of colitis. In genetically modified mice with diminished Hh signaling, no statistically significant difference in markers of fibrosis upon chronic colitis could be determined, neither histologically nor sonographically. Induction of acute colitis in transgenic mice bearing disinhibited Hh signaling did not lead to increased thickness of the *muscularis mucosae* or deposition of collagen fibers when compared to controls. However, PCR revealed an upregulation of fibrosis-associated genes in Hh overactivated mice. There was no difference in markers of fibrosis in mice with chronic colitis and overactivated Hh signaling in comparison to control mice. In mice treated with a clinically approved Hh inhibitor, Hh inhibition did not lead to

significant differences in colon fibrosis upon chronic colitis. We conclude that Hh signaling plays a limited role in the pathogenesis of fibrosis in IBD.

German abstract/Zusammenfassung

Der Hedgehog (Hh)-Signalweg spielt eine wichtige Rolle bei Organentwicklung und Homöostase, aber auch in Krankheitsprozessen. So weisen Basaliome und Medulloblastome oft aktivierende Hh-Mutationen auf. Im Kolon ist eine Mitwirkung des Hh-Signalwegs bei der Ausbildung der Gewebepolarität, der Homöostase von Stammzellen und mesenchymalen Zellen sowie der Karzinogenese beschrieben.

In dieser Studie wurde der Einfluss des Hh-Signalwegs auf Fibrose bei chronisch-entzündlichen Darmerkrankungen (CED) am Mausmodell untersucht. Bei CED, mit den Hauptvertretern Morbus Crohn und Colitis ulcerosa, sind unterschiedliche Anteile des Gastrointestinaltrakts betroffen. Neben den Symptomen der Entzündung leiden viele Patienten unter einer Fibrose, die durch Stenosen oder Fistelbildung zu weiteren Beschwerden führt.

Ein fibrogener Einfluss des Hh-Signalwegs findet sich z. B. bei der Leberzirrhose und Systemischen Sklerose sowie bei Tiermodellen der Lungen- und Nierenfibrose. Im Kolon aktivieren von Enterozyten freigesetzte Hh-Liganden den Signalweg in stromalen, mesenchymalen Zellen (Fibroblasten, Leiomyozyten). Der Fokus dieser Arbeit lag daher auf Veränderungen des stromalen Hh-Signalwegs im Kontext eines Kolitismodells.

Eine akute oder chronische Kolitis in Mäusen wurde durch ein chemisches Agens induziert. Mittels histologischer und sonografischer Methoden wurde das Ausmaß der intestinalen Fibrose evaluiert und zwischen verschiedenen Gruppen verglichen. Als Parameter für die Fibrose wurde der Durchmesser der Kolonwand und der *Muscularis mucosae* sowie die histochemische Anfärbung von Kollagenfasern genutzt. Bei der akuten Kolitis erfolgte die Bestimmung der Expression Hh- und fibroseassoziierter Gene mittels PCR. Um den Einfluss des stromalen Hh-Signalwegs näher zu beleuchten, wurden transgene Mäuse mit hoch- oder herunter-reguliertem Signalweg und medikamentöse Interventionen eingesetzt.

Histologisch zeigte sich wie erwartet eine Kolitis. In genetisch modifizierten Mäusen mit verringertem Hh-Signalweg ließ sich weder histologisch noch sonografisch ein statistisch signifikanter Unterschied hinsichtlich der Fibrose nach chronischer Kolitis im Vergleich zu Kontrollmäusen erkennen. Nachdem in transgenen Mäusen mit aktiviertem Signalweg und Kontrollen eine akute Kolitis induziert wurde, fanden sich keine signifikanten Unterschiede der Dicke der *Muscularis mucosae* oder der Ablagerung von Kollagen. Die PCR zeigte eine Hochregulierung von fibroseassoziierten Genen in Mäusen mit überaktivem Hh-Signalweg. Im

selben Mausmodell und in Kontrolltieren wurde ebenfalls eine chronische Kolitis induziert, der genetisch verursachten Überaktivierung des Signalwegs wurde hier teilweise durch einen medikamentösen Hh-Inhibitor entgegengewirkt. Weder durch Hh-Aktivierung noch durch medikamentöse Hemmung ließ sich ein signifikanter Unterschied hinsichtlich der Fibrose erkennen. Daraus lässt sich folgern, dass Hh nur einen begrenzten Einfluss auf die Fibroseentstehung bei CED ausübt.

2. Introduction

2.1 Hedgehog signaling pathway

The Hh signaling pathway was first described in a genetic screen performed on cuticle embryos of *Drosophila melanogaster*, demonstrating an effect of Hh mutations on *Drosophila* body segmentation (1). The Hh pathway is evolutionary highly conserved and plays a critical role also in mammals, where Hh signaling is encoded by three paralogous genes: Sonic (*SHH*/*Shh*)-, Indian (*IHH*/*Ihh*)- and Desert Hedgehog (*DHH*/*Dhh*) (2). They play a pivotal role in embryonic and post-embryonic body-tissue patterning, with reduction of Hh activity leading to morphological deficits, as severe as holoprosencephaly (failure of forebrain development leading to complex morphological craniofacial alterations) and cyclopia, the failure to develop two separate eye sockets (3, 4). Moreover, the physiological role of Hh in tissue repair, homeostasis and stem cell maintenance has been a subject of profound research (5, 6). The signaling pathway's impact on disease has been linked to a plethora of conditions, ranging from alopecia and depression to complex syndromes like Down syndrome as well as cancer (7-9). Regarding carcinogenesis, Hh is involved in maintenance of cancer stem cells, cancer progression (in both ligand- and non-ligand-dependent fashion), and in tumor regulation by neoangiogenesis, cell cycle control and downregulation of pro-apoptotic factors (10-14). For instance, mutations of the tumor suppressor gene *PTCH1*, encoding for the Hh suppressor protein patched homolog 1 (PTCH1), were found in basal cell carcinoma and medulloblastoma, both in sporadic cases and in hereditary tumors in Gorlin syndrome (3). Moreover, its upregulation has been linked to the promotion of metastasis in various malignancies (15).

Under physiological conditions in mammals, the three Hh effector molecules are synthesized as precursor proteins bearing a signaling amino-peptide (N)-terminal domain and a carboxy (C)-terminal domain, which catalyzes the transfer and esterification of a cholesterol molecule to the N-terminal domain (3). This enables the Hh polypeptides to associate with the cell membrane’s lepidic structure (11). To complete the biochemical processing needed for Hh-dependent pathway activation, palmitoylation of the N-terminal domain is required (3, 11).

To activate the Hh signaling cascade, Hh molecules bind to the twelve-span transmembrane receptor Patched 1 (PTCH1, ref. 3). Upon ligand binding, PTCH1 releases its repression of the G-protein coupled seven domain transmembrane protein Smoothened (SMO), leading to its translocation to the cell surface and accumulation in primary cilia, which also acts as a chemosensor detecting extracellular Hh ligands (16, 17).

The final part of Hh signaling is executed by the three GLI transcription factors, of which GLI1, in humans encoded by Glioma-Associated Oncogene Homolog 1 (GLI family zinc finger 1, *GLI1*)

on Chromosome 12q13.3, is the best described (18). The members of the GLI transcription factor family bear DNA-binding zinc-finger domains (18). While GLI1 acts as a transcription activator, GLI2 and 3 can have an activating or repressive effect on gene transcription (19). Hh related gene transcription is regulated by the balance of activating (GLI^A) and repressing (GLI^R) forms of GLI (5). In its inactive state, PTCH1 inhibits SMO and therefore GLI^R is the dominant form, leading to an increase in the GLI3 level, whereas in activated Hh signaling GLI^A is upregulated, hence leading to stimulation of GLI-related gene expression (5). Among those target genes *PTCH1*/*Ptch1* is found, therefore regulating Hh signaling in a negative feedback loop (3, 5, 11). Notably, besides the aforementioned so-called canonical Hh pathway, different non-canonical routes have been described that act either unrelatedly to Smoothened-Patched interaction or in a GLI independent manner (20).

In the colon, Indian Hedgehog (IHH) acts as the main ligand under homeostatic conditions (21). Following secretion by differentiated enterocytes, IHH activates downstream signaling in the stroma in an exclusively paracrine way (21). Mesenchymal cells such as (myo)fibroblasts and smooth muscle cells are the main responsive elements of Hh signaling (21, 22). Epithelial cells in the intestine are not Hh responsive, with the exception of a rare epithelial cell population found in the small intestine, located above Paneth cells (23, 24). In humans, the mRNA expression levels of the Hh pathway components *GLI1* and *PTCH1* increase from the ascending colon to the sigmoid colon (25). During development, deficiency of either Hh ligands or homozygous loss of GLI activity leads to severe gastrointestinal malformations in mice (26). It has been shown by the host laboratory that in a murine model of colitis-associated colorectal cancer downstream Hh activity is diminished and restricted to the stroma, and that attenuated Hh signaling promotes tumorigenesis (27).

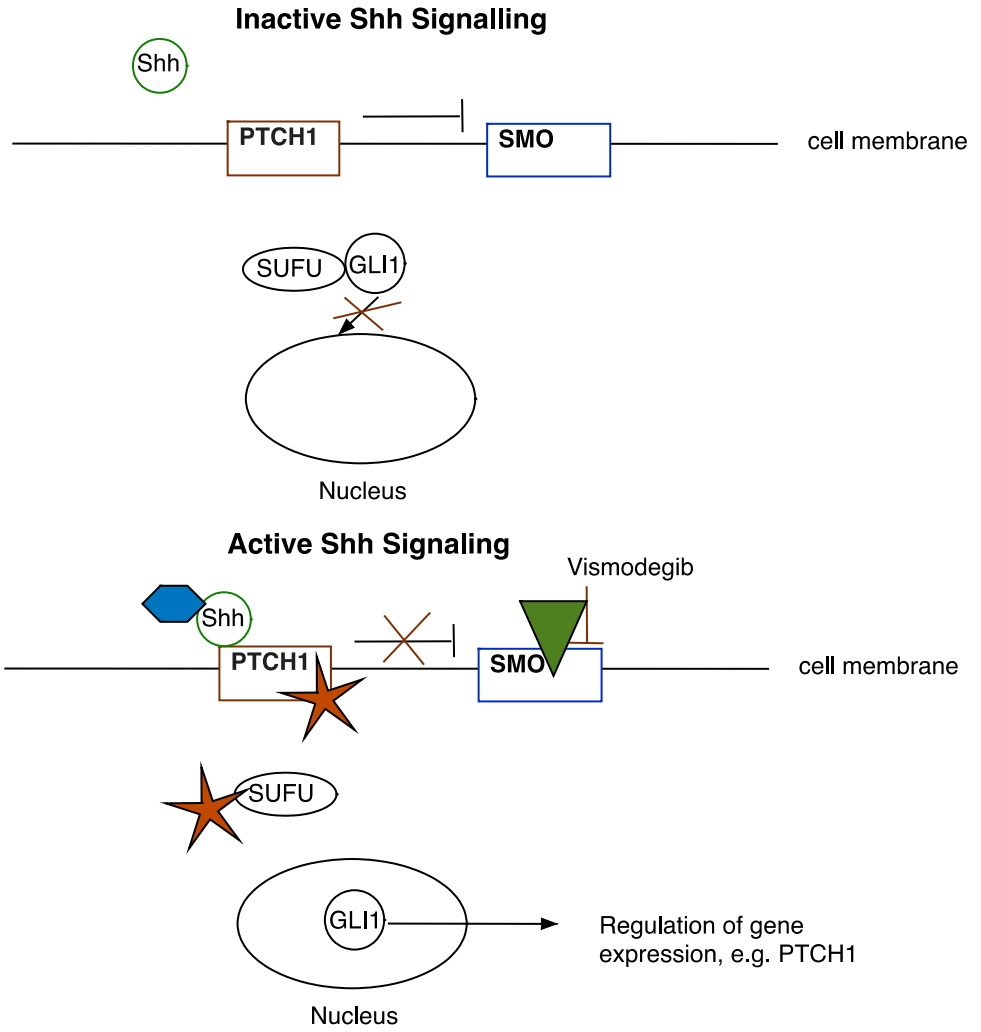

Figure 1: Schematic overview of inactive (top) and active (bottom) Hh (Hedgehog) signaling, Vismodegib as inhibitor of Hh signaling and common modes of pathologic pathway activation (adapted from ref. 28). In inactive Hh signaling (absence of a binding ligand, e.g. Sonic hedgehog, Shh) PTCH1 (Patched 1) suppresses SMO (Smoothened) and SUFU (Suppressor of Fused) withholds GLI1 (Glioma-associated oncogene homolog 1) in the cytoplasm. Upon ligand-binding (Shh) PTCH1 releases its inhibition of SMO, leading to accumulation of GLI1 in the nucleus and gene regulation. Vismodegib (GDC-0449) is a Hh inhibitor, binding directly to SMO (28). Hh signaling can be pathologically activated by i) ligand overexpression (blue hexagon) in an autocrine or paracrine way, ii) loss of function of suppressing genes (PTCH1, SUFU; orange star), iii) gain of function of pathway activators (SMO; green triangle) (29)

2.2 Inflammatory bowel disease

Inflammatory bowel disease (IBD) is a chronic inflammatory disorder of multifactorial etiology, with genetic and environmental factors leading to a dysregulation of the mucosal immune system (30). IBD comprises two main entities, Crohn's disease and ulcerative colitis (UC) (31, 32). The highest incidences of IBD are found in Europe (in particular in Scandinavia and the United Kingdom) and North America (31). In northern Europe, the total incidence rate for IBD has been determined as 6.3 cases for Crohn’s disease and 11.4 cases for UC per 100,000 persons per year, whereas the rate in southern Europe is notably lower (31). The respective prevalence has been

described to vary from 1.5 to 213 cases per 100,000 persons for Crohn's disease and from 2.4 to 294 per 100.000 persons for UC (31). Incidence and prevalence rates have shown a worldwide increase, and additionally in areas with previously low occurrence of IBD, such as newly industrialized countries (31, 33). This has not only been partly attributed to the disclosure of previously undiagnosed IBD cases due to advances in and better access to healthcare, but also to the westernization of societies, changing dietary and sanitary conditions, and other lifestyle factors (33).

Both entities present with typical, yet sometimes overlapping clinical features (Table 1; ref. 34). Regarding hallmarks, Crohn's disease presents as a discontinuous, transmural inflammation that may affect the whole gastrointestinal tract, while UC shows no transmural inflammation and is usually limited to the colon, although so-called "backwash ileitis" can occur (34). Notably, in UC patterns of Crohn's disease can also be found, e.g. transmural inflammation in patients who received ileal pouch anal-anastomosis (35).

	Crohn's disease	**Ulcerative colitis**
Sex ratio (♂:♀)	2:1	1:1
Affection of upper-gastrointestinal tract	Possible	Not found
Affection of the small bowel	Yes	Only in "backwash ileitis"
Colonic obstruction	Common	Rare
Perianal manifestations and fistulae	Common	Not found
Hematochezia	Rare	Common
Passing mucus per rectum	Rare	Common
Extra-intestinal manifestations	Common	Common

Table 1: Typical clinical features of IBD (adapted from ref. 34)

The most frequent extra-intestinal manifestations can be divided into three subgroups (36). Firstly, common immune-related extra-intestinal manifestations of the musculoskeletal system (arthritis), the skin (pyoderma gangrenosum, erythema nodosum) and the visual system (uveitis, scleritis). Secondly, the variety of IBD-associated autoimmune disorders consists of spondyloarthropathies, diabetes mellitus type 1, diseases of the hepatobiliary tract (primary sclerosing cholangitis), thyroid diseases, and disorders from the spectrum of myositis and vasculitis. The third subgroup comprises extra-intestinal complications induced by inflammatory events (anemia, amyloidosis), malnutrition (growth failure, fatty liver disease) or therapy (steroid osteopathy).

While patients suffering from UC- and Crohn's disease-related ileocolitis exhibit an increased risk for acquiring colon cancer, patients affected by Crohn's disease-associated enteritis are additionally prone to develop small-bowel cancer (34).

The diagnostic procedure in IBD includes taking the patient's history, physical examination, laboratory tests of blood and stool samples as well as ileocolonoscopy, with the possibility of taking biopsies for histopathological evaluation (32). During endoscopic examination, certain features can be seen to distinguish between Crohn's disease and UC. Crohn's disease, a transmural inflammation, characteristically presents with deep ulcerations, often of longitudinal shape ("snail tracks"), inflamed areas containing normal mucosa ("skip lesions"), a so-called cobblestone appearance of the ileum and occasional strictures as well as mucosal edema (32). In the setting of mucosal inflammation in Crohn's disease, features of a continuous, uniform disease with flat ulcerations, mucosal edema and a circumferential pattern of inflammation can be identified (32).

Histopathological distinction between Crohn's disease and UC can prove difficult, with pathognomonic attributes being absent in some cases (32). Histologically, Crohn's disease is typically characterized by (not always detectable) granulomas and a discontinuous, transmural inflammation; in contrast, UC exhibits a continuous pattern of inflammation, limited to the mucosa (32). In acute/active IBD, the histological features consist of neutrophil granulocytes infiltrating the mucosa, leading to cryptitis and crypt abscesses (in UC) and loss of epithelial integrity with erosions and ulcers (32). In a chronic course of disease, disturbed epithelial architecture (crypt shortening or loss, crypt branching, reduced number of goblet cells), a lympho-plasmacellular infiltration within the *lamina propria*, metaplasia (pyloric gland metaplasia, Paneth cell metaplasia) and mucosal/submucosal fibrosis can be detected (37).

Factors influencing the risk of IBD include geographical distribution, dietary and sanitary conditions, smoking behavior and infections (38). On a genetic level, a multitude of susceptibility regions have been reported, e.g. *IBD1-9* and IBD-associated genes such as *NOD2* and *CARD15* (38). Over 200 single nucleotide polymorphisms are currently described to be associated with an increased risk for IBD (39). In addition, the composition of the gut microbiome and its link to IBD has been a matter of extensive research, however no single cause for the diseases has been identified (40).

The gastrointestinal immune system plays a key role in mediating IBD. As the first line of innate immunity, the intestinal epithelium regulates the interplay between intestinal commensals and lymphoid tissue (38). Derogation of the epithelium's integrity, such as deregulation of tight

junctions, increased permeability between epithelial cells, or decreased secretion of mucus, immunoglobulin A and *defensins*, all impair that barrier and therefore enhance inflammation and are pathogenetic factors for IBD (38). Furthermore, receptors of the innate immune system (NOD-like receptors, toll-like receptors and other pattern-recognition receptors) expressed on epithelial cells, innate lymphoid cells (ILC) such as natural killer cells (NK-cells), and antigen-presenting cells (dendritic cells, macrophages) in the subjacent *lamina propria* are involved in the gut's non-specific immune system not only by shaping the immune response to intestinal microbes, but also by maintaining self-tolerance, and disturbances of those elements have been linked to IBD (38, 41).

The adaptive immune system in IBD is mediated mostly by CD4+ T-cells (42). While Crohn's disease seems to be dominated by the T helper cell (Th) 1 subgroup, denoted by secretion of interferon-γ (IFNγ) and tumor necrosis factor alpha (TNF-α), UC is mediated through Th2-cells, with interleukin (IL)-4, IL-5 and IL-13 being the main effector cytokines (41, 43). The Th17 subgroup has been described as an important mediator of inflammation in both entities (41). Via secretion of IL-6 and IL-17, Th17-cells are able to stimulate the synthesis of pro-inflammatory cytokines (chemokines, IL-1, IL-6, TNF-α) in epithelial cells, fibroblasts and macrophages, thereby enhancing inflammatory response in IBD (41). Furthermore, mutations impairing the function of IL-10, a powerful anti-inflammatory cytokine, augment the susceptibility for UC and increase the severity of IBD (44). The impact of B-cells has been less well studied, but the existence of certain antimicrobial antibodies (anti-*Saccharomyces cerevisiae* and anti-flagellin antibodies) in patients suffering from IBD suggests a pathology involving B-cells (45).

2.3 IBD and Hedgehog signaling

The fact that the human *GLI1* gene (12q13.3; Mendelian Inheritance in Man [MIM]: 165220) is located within the aforementioned *IBD2* susceptibility region (12p13.2-q24.1; MIM: 601458), along with the finding of downregulated *GLI1* expression in inflamed biopsies of UC patients, has suggested an involvement of Hh signaling in IBD pathogenesis (46, 47). A haplotypic variation of *GLI1* is strongly associated with IBD in the northern European population (25). Knockout of intestinal Hh leads to spontaneous inflammation in mice, and isolated colon mesenchyme (lacking Hh ligand expression from the epithelium) shows a downregulation of Hh and upregulation of inflammatory pathways, an effect that can be reduced by adding exogenous Hh ligands, suggesting an important role of Hh in intestinal inflammation (48). In $Gli1^{+/LacZ}$ reporter mice, which lack one functional *Gli1* allele, chemical induction of colitis leads to more severe symptoms and histopathological findings compared to wildtype (WT) littermates (25). Similar results were seen after abolishing Hh signaling by genetic *Smo* deletion or pharmacological inhibition (49). In

contrast, knockout of one *Ptch1* allele dampened dextran sodium sulphate (DSS)-induced colitis in mice (49).

In mucosal biopsies from patients suffering from Crohn's disease or UC, significantly lower expression of *SHH*/SHH, *IHH*/IHH and *GLI1*/GLI1 could be determined on the protein and messenger ribonucleic acid (mRNA) level, and Hh pathway components modulated inflammatory cytokines in explanted human colons (50). Microarray analysis of gene expression confirmed the downregulation of Hh pathway components in IBD and non-IBD colonic inflammation (25). On the other hand, mucosal upregulation of the Hh ligand *SHH*/SHH and *PTCH1*/PTCH1 was detected on the mRNA and protein level in inflamed, patient-derived colon samples (51). Notably, the spatial expression pattern of Hh components was also altered, losing its gradient from strong expression in the basal cell layer to weak expression in luminal enterocytes (51).

Controversial findings exist about the mechanistic link between Hh signaling and inflammation. Whereas Hh-responsive CD11b+ myeloid cells and CD11c+ dendritic cells were observed in ulcers in DSS colitis, *in vitro* and *in vivo* analysis could not determine a direct response of those cells to Hh signaling (22, 25). Hh responsiveness was not seen in infiltrating CD3+ T-lymphocytes (25). A comparison between $Gli1^{+/LacZ}$ mice and WT mice after DSS-induced colitis revealed increased levels of pro-inflammatory cytokines and chemokines (such as IL-2, IL-4, IL-6, IFNγ, and Cxcl5) in the Hh-downregulated $Gli1^{+/LacZ}$ cohort (25). Notably, mRNA levels of the anti-inflammatory cytokines *Tgf-β* (transforming growth factor β1) and *Il-10* (interleukin 10) did not show a significant up- or downregulation (25). Additionally, TGF-β can also exhibit a pro-inflammatory function (44).

2.4 Fibrosis in IBD

Intestinal fibrosis is a common pathological feature of IBD. Over 10 % of patients with Crohn's disease present with strictures or fistulae at the time of initial diagnosis (52). After ten years, strictures can be found in approximately half of the patients (52). Furthermore, complications related to the forming of strictures and fistulae account for the majority of surgical procedures in Crohn's disease (52). In Crohn's disease, the ileum and ileocolonic region are predominately affected by fibrotic complications, but strictures can affect the whole gastrointestinal tract (52). Therapeutic implications include endoscopic dilation, topical or systemic corticosteroid treatment and surgical resection (52). The emergence of new anti-inflammatory agents, such as antibodies against TNF-α (Infliximab), aminosalicylates or inhibitors of purine synthesis (azathioprine) did not lead to a significant reduction of intestinal complications or the requirement for surgery in UC (53). To date, no effective anti-fibrotic drug for IBD-driven intestinal fibrosis is available (54). Studies on the prevalence of fibrosis in UC show variable data, depending on the type of report

(radiological, endoscopic or surgical) and the definition of fibrotic complications (55). Strikingly, even though inflammation in UC is usually restricted to the mucosa and adjacent submucosa, strictures are a well-described finding in UC (55). The prevalence of benign strictures in UC has been described as between 1 % and 11.2 % (55). Notably, strictures in UC can show features of malignancy, especially after a long course of disease (55).

Fibrosis, the accumulation of collagen-rich extracellular matrix (ECM), is seen as a process induced by inflammation (56). Mesenchymal cells such as fibroblasts, myofibroblasts and smooth muscle cells are the key mediators of fibrosis (56). The activation of myofibroblasts can be induced by different factors. Growth factors, e.g., TGF-β, insulin-like growth factor (IGF) or platelet-derived growth factor (PDGF) play an important role in IBD-related fibrosis (56). In addition, a disturbed balance between ECM degrading matrix metalloproteinases (MMP) and their tissue inhibitors is involved in fibrosis (56). Activation of mesenchymal cells leads to deposition of different proteins in the ECM, such as fibronectin and tenascin, and of collagens, predominantly types I, III and V (57). In intestinal strictures in Crohn's disease, histological evaluation shows thickening of the *lamina muscularis mucosae* and *muscularis propria* as well as *submucosal* collagen deposition (57). In strictures derived from UC patients, not only has thickening and muscular hypertrophy of the *lamina muscularis mucosae* been detected, but also fibrosis of the *submucosa*, *muscularis propria* and even *subserosa* has been described (55).

The TGF-β/Smad (transforming growth factor beta 1/mothers against decapentaplegic homolog) signaling pathway is seen as the main mediator of fibrosis in IBD (58). Knockout of Smad7 dampens colitis and colitis-related fibrosis (58, 59). Additionally, pro-inflammatory cytokines like IL-1β, IL-6, IL-13, IL-17 or TNF-α enhance ECM deposition (60). Moreover, given the setting of inflammation in other organs (kidney, lung or heart), mature epithelial cells can go through a transformation into mesenchymal cells (epithelial-to-mesenchymal transition, EMT) and can thereby contribute to a pro-fibrotic environment, a process which is also discussed in IBD (61, 62).

2.4 Hh signaling in fibrosis

Hh signaling has been described as a driver of fibrosis in several organs. In the liver, activation of Hh mediates cirrhosis in non-alcoholic fatty liver disease, both in a murine model and human liver sections (63). In chronic hepatitis B and C infections, both common causes of liver cirrhosis, high expression of both Hh ligands and target genes can be found (64). Additionally, patients with advanced fibrosis show a higher expression of Hh target genes than those with less progressed fibrosis (64). Furthermore, Hh ligands are able to promote EMT in the liver of the rat, and treatment with the Hh antagonist GDC-0449 reduced liver fibrosis in a mouse model (65, 66). In the murine kidney, it has been shown that Shh signaling is involved in fibroblast activation and

thereby induction of renal interstitial fibrosis (67). Hh signaling is upregulated in fibrotic murine airway epithelium upon injury and in specimens of human idiopathic pulmonary fibrosis (68). Inhibiting the Hh pathway leads to the reduction of fibrosis in bleomycin-induced lung fibrosis in mice (69). Furthermore, the capacity of Hh in promoting fibrosis has been described, e.g., in the skin (systemic sclerosis) and the setting of acute and chronic pancreatitis (70, 71). In the heart, Shh upregulation seems to mitigate fibrosis after ischemia (72). In the intestine, loss of Ihh leads to intestinal fibrosis in mutant mice (73). A promotive role of Hh signaling in EMT has been postulated in various structures of the digestive system, such as the esophagus (74), pancreas (75) and bile duct (76).

Interestingly, recent studies have identified that Hh responsive cells in the murine intestinal mesenchyme express the fibroblast marker gp38 (podoplanin), as well as Gli1 expression colocalized with collagen III and platelet-derived growth factor receptor alpha (PDGFRα) expression in immunofluorescence (22). In addition, an overlap between Gli1 and desmin and/or α-smooth muscle actin positive cells was seen, at least partially (22). Furthermore, intestinal cells that had been sorted by flow cytometry showed an increase in *Gli1* and *Ptch1* mRNA expression in gp38+ cells compared to those expressing epithelial (epithelial cell adhesion molecule), leukocytic (CD45) or endothelial (CD31) membrane markers (22). These findings support a model in which Hh responsive cells are of mesenchymal nature and include fibroblasts, myofibroblasts and smooth muscle cells, which all play an important role in intestinal fibrosis.

2.5. The Hedgehog inhibitor Vismodegib

Vismodegib (GDC-0449, Erivedge®) is a small molecule inhibitor of Hh signaling (77). The United States Food and Drug Administration (FDA) approved the drug in 2012 for the treatment of basal cell carcinoma (77). To date, clinical trials for Vismodegib have been conducted *inter alia* for malignant tumors of the skin (advanced or metastatic basal cell carcinoma), the central nervous system (medulloblastoma), carcinomas of the prostate, lung, ovaries or pancreas, hematological neoplasias (B-cell lymphoma, chronic lymphocytic leukemia) and sarcomas (chondrosarcoma) (78). Side effects of Vismodegib treatment include fatigue, nausea and weight loss as well as muscle spasms, dysgeusia (disturbances in taste perception) and hair loss (77). There is controversial data on whether Vismodegib increases the risk of squamous cell carcinoma formation (78). Published data from the host laboratory also indicates that Hh inhibitor treatment may increase the risk of colon carcinoma formation in patients suffering from IBD (27).

Vismodegib binds to the transmembrane receptor SMO and thereby inhibits Hh signaling (77; see also Figure 1). Further SMO inhibitors include the steroidal alkaloid Cyclopamine, found in corn lilies (*Veratrum californicum*) and responsible for cyclopia in sheep upon uptake by pregnant

animals, as well as the widely used antifungal drug Itraconazole and newly developed inhibitors such as Sonidegib, Saridegib or Glasdegib (78).

2.6 Aims

The main aim of this study was to evaluate if activation or suppression of the Hh signaling pathway has an impact on colonic fibrosis in an experimental model of acute and chronic IBD. Previous studies suggest that Hh is a potent modulator of IBD, both in human samples and mouse models (22, 25, 49, 50). Since Hh responsive cells in the stroma are to a large extent (if not exclusively) of mesenchymal origin (21, 22), it can be hypothesized that Hh is a target pathway of colitis-associated intestinal fibrosis. To induce colitis-associated fibrosis, we employed the widely used DSS model (79-83). The extent of intestinal fibrosis was evaluated by different methods: small animal ultrasound (US) to measure the diameter of the colonic wall, scaling the thickness of the *lamina muscularis mucosae* on histological slides, and quantifying collagen-deposition with a histochemical method. In addition, clinical and histological parameters of colitis activity were monitored, and mRNA expression of Hh- and fibrosis associated genes was determined in the setting of acute colitis.

Primarily, we sought to investigate whether genetic manipulation of Hh signaling (reduction of pathway activity by knocking out the Hh effector *Gli1*) has an effect on fibrosis related to chronic colitis.

In another approach, the effect of increased Hh signaling (by using an inducible knockout of the Hh repressor *Ptch1*) in subepithelial and *lamina propria* fibroblasts was studied. To this end, we induced acute colitis in mice and assessed fibrosis as well as associated mRNA expression.

To rescue the genetically induced Hh overexpression, a pharmacological approach using the small molecule inhibitor Vismodegib was employed. In the setting of chronic DSS colitis, mice bearing a knockout causing conditional Hh activation (*Ptch1*) or controls were treated with Vismodegib or a vehicle and the fibrosis was evaluated.

3. Materials and methods

3.1 Materials

3.1.1 Equipment and consumables

	Supplier
Allegra 25 R centrifuge	Beckmann Coulter Life Sciences, Brea, USA
Applied biosystems 7500 Fast Real-Time PCR System	Applied biosystems, Warrington, UK
Applied biosystems MicroAmp Fast Optical 96-well Reaction Plate with Barcode (0.1 ml)	Applied biosystems
BD Microtainer SST Tubes	Becton, Dickinson and Company, Franklin Lakes, USA
BD Plastipak with Luer-Lock	Becton, Dickinson and Company
Bioruptor Sonicator	Diagenode, Liège, Belgium
Brand 8-well RealTime PCR-tubes, PP, single capped	BRAND GmbH + Co KG, Wertheim, Germany
Bright field microscope, Leica DMLB	Leica Microsystems GmbH, Wetzlar, Germany
Eppendorf centrifuge 5417C	Eppendorf AG, Hamburg, Germany
Galaxy Mini centrifuge	VWR International Ltd, Lutterworth, UK
Gilson pipetman (1-1000 µl)	Gilson Inc., Middleton, USA
Hitachi HV-F22CL scan camera	Hitachi Kokusai, Tokyo, Japan
INTEGRA Pipetboy	Integra Biosciences AG, Zizers, Switzerland
KEBO-Lab Reax 2000	KEBO Inredningar Sverige AB, Bromma, Sweden
KIATO Sterile Disposable Scalpel	Aditya Dispomed Products Pvt. Ltd, Kanpur, India
MENZEL Microscope Cover Slips, 24 x 60 mm	Gerhard Menzel GmbH, Braunschweig, Germany
Mettler Toledo precision scale	Mettler-Toledo AB, Stockholm, Sweden
Mini centrifuge C-1200	National Labnet Co., Edison, USA
MJ Research PTC-200 Peltier Thermal Cycler	MJ Research Inc., St. Bruno, Canada
Neptune Barrier Tips (10-1000 µl)	Biotix Inc., San Diego, USA
Olympus BX50 DIC/Nomarski microscope	Olympus Corporation, Tokyo, Japan
Olympus DP25 digital camera	Olympus Corporation
Pannoramic MIDI II slide scanner	3DHISTECH Ltd., Budapest, Hungary
SARSTEDT Centrifuge Tubes (15 ml, 50 ml)	SARSTEDT AG & Co., Nümbrecht, Germany
SARSTEDT Micro Tubes, 1.5 ml, PP, with attached PP cap	SARSTEDT AG & Co.

SARSTEDT Serological Pipettes (10 ml, 25 ml)	SARSTEDT AG & Co.
TECAN Infinite M200 PRO NanoQuant	Tecan Group Ltd., Männedorf, Switzerland
TECAN NanoQuant plate	Tecan Group Ltd.
TERUMO NEOLUS Hypodermic Needles	Terumo Europe N.V., Leuven, Belgium
Veet hair removal cream	Reckitt Benckiser, Solna, Sweden
VisualSonics Vevo 2100 LAZR Imaging Station	VisualSonics Inc., Toronto, Canada
VWR VDI 12 Homogeniser	VWR International, Radnor, USA

Table 2: Equipment and consumables

3.1.2 Chemicals and kits

	Supplier
2,4,6,-Trinitrophenol	Sigma-Aldrich, St. Louis, USA
2-Mercaptoethanol ≥ 99 %	Sigma-Aldrich
4-Hydroxytamoxifen, Minimum 70 % of Z-Isomer	Sigma-Aldrich
Aqua-Poly/Mount, mounting medium	Polyscience Inc., Warrington, USA
Azoxymethane (AOM)	Sigma-Aldrich
Corn oil	Sigma-Aldrich
Deoxynucleotide (dNTP) Solution Mix, 8µmol each dNTP	New England Biolabs, Ipswich, USA
Dextran sulphate sodium (DSS)	TdB consultancy, Uppsala, Sweden
Dimethyl Sulphoxide (DMSO) Hybri-Max	Sigma-Aldrich
Ethanol, Kemetyl Absolut Finsprit, 99.5 %	Kemetyl AB, Haninge, Sweden
Glutaraldehyde solution, Grade I, 50 % in H_2O	Sigma-Aldrich
Hydrochloric acid, 1N	Sigma-Aldrich
Isoflurane	Baxter Medical AB, Kista, Sweden
$MgCl_2$ 1M	Sigma-Aldrich
NONIDET P-40, 0.1 %	BDH Laboratory Supplies, Dorset, UK
Oligo$(dT)_{12-18}$ Primer 25 µg (0.5 µg/µl)	Invitrogen, Carlsbad, USA
Paraformaldehyde (PFA)	In-house preparation
Potassium hexacyanoferrate (II) trihydrate	Sigma-Aldrich
Potassium hexacyanoferrate (III)	Sigma-Aldrich
Power SYBR Green PCR Master Mix	Applied Biosystems
Quiagen RNase-Free DNase Set Buffer	Quiagen GmbH, Hilden, Germany
Quiagen RNase-Free water	Quiagen GmbH
Quiagen RNeasy Mini Kit	Quiagen GmbH
RNase Inhibitor Human placenta, 40,000 U/ml	New England Biolabs
Siriusrot F3BA	Waldeck GmbH & Co KG, Münster, Germany

SuperScript III Reverse Transcriptase 10,000 U (200 U/µl)	Invitrogen
Tamoxifen ≥ 99 %	Sigma-Aldrich
Ultrasound gel	Parker Laboratories Inc., Fairfield, USA
Vismodegib V-4050, free base, >99 %	LC Laboratories, Woburn, USA
X-Gal (5-bromo-4-chloro-3-indolyl-β-D-galactopyranoside)	Sigma-Aldrich
Xylene, histological grade	Sigma-Aldrich

Table 3: Chemicals and kits

3.1.3 Solutions

	Components
Phosphate-buffered saline (1x PBS)	137 mmol/L NaCL 2.7 mmol/L KCl 10 mmol/L Na_2HPO_4 1.8 mmol/L KH_2PO_4
Picric acid solution	1.3 % 2,4,6,-Trinitrophenol in H_2O
Sirius Red solution	0.1 % Siriusrot F3BA in picric acid solution
X-Gal fixative	2 % Paraformaldehyde in 1x PBS 0.2 % v/v Glutaraldehyde
X-Gal rinse buffer	2 mM $MgCl_2$ 0.1 % NONIDET P-40 in 1x PBS
X-Gal staining solution (stock solution)	2.5 ml of 40 mg/ml X-Gal 1 ml of 5 mM Potassium hexacyanoferrate (III) ($K_3Fe(CN)_6$) 1 ml of 5 mM Potassium hexacyanoferrate (II) trihydrate ($K_4Fe(CN)_6$) in 100 ml rinse buffer

Table 4: Solutions

3.1.4 RT-PCR primer

Primer sequences were retrieved from previous publications and verified by using the Primer-Basic Local Alignment Search Tool (Primer-BLAST) by the National Center for Biotechnology Information, Bethesda, USA.

Gene of interest	**Product on target template** (according to Primer-BLAST)	**Sequence (5'→3')** **F=Forward** **R=Reverse**
α-Sma	actin, alpha 2, smooth muscle, aorta (Acta2), mRNA	F: AAACAGGAATACGACGAAG R: CAGGAATGATTTGGAAAGGA
Arp	ribosomal protein, large, P0, mRNA	F: TGCACTCTCGCTTTCTGGAGGGTGT R: AATGCAGATGGATCAGCCAGGAAGG
Col1a1	collagen, type 1, alpha 1, mRNA	F: GCCGAACCCCAAGGAAAAGAAGC R: CTGGGAGGCCTCGGTGGACATTAG
Col3a1	collagen, type 3, alpha 1, mRNA	F: TCCCCTGGCTCAAATGGCTCAC R: GCTCTCCCTTCGCACCGTTCTT
Gli1	GLI-Kruppel family member GLI1, mRNA	F: CGTTTAGCAATGCCAGTGACC R: GAGCGAGCTGGGATCTGTGTAG
Ptch1	patched 1 (Ptch1), mRNA	F: TTGGGATCAAGCTGAGTGCTG R: CGAGCATAGCCCTGTGGTTCT
Tgf-β	transforming growth factor, beta 1, mRNA	F: TTGCCCTCTACAACCAACACAA R: GGCTTGCGACCCACGTAGTA

Table 5: RT-PCR primer

3.1.5 Software

	Provider
7500 Fast Real-Time PCR System software (v2.0.6)	Applied biosystems, Warrington, UK
CellSense	Olympus, Tokyo, Japan
GraphPad Prism 7	GraphPad Inc., La Jolla, USA
i-control	Tecan Group Ltd., Männedorf, Switzerland
ImageJ 1.52a	National Institutes of Health, Bethesda, USA
MRI Fibrosis Tool by Gabriel Landini	http://dev.mri.cnrs.fr/projects/imagej-macros/wiki/Fibrosis_Tool
Pannoramic viewer 1.15.4.43061	3DHISTECH Ltd., Budapest, Hungary
VisualSonics Vevo software (v.1-5.0)	VisualSonics Inc., Toronto, Canada

Table 6: Software

3.1.6 Databases

	Provider
HUGO Gene Nomenclature Committee (HGNC)	HGNC, European Bioinformatics Institute (EMBL-EBI), Cambridge, UK (https://www.genenames.org/; retrieved 16 June 2019
Mouse Genome Informatics (MGI)	The Jackson Laboratory, Bar Harbor, USA (http://www.informatics.jax.org/; retrieved 16 June 2019)
Primer-Basic Local Alignment Search Tool (Primer-BLAST)	National Center for Biotechnology Information, Bethesda, USA (https://www.ncbi.nlm.nih.gov/tools/primer-blast/index.cgi; last accessed 16 June 2019)
Universal Protein Resource (UniProt)	UniProt consortium (EMBL-EBI; SIB, Geneva, Switzerland; PIR, Washington, USA) (https://www.uniprot.org/; retrieved 16 June 2019)

Table 7: Databases

3.2. Methods

3.2.1 Mice, genetic modifications and pharmacological interventions

All mice were kept in the animal facility of Karolinska University Hospital, Huddinge, Sweden, under specific pathogen-free conditions. Animals were housed in groups in enriched standard-cages in an air-conditioned atmosphere with a controlled 12 h light-dark cycle. A standard chow and drinking water were provided *ad libitum*. The mice used were at >6 weeks of age. Euthanasia was carried out by cervical dislocation at the experimental endpoint or when mice showed increased signs of suffering, evaluated by a scoring system and adhering to local ethical guidelines. Necropsy was performed right after sacrificing and colonic tissue was harvested, which was either

fresh-frozen and stored at -80°C, or fixated for histology (4 % PFA in 1x PBS) or X-Gal staining (see below).

Studies were covered by the ethical permits S69/12, S138/12, S10/15, S15/15, and extensions (Department of Agriculture, *Jordbruksverket*, Sweden). The experimental designs aimed to follow the 3R's policy (replacement, reduction, refinement) of animal research (84).

All transgenic mice were backcrossed to a C57BL/6 background. Genotyping was performed by analyzing sequence-specific melting points in a reverse transcription polymerase chain reaction (RT-PCR)-assay (for *Ptch1*) or by polymerase chain reaction (PCR) based amplification of the sequence in question (*Gli1*^{LacZ}, *Col1a2Cre*).

A concise overview of the mouse models used in this study can be found in Table 8.

C57BL/6: An inbred strain and common murine model for human diseases. Mice were obtained from Scanbur AB, Sollentuna, Sweden.

***Gli1*$^{+/lacZ}$**: Transgenic *Gli1*$^{+/lacZ}$ mice (in the following: *Gli1*^{LacZ}) bear a replacement (knock-in) of encoding sequences of the *Gli1* gene by *lacZ*, a bacterial gene that is part of the *lac* operon (Figure 2; ref. 85, 86). Therefore, these mice lack one functional copy of the Hh main effector *Gli1*, as previously described (85). Furthermore, the insertion of the *lacZ*-sequence (encoding for β-galactosidase) enables the use of X-Gal staining (see below) as a read out for *Gli1*-activation (87). *Gli1*^{LacZ} mice were originally developed in Alexandra Joyner's laboratory (85).

Figure 2: Schematic overview of Gli1^{LacZ} *mice (adapted from ref. 85). Encoding sequences of the Gli1 gene are replaced by the bacterial lacZ gene (orange). 5'UTR: 5' untranslated region; ATG: initiator codon*

Cre-Lox-System: The Cre-Lox recombination system has become a valuable tool to genetically modify specific cells in living organisms. It makes use of the enzyme cyclization recombinase (Cre) to delete, integrate, invert or translocate selected DNA sequences (88). Cre catalyzes cleavage and reassignment of DNA between two specific base sequences, for which the palindromic *LoxP* site serves as recognition site (89). Through flanking of a specific gene sequence by two *LoxP* sites, Cre binding sites are introduced to the genome (89). Arrangement of *LoxP*-sequences in the same direction leads to excision of the embedded DNA in the form of a circular fragment that gets disposed of, or "floxed" (88). Antidromic *LoxP* sites are necessary for the inversion of DNA fragments (90). Placing *LoxP*-sites on distinct DNA molecules allows for

intermolecular recombination, i.e., integration and translocation (88). Modern Cre proteins have the further advantage of being Tamoxifen inducible, and are then termed Cre-ERT (91). These enzymes are activated only when tamoxifen is present, i.e., they cut at *Lox* sites in the presence of the drug, while endogenous estrogen is not sufficient to activate Cre (89). By using this technique, specific knockout is possible, e.g. the PTCH1-receptor in all cells expressing the *Col1a2*-promoter by Tamoxifen application (27). As a result of this inducible knockout of *PTCH1*, the Hh pathway can be activated permanently at any desired point in time (89, 92).

***Col1a2CreER;Ptch$^{+/fl}$*:** As a double-transgenic mouse model of stromal activation of the Hh pathway, *Col1a2CreER;Ptch$^{+/fl}$* (termed *Col1a2;Ptch$^{+/fl}$* in the following) were generated. In this model, a tamoxifen-inducible Cre recombinase is expressed under a Collagen1a2 promoter, which is active in the majority of subepithelial and lamina propria fibroblasts (89). A fibroblast-specific expression site and a minimal promoter of the *Col1a2* gene regulate the expression of tamoxifen-inducible Cre, followed by a polyadenylation signal (89, 93). *Ptch1$^{+/fl}$* mice bear *loxP* sites around exon 2 of one *Ptch1* allele (92). Tamoxifen administration leads to Cre activation and thus site-specific recombination at *LoxP* sites, effectively creating a *Ptch1* knockout (by "floxing", hence the ^{fl} in the model's denomination) exclusively in *Col1a2* expressing cells by removing *Ptch1* exon 2 (Figure 3; ref. 27).

Col1a2;Ptch$^{+/fl}$ mice were generated by crossing *Col1a2CreER mice* (B6.Cg-Tg[Col1a2-cre/ERT]7Cpd/J, The Jackson Laboratory, Bar Harbor, USA; ref. 89) with Ptch1neo[Δ]Ex2[Δ] mice (27, 92).

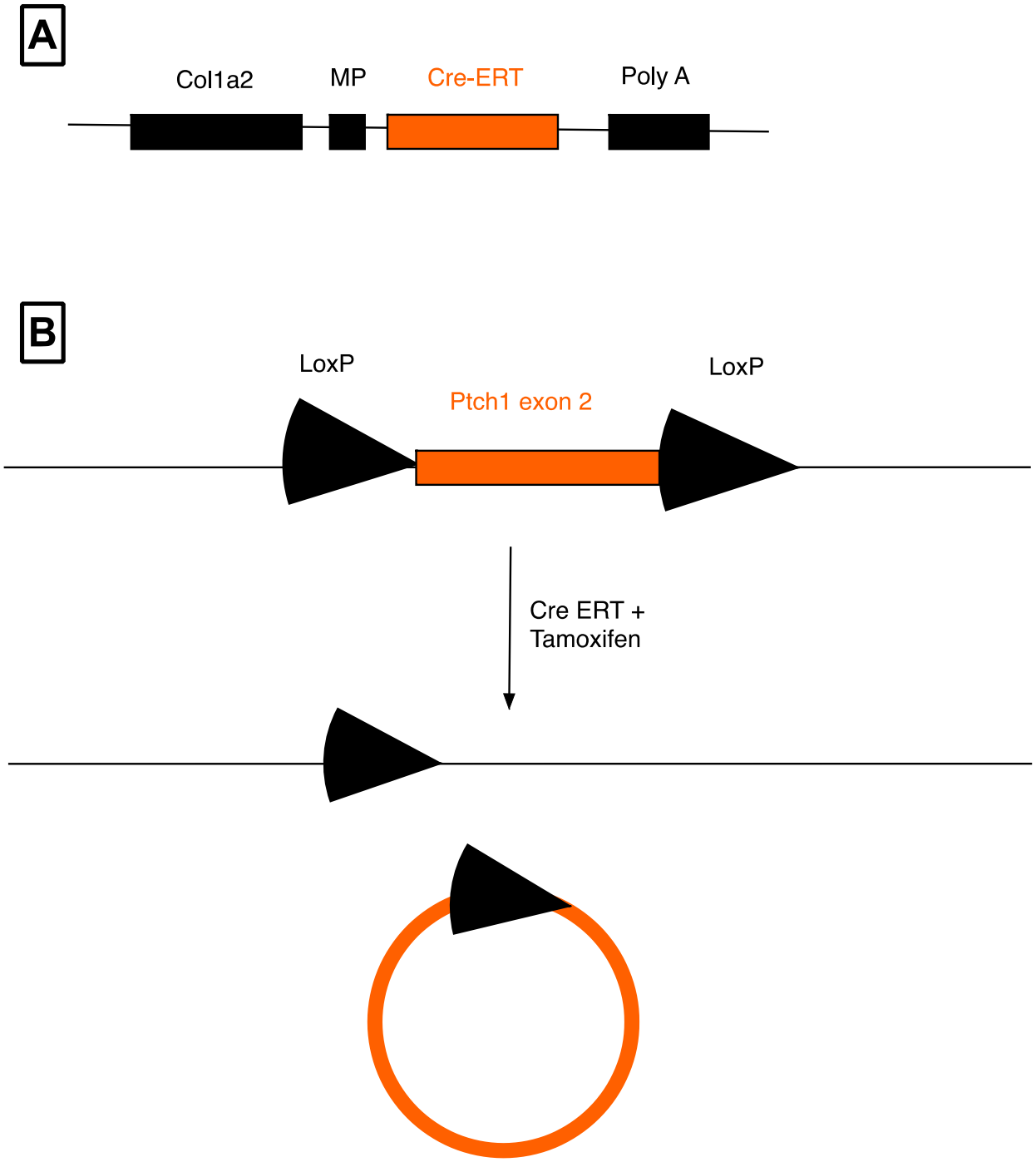

Figure 3: Schematic overview (adapted from ref. 89, 93) showing inducible heterozygous knockout of Ptch1 exon 2 in Col1a2;Ptch$^{+/fl}$ mice. A) Tamoxifen-inducible Cre recombinase (Cre-ERT) is expressed under a collagen 1a2 promoter. B) Activation of Cre-ERT by Tamoxifen leads to deletion of Ptch1 exon 2 by homologous recombination of similarly oriented LoxP sites (black arcs); the deleted DNA becomes a circular fragment and gets abolished (bottom). MP: Minimal promoter; Poly A: Polyadenylation signal

Genotype	Termed as	Genetic alteration	Effect	Reference
C57BL/6	WT	none (Wildtype)		
Gli1$^{+/lacZ}$	*Gli1*^{LacZ}	knock-in of bacterial *lacZ* gene (encoding β-galactosidase) to *Gli1*	Lack of one functional copy of *Gli1;* Readout of *Gli1* expression by X-Gal staining	(85)
Col1a2CreER;Ptch$^{+/fl}$	*Col1a2;Ptch*$^{+/fl}$	Tamoxifen inducible Cre recombinase under Collagen1a2 promoter; *loxP* sites around exon 2 of *Ptch1*	Knockout of *Ptch1* after Tamoxifen treatment, preferentially in fibroblasts	(89)

Table 8: Mouse models used in this study

DSS colitis model: The dextran sodium sulphate (DSS) model is a widely used murine model to mimic acute or chronic human IBD (79). DSS is an anionic, water-soluble, sulphated polymer that, upon ingestion, forms vesicles with medium-chain length fatty acids in the colon (80). Those vesicles are able to enter the cytoplasm of colonic epithelial cells, a process that hypothetically activates pro-inflammatory pathways (80). Typically, after three to five days, mice start to present with symptoms of colitis, e.g., diarrhea, bloody stools and weight loss (81). Additionally, an upregulation of pro-inflammatory cytokines can be seen (81). DSS colitis is characterized by mucosal lesions with mixed-cellular mucosal and submucosal inflammation as well as crypt loss, especially in the distal colon (80). Histological and clinical characteristics resemble those of human IBD, notably those of UC (82). Hh signaling seems to shape the inflammatory activity in DSS-induced IBD in mice through GLI1 (25). It has been shown that DSS-induced colitis leads to intestinal fibrosis in mice (83). Azoxymethane (AOM), an alkylating agent used in combination with DSS as a model of inflammation-driven carcinogenesis (94), has been administered intraperitoneally (i.p.) to some mice in experiments that evaluated the effect of Hh signaling on colonic carcinogenesis. While multiple tumors develop in the AOM/DSS model throughout the colon, large areas of the intestinal epithelium are devoid of neoplastic or dysplastic changes (95, 96). In a subset of experiments, we took advantage of this fact to analyze fibrosis in chronic colitis of the AOM/DSS model, which at the same time reduced the number of laboratory mice used.

Tamoxifen: To activate Cre recombinase in *Col1a2;Ptch*$^{fl/fl}$ mice, 5 mg Tamoxifen dissolved in corn oil (sonication at 37°C) was administered intraperitoneally at the experimental starting point. For topical activation of the Cre-Lox-System in the colon, 4OH-Tamoxifen was dissolved in 99.5 % ethanol (27). After vortexing, oil was added, and the suspension was sonicated in a water bath at 37°C for 30 min. In total, 1 mg 4OH-Tamoxifen per 25 g body weight was applied to the murine colon, using a flexible plastic gavage needle.

Vismodegib (GDC-0449): A small-molecule antagonist of Hh signaling, acting by inhibiting SMO (77; see Figure 1). GDC-0449 was injected intraperitoneally (25 mg per kg body weight, dissolved in dimethyl sulfoxide [DMSO]) twice daily, six days per week (27).

3.2.2 Histological methods

Formalin-fixed, paraffin-embedded (FFPE) tissue: In brief, freshly harvested colon samples were fixed overnight (4 % PFA in 1x PBS at room temperature), cut longitudinally, dehydrated in 70 % ethanol, cleared in xylene, embedded in paraffin and cut in four µm thick sections following a standard procedure. Processing of FFPE tissue and H&E staining was performed by ZeMAC histoanalys AB, Huddinge, Sweden.

Hematoxylin & Eosin (H&E) staining: A bichromatic staining method, which is one of the most common histological stains, was performed according to a standard protocol (97) on FFPE tissue.

LacZ ("X-Gal") staining: X-Gal staining is a histochemical method to visualize *lacZ* activity making use of the *Escherichia Coli lacZ* gene, which encodes for the bacterial enzyme β-galactosidase (β-gal) that catalyzes the hydrolysis of β-galactoside into monosaccharides (87). For staining purposes, the β-galactoside X-Gal (5-bromo-4-chloro-3-indolyl-beta-D-galactopyranoside) is cleaved by β-gal into galactose and 5-bromo-4-chloro-3-hydroxyindole. Oxidation of the latter one leads to blue-colored 5,5-dibromo-4,4-dichloro-indigo, which can be seen in brightfield microscopy (87).

Using this approach with transgenic *Gli*$^{/LacZ}$ reporter mice allows the assessing of *lacZ* positivity as readout of gene expression (87). LacZ staining was conducted according to a modified previously published protocol (98).

Briefly, to perform (whole-mount) X-Gal staining, freshly obtained colon samples were fixated for one hour at room temperature in X-Gal fixative (Table 4). Thereafter, samples were washed twice gently in X-Gal rinse buffer (Table 4). Next, samples were put in pre-warmed (37°C, 1 hour) X-Gal staining solution (Table 4) and incubated at 37°C for 24 hours. After two washing steps

with rinse buffer, samples were carried over for fixation in cold 4 % PFA in 1x PBS for four hours at room temperature, and finally dehydrated in 70 % ethanol. After paraffin embedding, the samples were sectioned, counterstained with eosin and mounted with a water-based mounting medium between cover slips.

Sirius Red staining: Sirius Red is an anionic dye bearing sulphonic acid groups that are able to react with basic groups of collagen fibers and is a widely used histochemical method for staining collagen I, II and III molecules (99). In polarized light microscopy, collagen type I fibers show a yellow-red birefringence, whereas collagen type III fibers appear greenish (100).

FFPE tissue was cut into 4 µm thick slices, dried overnight and incubated for 40 min. at 60°C right before staining. After deparaffinization (3 x 5 min. in xylene) and rehydration (in 100 %, 96 %, 70 % ethanol, two min. each; followed by one min. in tap water), specimens were incubated for one hour in 0.1 % Sirius Red solution adjusted to pH 2. Differentiation was carried out in 0.01 % 1N Hydrochloric acid (HCl) for two min. and slides were washed for one min. with tap water. After dehydration in ascending ethanol series (70 %, 96 %, 100 %, three changes; two min. each) and clearance in xylene (3 x 5 min.), samples were mounted between cover slips.

3.2.3 Measurement of *lamina muscularis mucosae*

The assessment of the thickness of the *lamina muscularis mucosae* as a readout of intestinal fibrosis in a murine model has been described before (83). We determined the thickness of the *lamina muscularis mucosae* on micrographs of H&E stained slides. Pictures were obtained on an Olympus BX50 DIC/Nomarski microscope with an attached Olympus DP25 digital camera. Measurements were performed on three different, randomly chosen areas (400-fold magnification) using the CellSense software measuring tool, and the arithmetic mean per sample was calculated. Measurements were performed blinded to genotype and treatment group.

3.2.4 Collagen quantification

To quantify fibrosis by means of collagen deposition, pictures of Sirius Red stained slides were obtained using a Pannoramic MIDI II slide scanner. Analysis of the scanned images was performed using ImageJ and the 3DHISTECH PannoramicViewer software. The relative area of fibrosis was determined by measuring the relative area of Sirius Red stained collagen fibers. To do so, a freely available Plugin for ImageJ (MRI Fibrosis Tool by Gabriel Landini, http://dev.mri.cnrs.fr/projects/imagej-macros/wiki/Fibrosis_Tool) was used with preset threshold settings. The application of that approach to determine the amount of fibrosis in various organ systems has been described previously (101-103). Five randomly picked image sections were acquired (100-fold magnification) per scanned sample. After selection of the respective region of interest (all layers or *lamina muscularis mucosae* alone) the MRI Fibrosis tool was applied. The

measured area of fibrosis was expressed relative to the whole area analyzed. Measurements were performed in a blinded manner.

3.2.5 Small animal ultrasound

Mouse US was performed using a VisualSonics Vevo 2100 LAZR Imaging station as described above (104). Under volatile anesthesia (adjusted to a continuous supply of approximately 0.5-1.5 % v/v isoflurane with medical air), a customary topical depilatory cream was applied to the abdominal region for hair removal. Vital signs of the animal were monitored continuously, and animals were placed on a heated plate. After application of US gel, image acquisition was performed in B-Mode at 40 MHz on mice in a supine position. To enhance intraluminal contrast, US gel was gently applied to the colon, using a rectally inserted flexible plastic gavage tube. Measurement of colon wall thickness was done three times for different positions of the mice (proximal, middle and distal colonic regions) using VisualSonic Vevo software, and the arithmetic means were calculated. The utilization of mouse US to determine colon wall thickness has been reported previously (105), and the method showed an increase in colon wall thickness upon chemically induced colitis, which correlated with the severity and progression of colitis as well as with clinicopathological parameters (106, 107). It has been shown in rats that both DSS and trinitrobenzenesulfonic acid (TNBS, another chemical agent used for colitis induction in rodents) induce colitis, leading to changes in colon wall thickness which can be determined sonographically (107, 108). A representative US picture can be seen in Figure 4.

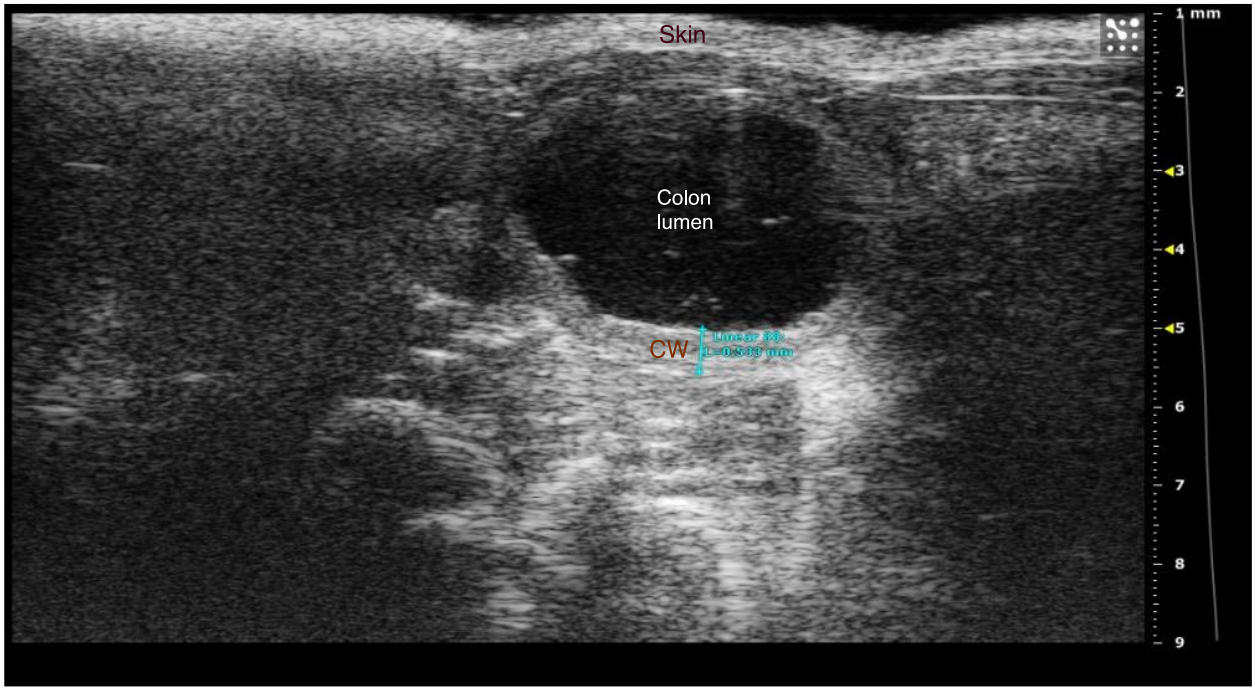

Figure 4: Representative US (B-Mode) picture of murine colon. CW: Colon wall; measurement (performed with Vevo software) showing a colon wall thickness of 0.533 mm

3.2.6 Colitis activity

To evaluate the inflammatory activity during the course of colitis, the body weight was measured daily. The consistency of feces and of passed blood was monitored on a daily basis. If applicable, the entire colon length was measured upon necropsy, since shortening of the colon has been described as a feature of acute DSS colitis (109).

For histological evaluation of colitis severity, a previously described histological scoring system was used with slight modifications (80). On H&E stained slides, histological alterations due to inflammation were assessed and scored (Table 9). Longitudinally cut colon samples were evaluated and a respective score was assigned to the most severe finding. A total histological score was calculated by summing the respective scores for inflammation and epithelial damage.

Score	Inflammation	Epithelial damage
0	rare inflammatory cells in lamina propria	no crypt damage
1	increased number of granulocytes in lamina propria	loss of basal one-third of crypts
2	confluence of inflammatory cells into the submucosa	loss of basal two-third of crypts
3	transmural inflammation	entire crypt loss
4		epithelial erosion
5		confluent erosion

Table 9: Histological scoring system for evaluation of colitis (extent of inflammation and epithelial damage)

3.2.7 Isolation of RNA

A total of 20-30 mg of fresh frozen (-80°C) colonic tissue was disrupted using a VDI 12-Homogeniser and 600 µl RLT-Lysis-Buffer per sample. To eliminate ribonuclease activity during this process, 60 µl 2-Mercaptoethanol was added to every sample. After centrifugation of the lysate (3 min., full speed), insoluble cellular material was discarded and the supernatant was removed by pipetting, transferred to a new reaction tube and an equal volume of 70 % ethanol was added. From that mixture, an aliquot of a maximum 700 µl was carried over to a spin column fixed in a 2 ml collection tube. Several steps of centrifugation (15 s at 8000 x g) were performed and the flow-through was discarded, until no liquid was left. Subsequently, RNase digestion was performed (RNase-Free DNase Set) according the producer's protocol. Thereafter, 500 µl RPE-Buffer was

added twice to the spin columns, which were centrifuged for 15 s and 2 min., respectively, at 8000 x g, with discarding of the flow-through. To elute ribonucleic acid (RNA), the spin columns were placed in a new 1.5 ml collection tube, 45 µl RNase free water was added and it was centrifuged for 1 min. at 8000 x g. To determine the concentration and purity of the eluted sample-RNA, 2 µl was measured with a TECAN Infinite® M200 PRO NanoQuant spectrometer. After blanking, the total RNA concentration per sample was calculated by the spectrometer software as follows:

RNA concentration (ng/µl) = absorbance at 260 nm x 1000 (ng/µl)

To receive an estimate of RNA quality, the ratio of absorbance measurements at 260 nm (for nucleic acids) and 280 nm (for proteins) (OD260/OD280) was calculated. RNA with a ratio between 1.9 and 2.1 was considered pure (110).

3.2.8 Generation of cDNA

Since direct amplification of mRNA by PCR is not possible, generation of complementary DNA (cDNA) is required. This process, named reverse transcription, is executed by the enzyme reverse transcriptase (RT), derived from Moloney murine leukemia virus (111). Reverse transcription of mRNA was performed by using a SuperScript® III Reverse Transcriptase-Kit. In the first step, a Reverse Transcription Master-Mix (+RT) was prepared (Table 10).

4 µl 5X First Strand Buffer
1 µl RNase Inhibitor Human Placenta
1 µl 0.1 M DTT
1 µl SuperScript III Reverse Transcriptase (200 units/µl)

Table 10: Reverse Transcription Master-Mix, amounts per sample

To generate non-template controls (NTCs), another Master-Mix (-RT) was prepared, in which the reverse transcriptase was substituted by 1 µl RNase free water.

Afterwards, two (template and NTC) reaction mixtures per sample were prepared in separate 0.2 ml PCR-tubes (Table 11).

1 µl Deoxynucleotide (dNTP) Solution Mix
1 µl Oligo(dT)$_{12-18}$ Primer (0.5 µg/µl)
2.5 µg total RNA
RNAse free water *ad* 13 µl

Table 11: Reverse Transcription reaction mixture, per tube

The amount of RNase free water (dH_2O) was calculated as follows: *Amount of dH_2O = 13 µl (total amount per tube) – 1 µl dNTP mix - 1 µl Oligo(dT)$_{12-18}$ Primer – template RNA (amount of sample containing 2.5 µg total RNA)*

After incubation (5 min. at 65°C, 1 min. on ice) 7 µl Master-Mix (with reverse transcriptase or water, respectively) was added per template or NTC. Subsequent reverse transcription was

performed by using a MJ Research PTC-200 Peltier Thermal Cycler. The cycler program was set up at 55°C for 50 min.

3.2.9 Semi-quantitative real-time PCR

We applied a fluorescence-based semi-quantitative real-time PCR to analyze gene expression by means of the amount of mRNA. During the exponential phase of the performed PCR, the fluorescent dye SYBR green I intercalates with (previously generated) double-strand cDNA, thereby increasing fluorescence (112). With the increase of double-stranded cDNA, the fluorescence signal increases as well (113). The cycle in which the fluorescent signal rises significantly over the background is termed cycle threshold (CT; ref. 113). Applying the delta-CT method (see below) enables us to quantify gene expression in a semiquantitative manner (113, 114). Real-time PCR was performed with a 7500 Fast Real-Time PCR System according to the manufacturer's protocol. A proprietary Power SYBR® Green PCR Master-Mix was used, according to the manufacturer's product bulletin consisting of SYBR® Green I Dye, AmpliTaq Gold® DNA Polymerase, dNTPs, buffer components and ROX as passive reference dye. Initially, a reaction mixture was prepared for triplicates of every gene of interest (Table 12).

13 µl SYBR Green Master Mix
16 µl dH_2O
0.25 µl Forward-Primer
0.25 µl Reverse-Primer

Table 12: Real-Time PCR reaction mixture, x amount of required samples/NTCs

Afterwards 0.5 µl template cDNA (or non-template controls, respectively) was added, giving a total volume of 30 µl, which was aliquoted into a PCR reaction plate, receiving a reaction volume of 10 µl per well. Analysis was performed with three technical replicates per sample.

Determination of semiquantitative mRNA expression was carried out by applying the delta CT (ΔCT) method (115) to the arithmetic means of the three technical replicates per sample. At first, CT values from a housekeeping gene (*Arp*) were subtracted from the CT values of target genes ($\Delta CT = CT_{\text{target gene}} - CT_{\text{housekeeping gene}}$). Then, the ΔCT of different groups of interest was set in relation to control groups to gain ΔΔCT-Values ($\Delta\Delta CT = \Delta CT_{\text{Treated}} - \Delta CT_{\text{control}}$). Exponential ΔΔCT-values were normalized and expressed as n-fold changes in mRNA-expression (n-fold change= $2^{-\Delta\Delta CT}$). PCR experiments were in part performed by Mr. Leonard Kirn.

3.3 Statistics

For statistical evaluation, the arithmetic mean and standard error of the mean (SEM) of technical replicates was calculated. Statistical tests were performed using GraphPad Prism 7 software. To determine the level of significance, an unpaired Student's *t*-test (*t*-test), multiple *t*-test or analysis

of variance (ANOVA; ref. 116) were used, where applicable. Post-hoc analysis for the false discovery rate (FDR) was performed using the two-stage linear step-up procedure of Benjamini, Krieger and Yekuteli (117). A p-value ≤0.05 was considered significant, and a p-value ≤0.001 as highly significant. Correlation (ρ) was determined by Spearman's rank correlation coefficient. Results are shown in graphs with error bars representing SEM or box-whisker plots with whiskers going from the minimal to maximal value.

3.4 Experimental setups

3.4.1 Experiment A – Chronic colitis in *Gli*^{LacZ} mice

In the *Gli1*^{LacZ} group, DSS was applied to the drinking water at a concentration of 2 %. A higher concentration has been shown to be associated with increased morbidity and mortality in mice bearing that genotype (25). Initially in this cohort, AOM was injected i.p. at day 0 at a concentration of 12.5 mg per kg bodyweight. DSS application started at day 5 and continued for five consecutive days, followed by two weeks of normal drinking water as described previously (118). The regimen was repeated twice. US measurements of the bowel wall were performed at days 84 and 129. Mice were sacrificed at the earliest at day 137, when chronic colitis had developed. For a schematic overview of the experimental setup see Figure 5.

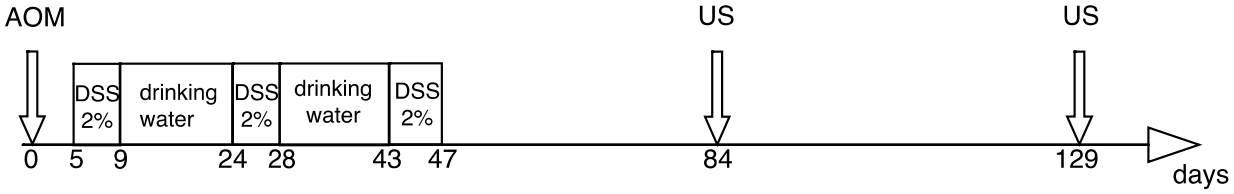

Figure 5: Schematic experimental setup in Gli1^{LacZ} *mice and controls (experiment A). DSS: dextran sodium sulphate; US: ultrasound*

3.4.2 Experiment B – Acute colitis in *Col1a2;Ptch*$^{+/fl}$ mice

Transgenic *Col1a2;Ptch*$^{+/fl}$ mice (n=7) bearing an inducible knockout of *Ptch1* (encoding for the Hh repressor PTCH1) in *Col1a2* expressing cells received an intraperitoneal injection of Tamoxifen at day 0, leading to activation of Cre recombinase, *Ptch1* knockout in *Col1a2* expressing fibroblasts and consequently an upregulation of the Hh pathway (27). Acute colitis was induced by application of one course (five consecutive days) of 3 % DSS, starting one week after Tamoxifen administration. Age-matched mice without Cre recombinase (n=7) served as controls and received similar treatment with Tamoxifen and DSS. Additionally, non-DSS-treated control mice (n=7) were used. Mice were sacrificed one week after DSS treatment ended. A schematic overview is depicted in Figure 6. Control mice had either no Cre recombinase, or no floxed alleles or both.

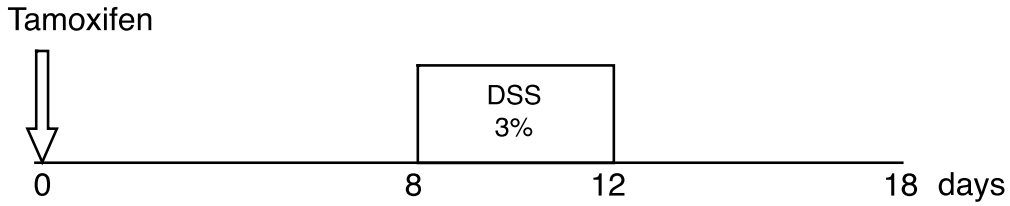

Figure 6: Experimental setup of acute colitis in Col1a2;Ptch$^{+/fl}$ mice (experiment B)

3.4.3 Experiment C – Chronic colitis in *Col1a2;Ptch$^{+/fl}$* mice

To assess the effect of pharmacological Hh inhibition on fibrosis in chronic colitis, five differently treated groups of mice were analyzed (Table 13). The groups consisted of either *Col1a2;Ptch$^{+/fl}$* transgenic mice (lacking one *Ptch1* allele and therefore exhibiting increased Hh signaling after Tamoxifen treatment) or controls. Pharmacological intervention was carried out by applying Vismodegib (Hh-inhibitor acting on SMO) or DMSO as vehicle control.

Where applicable (Table 13), 4-Hydroxytamoxifen (4-OH-Tamoxifen) was given at day 0 to induce Cre recombinase, leading to deletion of one *Ptch1* allele in *Col1a2;Ptch$^{+/fl}$* mice. Notably, 4-OH-Tamoxifen was applied intrarectally to ensure topical activation of Cre recombinase in the colon and reduce systemic recombination (27). To control for possible effects of Tamoxifen, one group of control mice received Tamoxifen treatment. AOM was given i.p. as described above, and 5 days after AOM treatment, all mice started a course of 2 % DSS for five days, followed by 14 days with normal drinking water. That regimen was repeated twice, and US was performed after termination of the last cycle. Depending on the assigned study group, mice received an intraperitoneal injection twice daily of either the SMO inhibitor Vismodegib (GDC-0449; 25 mg per kg body weight, dissolved in DMSO) or vehicle for six days per week (Figure 7). Mice were sacrificed at day 72.

Group	Transgene / control	4-OH-Tamoxifen treatment	Vismodegib / vehicle	n=
A	*Col1a2;Ptch$^{+/fl}$*	1 mg / 25g body weight	Vehicle	13
B	*Col1a2;Ptch$^{+/fl}$*	1 mg / 25g body weight	Vismodegib	9
C	Control	None	Vismodegib	10
D	Control	1 mg / 25 g body weight	Vehicle	11
E	Control	None	Vehicle	16

Table 13: Experimental setup of differently treated cohorts (chronic colitis in Col1a2;Ptch$^{+/fl}$ mice; experiment C)

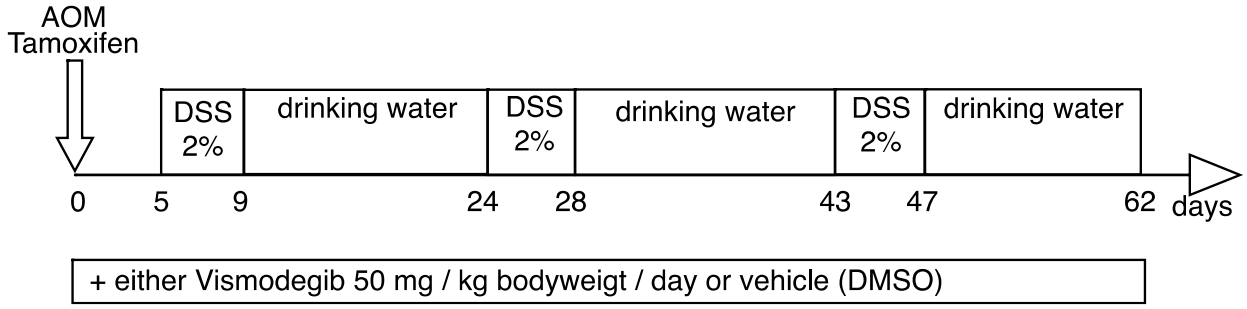

Figure 7: Scheme of treatment regimen (experiment C) in mice that received AOM i.p., 4OH-Tamoxifen rectally, three courses of 2 % DSS for colitis induction and either Vismodegib or vehicle treatment

4. Results

4.1 Colitis activity in a DSS model of chronic colitis

A scoring system to assess the colitis activity histologically (on *post-mortem* samples) was applied to the experiments using a chronic model of DSS colitis.

4.1.1 Experiment A – Colitis activity in Gli^{LacZ} mice with genetically inhibited Hh signaling

When comparing Gli^{LacZ} mice and controls, a statistically significant difference was observed, in that control mice exhibited higher colitis activity (mean score in Gli^{LacZ}: 1.4 ± 0.3; mean score for controls: 2.6 ± 0.4; n=7 in each group; p=0.0489, unpaired *t*-test; Figure 8). There was no significant difference in body weight during the course of colitis (p>0.05; multiple *t*-test) between Gli^{LacZ} mice and wildtype controls.

Histologically, Gli^{LacZ} mice and their respective controls (all received three cycles of DSS and were sacrificed at least 90 days after DSS treatment ended) showed a mild chronic colitis. Inflammatory cells were predominantly of mononuclear nature, and only one mouse showed an increased number of neutrophilic granulocytes in the *lamina propria.* Assessment of the crypts of Lieberkühn revealed crypt loss or evidence of epithelial regeneration with crypt branching or shortening. Crypt shortening was defined as an increased gap between the crypt base and *lamina muscularis mucosae* (79, 82). Whereas crypt shortening affected the vast majority of crypts in both cohorts, in Gli^{LacZ} mice on average 0.16 and in wildtype mice 0.09 branched crypts per high-power field (400-fold magnification) were counted. Representative micrographs are shown in Figure 10.

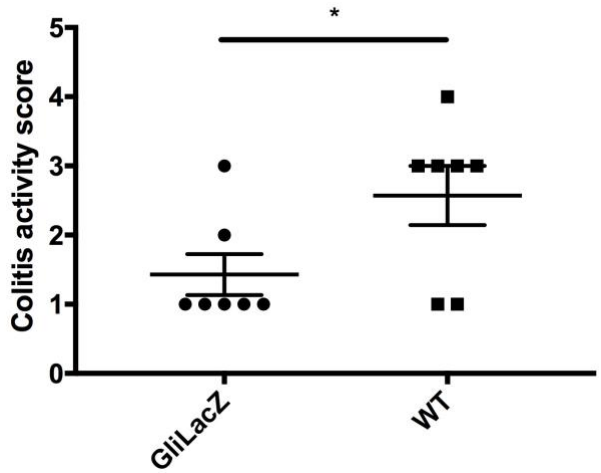

*Figure 8: Histological colitis activity score for Gli^{LacZ} and control mice (experiment A). * denoting a statistically significant difference (p≤0.05)*

4.1.2 Experiment C – Colitis activity in $Col1a2;Ptch^{+/fl}$ mice with genetically activated Hh signaling

We compared the histological colitis activity in $Col1a2;Ptch^{+/fl}$ mice with genetically induced activation of stromal Hh signaling to controls in several control groups, and upon Vismodegib treatment (Table 13). All mice received three cycles of DSS and were sacrificed 24 days after the

last DSS cycle ended. Two different pharmacological interventions were applied. At the beginning of the experiment, Tamoxifen was administered to induce Cre recombinase in *Col1a2;Ptch*$^{+/fl}$ mice and controls (Figure 9 A). Furthermore, mice received either the Hh inhibitor Vismodegib or vehicle to assess whether any effect of *Ptch1* knockout in the stroma could be overcome by inhibition of the downstream receptor SMO. In parallel, two groups of WT mice were treated with Vismodegib or vehicle; these mice did not receive Tamoxifen (Figure 9 B), so as to assess the effect of Vismodegib treatment independent of Tamoxifen.

Neither in *Col1a2;Ptch*$^{+/fl}$ mice (with or without Vismodegib) and Tamoxifen treated controls (Figure 8 A; ANOVA with FDR), nor in WT mice treated with Vismodegib or vehicle (Figure 9 B; unpaired *t*-test), were statistically significant differences in histologic colitis activity scores seen.

In the *Col1a2;Ptch*$^{+/fl}$ cohort and controls, the histological changes were more severe and diverse than in *Gli*^{LacZ} mice and their respective controls. A cellular inflammatory infiltrate was mostly mononuclear or consisted of neutrophilic granulocytes within the *lamina propria,* but submucosal or transmural infiltration was detected in some mice. Furthermore, epithelial erosions, ulcerations and rare crypt abscesses were seen, and solitary lymphoid aggregates were numerous. Representative histological alterations are depicted in Figure 10. Rarely, multinucleated giant cells appeared, but granuloma formation was not noted.

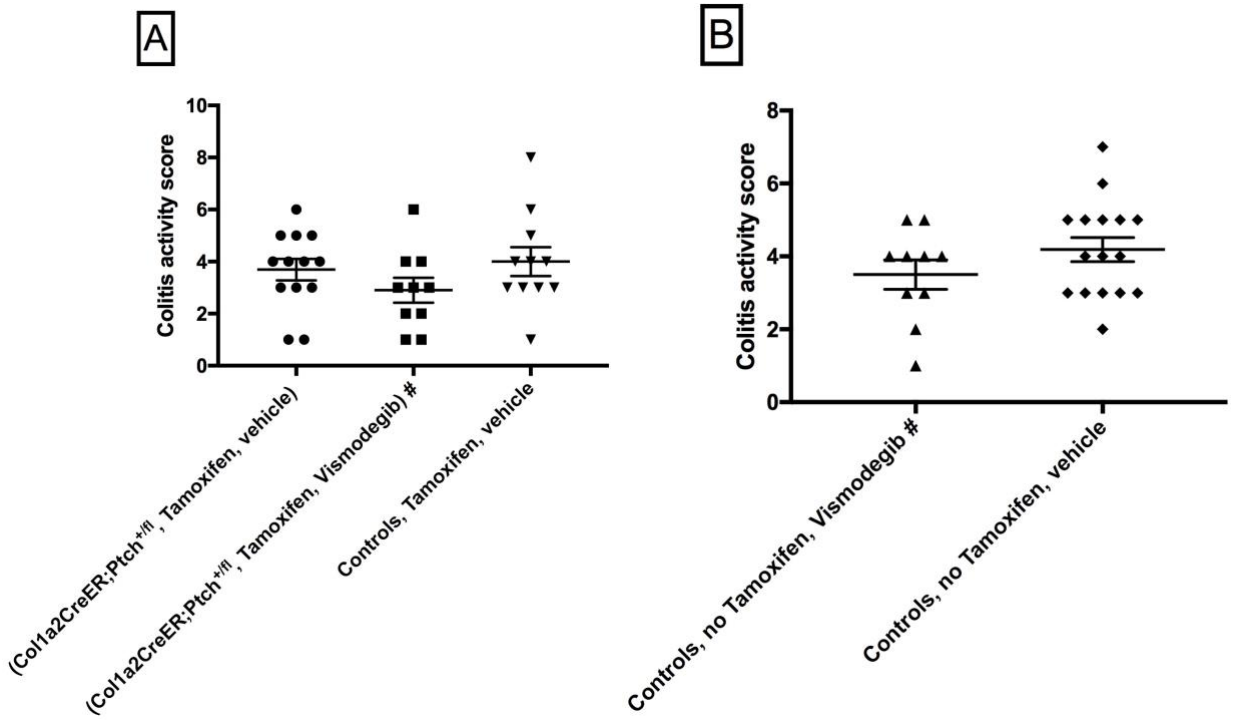

Figure 9: Histological colitis activity score (experiment C) for: A) Col1a2;Ptch$^{+/fl}$ *mice with Vismodegib or vehicle treatment and Tamoxifen-treated controls, B) Not Tamoxifen treated controls with Vismodegib or vehicle treatment. Mice with genetically activated Hh signaling in parenthesis, # denotes pharmacological Hh inhibition*

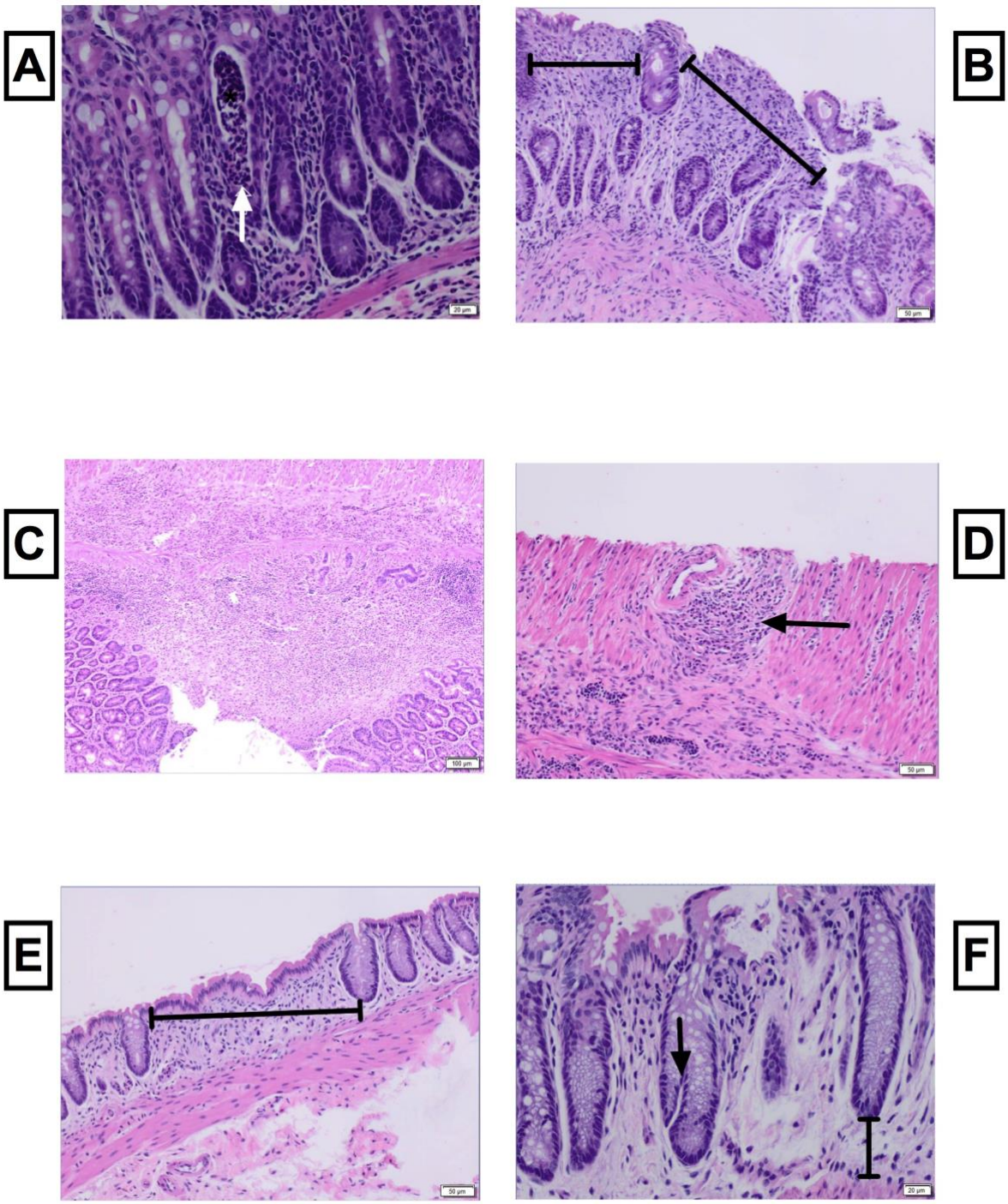

Figure 10: Representative images of histological findings in DSS-induced colitis (all H&E staining). A) Crypt abscess (white arrow; magnification 400-fold). B) Epithelial erosion and crypt loss (black bars; magnification 200-fold). C) Ulceration with mixed-cellular infiltrate affecting mucosa and submucosa (magnification 100-fold). D) Inflammatory infiltrate in muscularis propria (black arrow; magnification 200-fold). E) Crypt loss without signs of epithelial erosion (black bar; magnification 200-fold). F) Crypt branching (black arrow) and crypt shortening (black bar; magnification 400-fold)

4.2 Experiment A – Impact of mitigated Hh signaling on fibrosis in chronic colitis

To determine the effect of genetic Hh pathway inhibition on colonic fibrosis, *Gli1*$^{LacZ/LacZ}$ or *Gli1*$^{+/LacZ}$ mice (n=10, termed as *Gli1*^{LacZ} in the following), and C57BL/6 controls (n=7) were subjected to DSS-induced chronic colitis, after AOM injection at d0. Seven mice per group reached the experiment's endpoint.

4.2.1 Sonographic evaluation of colonic wall thickness

Colonic US was performed *in vivo* at two different time points after induction of chronic colitis (d84, d129). The thickness of the colonic wall as determined sonographically was used as a surrogate parameter for colonic fibrosis (107). Comparison of the mean colon wall thickness in *Gli1*^{LacZ} and control mice did not reveal a significant difference at either of the time points (d84: p=0.97; d129: p=0.4; multiple *t*-test; Figure 11 A). Means for the different time points and locations of measurements are shown in Table 14. Whereas colon wall thickness between early and late measurements correlated well in WT mice (ρ=0.943, p=0.017), the observed individual results per mouse were more heterogenous in *Gli1*^{LacZ} mice (ρ=-0.2, p=0.714). No US measurements were available for two mice at the later timepoint.

Time point / location	**Mean LacZ ± SEM [mm]**	**Mean WT ± SEM [mm]**	**p= (unpaired *t*-test)**
d84 proximal	0.369 ± 0.035	0.033 ± 0.026	0.401
d84 middle	0.3485 ± 0.022	0.357 ± 0.024	0.802
d84 distal	0.341 ± 0.029	0.341 ± 0.049	0.462
d129 proximal	0.338 ± 0.016	0.337 ± 0.015	0.954
d129 middle	0.303 ± 0.018	0.326 ± 0.026	0.482
d129 distal	0.330 ± 0.027	0.379 ± 0.029	0.264

Table 14: Mean values, SEM and p-values for US measurements at different time points (d84, d129) and locations (proximal, middle and distal colon; experiment A)

4.2.2 Histological evaluation of *lamina muscularis mucosae*

To assess if there was a successful deletion of one *Gli1* allele in *Gli1*^{LacZ} mice, we used X-gal staining on colonic tissue harvested right after euthanasia and determined β-gal activity in the colon exclusively in stromal cells, suggesting successful replacement of one *Gli1* allele with the lacZ gene (Figure 11 C).

On H&E-stained slides of colonic tissue, the diameter of the *lamina muscularis mucosae* was measured, and no significant difference between the two study groups was observed (mean *GliLacZ*: 30.4 µm ± 2.8 µm; mean controls: 27.7 µm ± 3.7 µm; p=0.564, unpaired *t*-test; Figure 11 B).

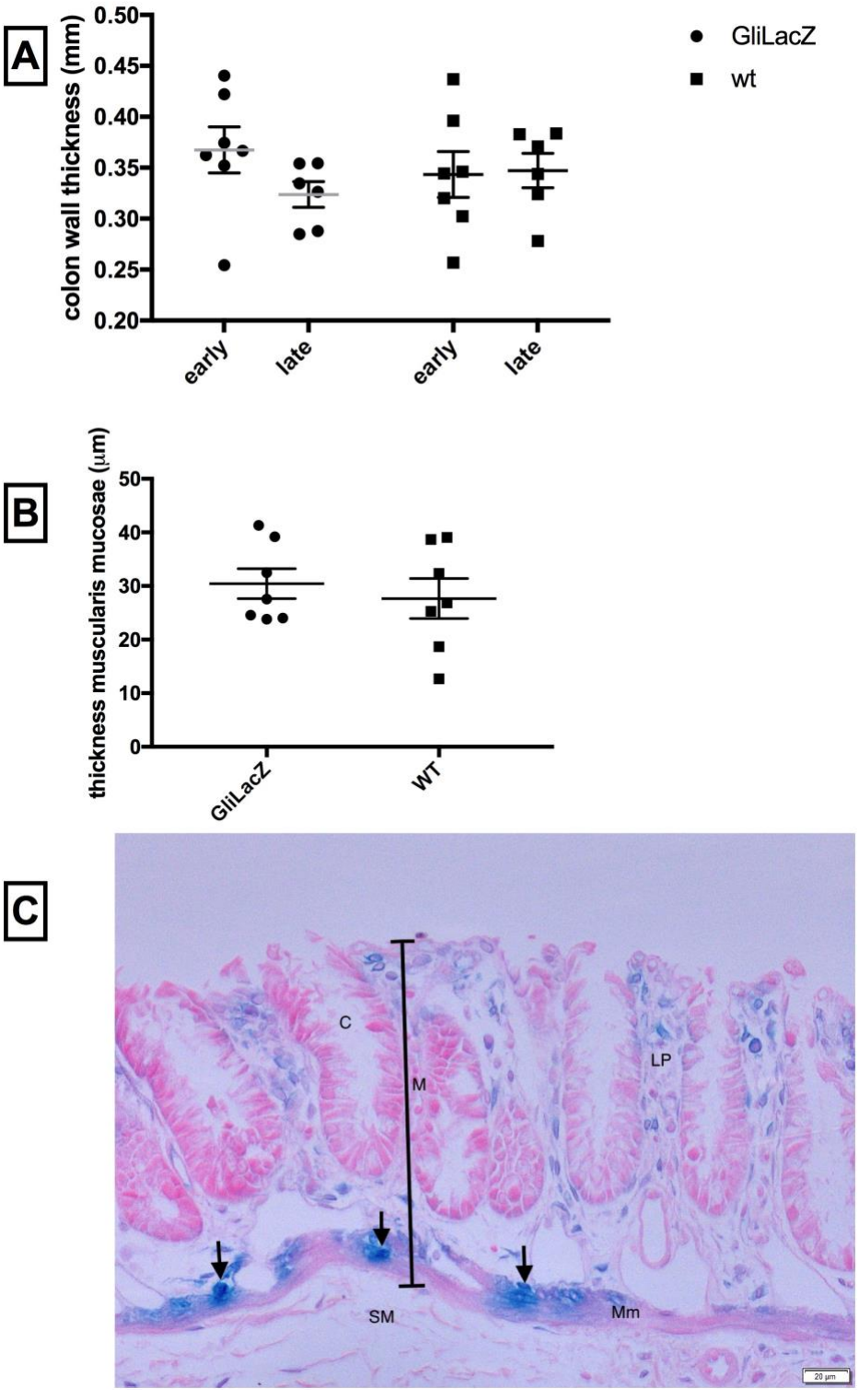

Figure 11: Experiment A – A) Colon wall thickness as determined by US at early (d84) and late (d129) time points. B) Histological evaluation of muscularis mucosae diameter in Gli1^{LacZ} and control mice. C) Representative picture showing X-gal stained cells in the lamina muscularis mucosae (arrows) and lamina propria; C: crypts of Lieberkühn, LP: lamina propria, M: mucosa, Mm: lamina muscularis mucosae, SM: tela submucosa (400-fold magnification, indicator bar: 20µm)

4.3 Experiment B – Impact of upregulated Hh signaling on fibrosis after acute colitis

4.3.1 Clinical parameters and colon length

There was no significant (p>0.05, multiple *t*-tests) difference in weight loss or clinical parameters (stool consistency, blood passing) between the two groups upon colitis-induction. *Post-mortem* evaluation revealed significantly decreased colon length in *Col1a2;Ptch*$^{+/fl}$ mice compared to DSS-treated controls (p=0.0127), and a highly significant difference between *Col1a2;Ptch*$^{+/fl}$ mice and age-matched controls that were not treated with DSS (p=0.0001, one-way ANOVA and multiple test correction [FDR, Benjamini, Krieger and Yekutieli]; Figure 12 A).

4.3.1 Histological evaluation of *lamina muscularis mucosae*

Histological assessment of the *lamina muscularis mucosae* diameter did not reveal any statistical significant difference (mean/SEM *Col1a2;Ptch*$^{+/fl}$: 143.2 µm ± 9.8 µm; mean/SEM controls: 174.3 µm ± 21.4 µm; p=0.2109, unpaired *t*-test; Figure 12 B) in DSS-treated mice with genetic Hh activation or controls.

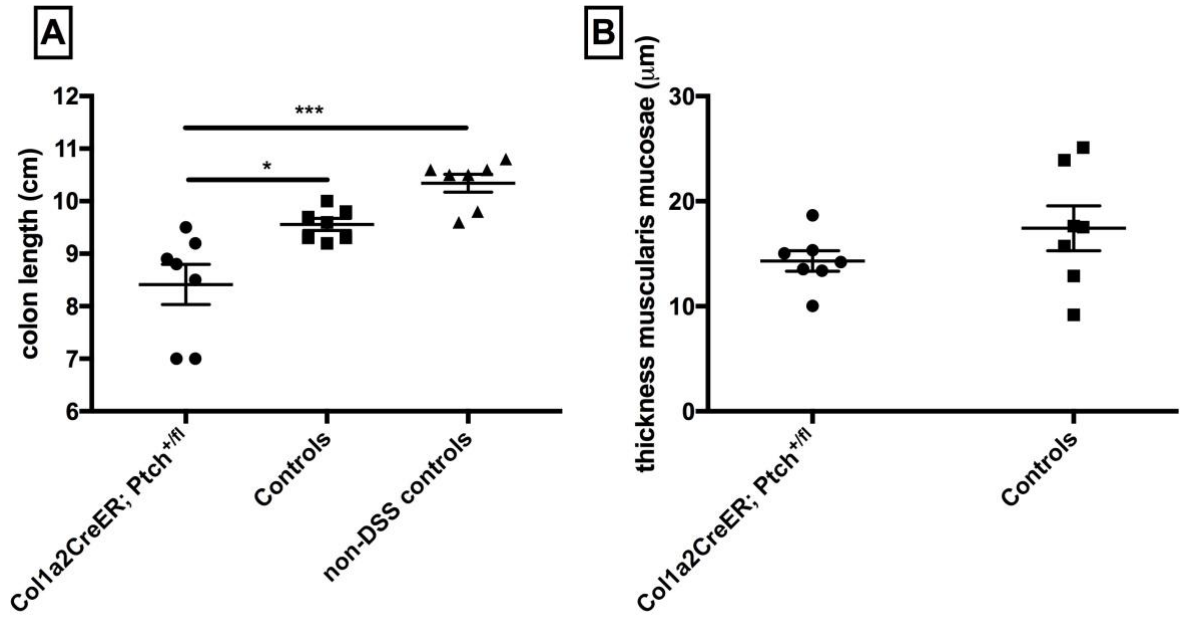

Figure 12: Experiment B – A) Colon length in DSS-treated mice and non-DSS controls measured upon necropsy. B) Histologically assessed thickness of lamina muscularis mucosae in Col1a2;Ptch$^{+/fl}$ *mice and controls. * denoting a statistically significant difference (p≤0.05), *** a highly significant one (p≤0.001)*

4.3.2 mRNA expression of Hh- and fibrosis-related genes

To assess the expression of Hh- and fibrosis-related genes after acute colitis, RT-PCR assays were performed and the relative mRNA expression between the two DSS-treated study groups was determined (Figure 13). A significantly different relative gene expression was detected in *Col1a2;Ptch*$^{+/fl}$ mice for *Gli1* (p=0.028), thereby confirming successful activation of downstream Hh signaling via *Ptch1*-knockout. The pro-fibrotic collagens *Col1a1* (Col1) and *Col3a1* (Col3) showed an increase in gene expression as well (p=0.044 and p=0.042 respectively, all multiple *t*-

test). An increase in expression levels in mice with stromal Hh activation was also seen for *Ptch1* and *α-SMA* (its gene *Acta2*,) while *Tgf-β*-levels showed a slight decrease, all without statistical significance.

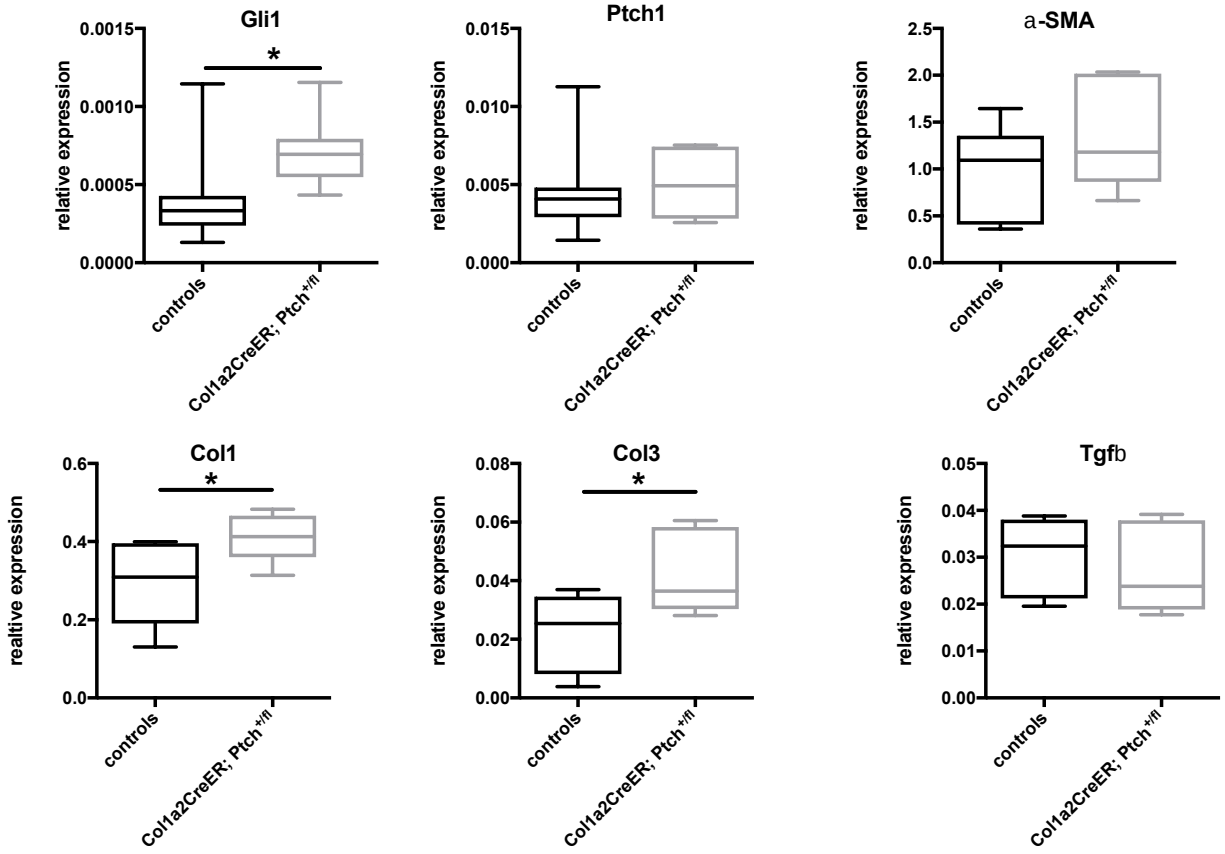

*Figure 13: Relative gene expression (compared to ARP as housekeeping gene) in Col1a2;Ptch$^{+/fl}$ mice and controls (experiment B). * denoting a statistically significant difference (p≤0.05)*

4.3.3 Assessment of Sirius Red stained collagen fiber deposition

To assess fibrosis by means of deposition of collagen fibers, Sirius Red stain was used on colonic tissue and the amount of fibrosis was quantified (for the whole colonic sample and *lamina muscularis mucosae*) using ImageJ software and a specific plugin. Tamoxifen-induced (5 mg i.p.) *Col1a2;Ptch*$^{+/fl}$ mice (n=6) and controls (n=7, with and without Tamoxifen injection) were challenged with acute colitis (one cycle of DSS 3 %, days 8-12). Mice were sacrificed at day 34.

No statistically significant difference (multiple *t*-test with FDR) was observed between *Col1a2;Ptch*$^{+/fl}$ mice and controls for the mean fibrotic area in the whole colonic sample examined (p=0.975) or in the *lamina muscularis mucosae* (p=0.469; Table 15, Figure 14).

In Figure 15, representative pictures of Sirius Red stained colonic samples (15 A) and the effect of applying the MRI Fibrosis Tool (15 B) are shown. A picture of collagen-typical birefringence under polarized light is shown for illustrative purposes (15 C).

	Mean fibrotic area [%] whole colonic sample	Mean fibrotic area [%] *lamina muscularis mucosae*
Col1a2;Ptch$^{+/fl}$ mice	21.17	61.53
Controls	21.27	58.12

Table 15: Mean values [%] for the fibrotic area in the whole colonic sample and lamina muscularis mucosae in Col1a2;Ptch$^{+/fl}$ *mice and controls, determined by Sirius Red staining (experiment B)*

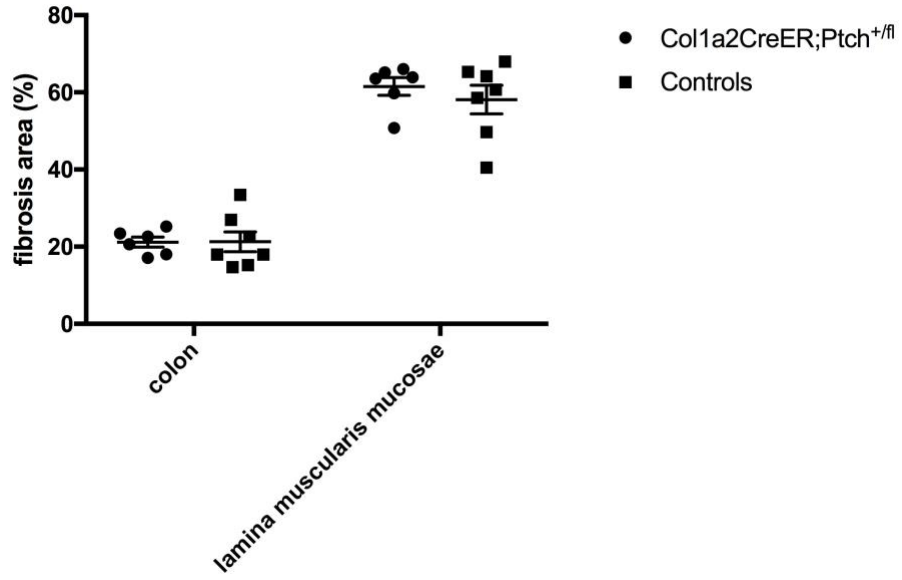

Figure 14: Quantification of fibrosis area in Col1a2;Ptch$^{+/fl}$ *mice and controls, shown for the whole colonic sample and lamina muscularis mucosae (experiment B)*

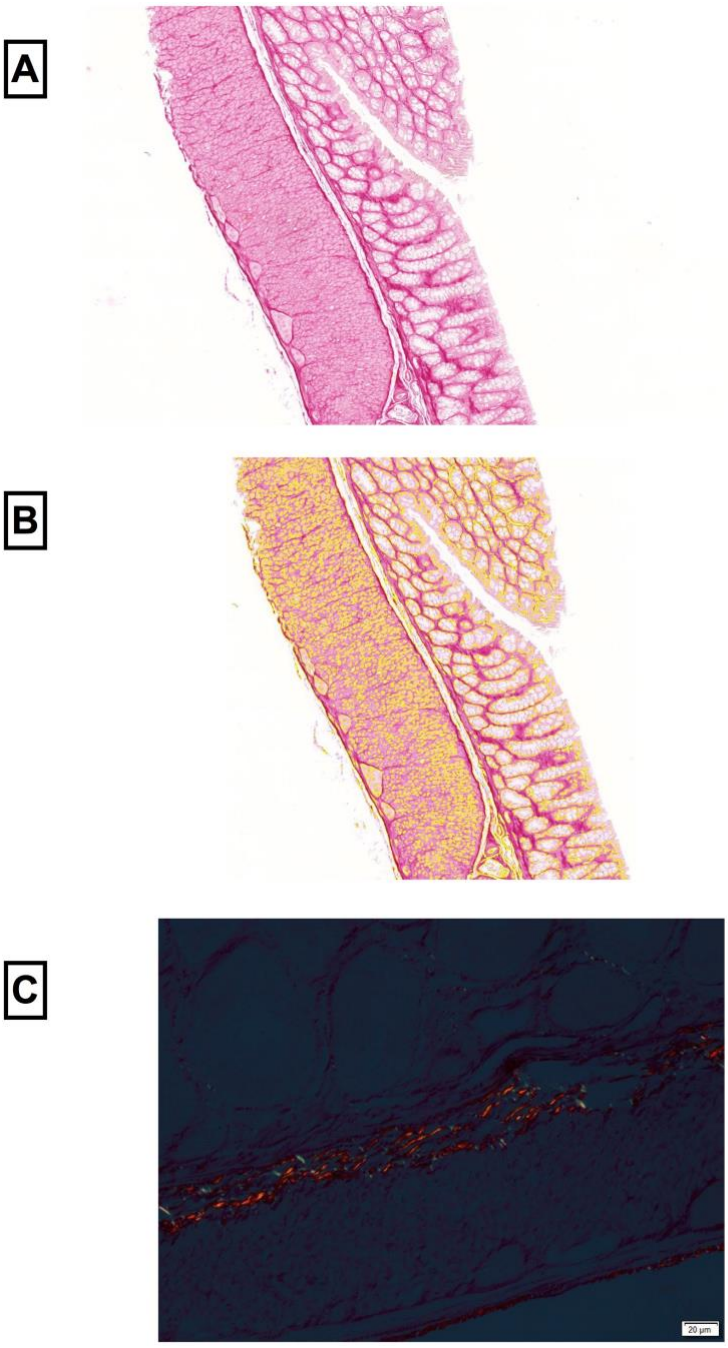

Figure 15: Sirius Red-stained murine colon: A) Representative micrograph of scanned slide, 100-fold magnification. B) Same picture after MRI Fibrosis Tool has been applied. C) Representative sample under polarized light, showing red-yellow birefringence, typical for collagen I (400-fold magnification, indicator bar: 20 µm)

4.4 Experiment C – Pharmacological inhibition of Hh activation and assessment of fibrosis

4.4.1 Sonographic evaluation of colon wall thickness

When comparing the average thickness of the colon wall as determined by US after termination of the last DSS cycle, no statistical significant difference was seen between the Tamoxifen-induced subgroups (*Col1a2;Ptch*$^{+/fl}$ with genetically activated Hh signaling and controls, with or without Vismodegib treatment; ANOVA with FDR, Figure 16A) and non-Tamoxifen injected controls (unpaired *t*-test, Figure 16 B).

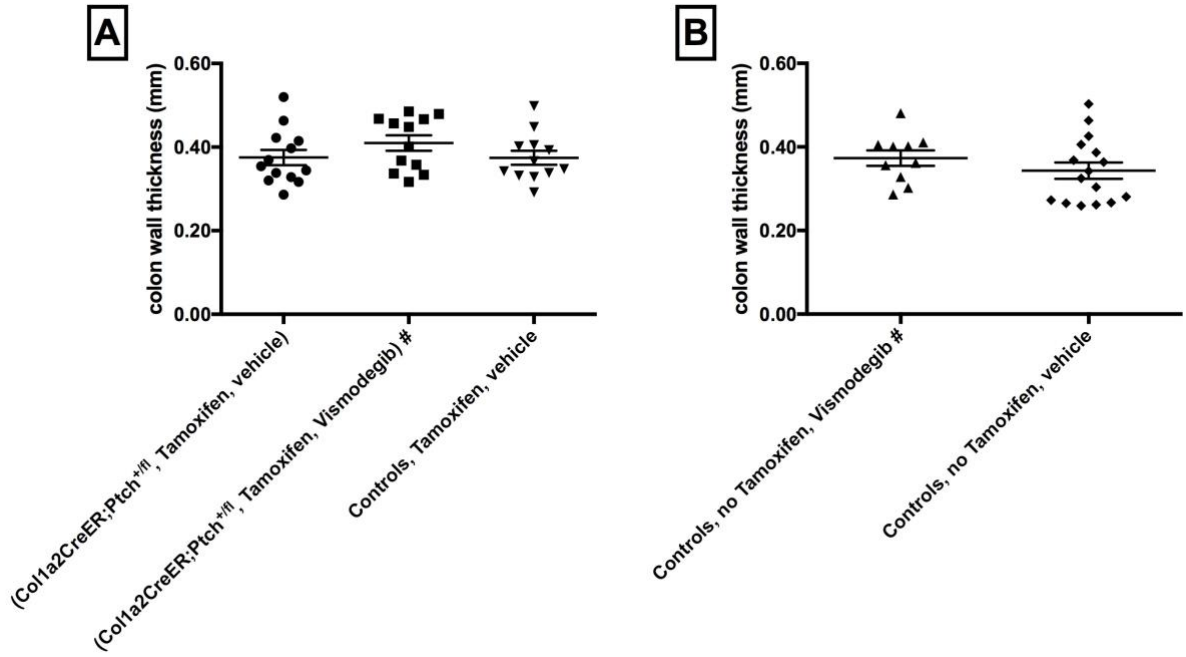

Figure 16: Experiment C – sonographically determined colon wall thickness in A) Col1a2;Ptch$^{+/fl}$ *mice with Vismodegib or vehicle treatment and Tamoxifen-treated controls. B) Not Tamoxifen treated controls with Vismodegib or vehicle treatment. Mice with genetically activated Hh signaling in parenthesis, # denotes pharmacological Hh inhibition*

4.4.2 Histological evaluation of *lamina muscularis mucosae*

Histological evaluation of the *lamina muscularis mucosae* thickness did not reveal any significant differences between the subgroups: Tamoxifen-treated and non-treated mice, (ANOVA with multiple comparison for FDR or unpaired *t*-test; Figure 17).

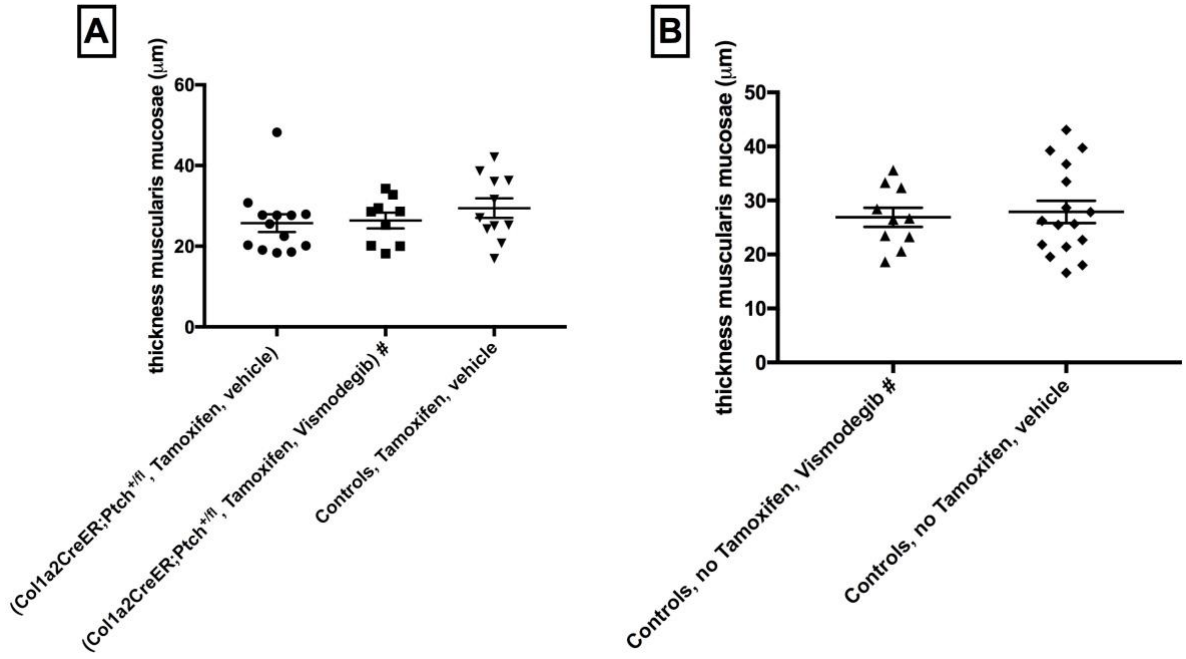

Figure 17: Experiment C – colon wall thickness determined by histological evaluation. A) Col1a2;Ptch$^{+/fl}$ mice with Vismodegib or vehicle treatment and Tamoxifen-treated controls. B) Not Tamoxifen treated controls with Vismodegib or vehicle treatment. Mice with genetically activated Hh signaling in parenthesis, # denotes pharmacological Hh inhibition

5. Discussion

5.1 Synopsis of results

The aim of this study was to assess whether manipulation of the Hh signaling pathway influences the fibrotic response in a murine colitis model. Chronic and acute colitis was induced by applying DSS in drinking water. The activity of the Hh pathway was altered either genetically or pharmacologically. Genetic modifications consisted of diminishing the pathway activity on the level of the transcription factor GLI1 (*Gli*^{LacZ} mice) or activating the pathway by disinhibition (*Col1a2;Ptch*$^{+/fl}$ mice). Vismodegib, an inhibitor of the pathway component SMO was administered for pharmacological Hh blockade. We examined intestinal fibrosis by ultrasound of the intestinal wall, measurement of colon length, histology and histochemistry as well as a PCR assay for analyzing transcription levels of fibrosis-associated genes. In addition, histological colitis activity scores were evaluated.

Initially, colitis activity and fibrosis in chronic colitis of *Gli*^{LacZ} and *Col1a2;Ptch*$^{+/fl}$ mice were investigated. When comparing the colitis activity scores, a statistically significant difference in the histological colitis activity between *Gli*^{LacZ} mice and WT controls was found. Average colitis activity scores were higher in WT mice. No significant difference in body weight loss between the two groups was noted. Interference with Hh signaling in *Col1a2;Ptch*$^{+/fl}$ mice and controls did not lead to a statistically significant difference in microscopically determined colitis activity.
Diminished Hh signaling in *Gli*^{LacZ} mice did not show significant differences of fibrosis as determined by intestinal wall US and histology in comparison to control mice. Different subgroups of *Col1a2;Ptch*$^{+/fl}$ mice (with or without Vismodegib treatment) and controls were compared, taking into account the sonographically determined colon wall thickness and the diameter of the *lamina muscularis mucosae* as measured on micrographs of colon samples. The results did not indicate a significant influence of genetic pathway upregulation or pharmacological Hh inhibition with Vismodegib compared to the vehicle treatment.

In acute colitis, differences in the colon length were found between mice with genetically activated stromal Hh signaling (*Col1a2;Ptch*$^{+/fl}$) and DSS-treated control mice. The colon was significantly shorter in *Col1a2;Ptch*$^{+/fl}$ mice, which exhibit genetically enhanced Hh signaling. However, the thickness of the *lamina muscularis mucosae* did not differ significantly. Using Sirius Red staining, no significant difference in the deposition of stained collagen fibers was seen between *Col1a2;Ptch*$^{+/fl}$ mice and controls. Compared to control mice, a significant upregulation of *Gli1* and collagen mRNA expression (*Col1a1* and *Col3a1*) in *Col1a2;Ptch*$^{+/fl}$ mice was determined.

In summary, upregulation of Hh related (*Gli1*) and fibrosis associated (*Col1a1* and *Col3a1*) mRNA in acute colitis was observed in the genetic model of Hh activation, suggesting that Hh signaling has an impact on the expression of fibrosis-related genes in acute colitis. However, this did not lead to significant changes in the fibrotic response in either acute or chronic experimental colitis, as assessed by sonography or histology. Therefore, the results suggest a limited effect, if any at all, of Hh activation on colitis-related fibrosis and do not substantiate the use of Hh inhibitors to prevent or treat intestinal fibrosis in IBD patients.

5.2 Colitis activity

Histological evaluation of DSS-induced colitis showed features of acute inflammation (e.g., infiltration of the *lamina propria* with neutrophil granulocytes, occasional crypt abscesses and epithelial erosions/ulcerations) as well as chronic alterations and features of regeneration (as disturbances of crypt architecture) as previously described (79, 82). The histological findings suggest that our DSS model did indeed lead to microscopical changes that were more similar to UC than Crohn's disease.

In the first approach (experiment A), we examined the extent of colitis in Gli^{LacZ} mice. A previous study described an association between a haplotypic *GLI1* variant and IBD in the northern European population (25). Inflamed colons from IBD patients showed a downregulation of *GLI1*/GLI1 on the mRNA and protein level (50). Gli^{LacZ} mice exhibit a monoallelic replacement of the *Gli1* gene and therefore show decreased GLI1 activity (25), in addition to their role as reporter mice (see 3.2.1). GLI1 acts as an activating transcription factor in the Hh signaling and knockout of one *Gli1* allele enables the establishment of a model for a reduced downstream Hh signaling pathway (25). Gli^{LacZ} mice without DSS treatment do not show clinical or histological features of colitis (25). In Gli^{LacZ} mice and respective controls, a statistically significant difference in histological colitis activity was noted, with controls showing more severe histological alterations. These findings are in contrast to previously published results that indicated that Gli^{LacZ} mice are more prone to DSS (3 %) induced colitis (25). In comparison to that study, we used a lower concentration of DSS (2 %) and assessed the histological activity after colitis with repetitive cycles, while the previous experiments were performed in the context of acute colitis (25), which may explain the differences in part. Another study, carried out by Lee et al., also in acute DSS colitis and with an even higher concentration of DSS (5 %), observed only a mild colitis enhancing

effect in *Gli*^{LacZ} mice (49). The authors of the latter study concluded that differences in the gut microbiota, animal housing or genetic background might account for the differences observed (49).

Next, we determined a histological colitis activity score in *Col1a2;Ptch*$^{+/fl}$ mice with overactivation of the Hh pathway (experiment C). This transgenic mouse strain bears a conditional, Tamoxifen inducible, Cre-mediated knockout of one allele of the SMO suppressor *Ptch1 (27)*. Inducible *Ptch1* knockout therefore leads to a reduced level of SMO inhibition, which results in a stimulation of GLI-mediated transcription (27, 92). Additionally, a fraction of *Col1a2;Ptch*$^{+/fl}$ mice and controls received Vismodegib, an inhibitor of SMO and thus Hh signaling (27, 77). This approach was used since Vismodegib treatment was able to overcome the effect of increased Hh signaling in *Col1a2;Ptch*$^{+/fl}$ mice in DSS colitis-induced colon cancer (27). There are several findings that prompted us to examine the role of more upstream Hh signaling in colitis. Expression levels of *PTCH1* and *SMO* are downregulated in IBD patient-derived colonic tissue (50). Ablation of *Smo*/SMO in mice by genetic or pharmacological (using the SMO antagonist XL-139) methods increases the severity of DSS colitis (49). Moreover, accelerated Hh signaling by genetic manipulation (in *Ptch*$^{+/fl}$ mice) or pharmacological pathway stimulation (with the SMO agonist SAG21k) results in protection from and amelioration of DSS colitis (49). We compared *Col1a2;Ptch*$^{+/fl}$ mice (with activated stromal Hh signaling) that received either Vismodegib or vehicle, as well as Tamoxifen-treated control mice that received vehicle treatment, but no statistically significant difference in histological colitis activity was found. Also, between WT mice treated with Vismodegib or vehicle, no significant difference of colitis activity could be found.

Thus, alterations in Hh signaling did not affect the histological colitis activity in the setting of chronic colitis in our hands. We could not confirm the marked decrease in colitis activity described in *Ptch*$^{+/fl}$ mice that underwent acute DSS colitis, challenged with 2 % DSS as also used in our study and 5 % DSS (49). Notably, the previous study (49) used whole body knockout mice, whereas in this study, the *Ptch1* knockout was limited to Collagen 1a2 expressing cells (i.e., fibroblasts; ref. 89). This means that in our study, Hh signaling was enhanced in Hh responsive and fibrogenic cells (21, 22, 56) only. 4-OH-Tamoxifen (to induce Cre-mediated deletion of one *Ptch1* allele) was applied intrarectally, ensuring a topical deletion in the colon. A whole-body knockout of *Ptch1* might therefore influence the inflammatory response in colitis differently than one limited to stromal cell elements. This might apply in particular to infiltrating mononuclear or intestinal myeloid cells, although the authors of the aforementioned DSS colitis study did not find *Gli1* expression in cells stained for the pan-lymphocytic marker CD45 or the myeloid

cells/macrophage proteins CD11b, CD11c or F4/80 (49). It has been shown in patient-derived samples of chronic pulmonary fibrosis that PTCH1 is present on lymphocytes and alveolar macrophages as well as that PTCH1 can be found on lymphocytes (but not granulocytes) in a model of murine lung fibrosis (68). The same study also confirmed that human CD4+ and CD8+ peripheral blood lymphocytes possess *PTCH1*/PTCH1 (mRNA and protein). The authors of that study propose that lymphocytic Hh signaling plays a role in pulmonary fibrogenesis, and that perhaps epithelial and lymphocytic cells communicate via Hh signaling to maintain the cellular response to injury (68). Additionally, mucosal CD4+ T-cells in human IBD express the Hh ligand (51). Conversely, absence of PTCH1 seems to neither activate canonical Hh signaling in murine lymphocytes, nor to impair cell proliferation or secretion of IFNγ (119). With regard to intestinal myeloid cells, there are controversial opinions as to whether or not these cells are Hh reactive and able to shape the inflammatory response of the intestine (22, 48). Dysfunction of the vascular endothelia also participates in the pathogenesis of IBD (120). Endothelial cells carry the PTCH1 receptor and SMO (121, 122), so that a whole-body knockout of *Ptch1* or manipulation of SMO might be capable of altering the vascular performance as well. In the brain, for example, it has also been shown that interrupted Hh signaling disturbs the endothelial function, thereby disturbing the blood-brain barrier (122). A similar mechanism might also occur in the vessels of intestines affected by colitis. Taking these findings together, the differences observed between our experiments (conditional *Ptch1* knockout in fibroblasts, in parts combined with antagonizing SMO) and the study using a whole-body knockout partly in combination with SMO stimulation (49) could be explained by the diverse cell populations involved in colitis and the variable approaches of targeting them. The different DSS schemes (acute or chronic) could also be partly responsible for the observed difference.

In order to take into account the different strategies of manipulating the Hh pathway in chronic colitis (general inhibition in Gli^{LacZ} mice or conditional, targeted activation in $Col1a2;Ptch^{+/fl}$ mice), we compared the histological colitis activity score between these groups. Histological evaluation showed a marked increase of colitis scores in the $Col1a2;Ptch^{+/fl}$ experiment compared to the experiment employing Gli^{LacZ} mice and their respective controls. Presumably, this could be due to the fact that the $Col1a2;Ptch^{+/fl}$ experiment ended 24 days after the last DSS cycle, compared to 90 days in the Gli^{LacZ} experiment, and hence acute inflammatory changes were regressive. This setup allowed us to assess more subacute alterations in the $Col1a2;Ptch^{+/fl}$ experiment, whereas for the Gli^{LacZ} cohorts, US at different time points and a longer course of regeneration enabled the evaluation of more chronic changes. The DSS concentration was the same

in both experiments. An actual effect of the genetic or pharmacological alterations on colitis activity appears to be less likely, since WT controls in the *Col1a2;Ptch*$^{+/fl}$ experiment also showed increased colitis scores compared to the controls that were used for the *Gli*^{LacZ} mice.

5.3 Impact of up- or downregulated Hh signaling on intestinal fibrosis in chronic colitis

Fibrosis, the excessive accumulation of extracellular matrix proteins such as collagens and fibronectin, is a result of local inflammation and a common feature of IBD (52, 56). Intestinal fibrosis is executed by mesenchymal cells (smooth muscle cells, myofibroblasts, fibroblasts) and is fostered by impaired tissue degradation (52). Furthermore, in addition, pericytes, bone-marrow derived stem cells, endothelial and epithelial (then termed epithelial-to-mesenchymal transition, EMT) cells can acquire mesenchymal properties and produce extracellular matrix in the gut (123). Intestinal fibrosis can be stimulated by autocrine signaling of mesenchymal cells, paracrine signals secreted by immune cells or molecular patterns from damaged cells or microorganisms (123). The composition of the gut microbiome or dietary factors can shape the fibrotic response (123). IBD-related fibrosis is mediated *inter alia* by growth factors, e.g., TGF-β, insulin-like growth factor (IGF) or platelet-derived growth factor (56). A promoting role of Hh signaling on fibrosis has been described for the liver, kidney, lung, skin and pancreas, whereas in the heart, Hh mitigates fibrosis induced by ischemia (63-72). Loss of epithelial Ihh ligand leads to increased intestinal fibrosis in mice, as assessed by light microscopy (73). In the esophagus and the biliary tract, Hh signaling can also induce EMT (74, 76). Since intestinal mesenchymal cells are Hh responsive (expressing PTCH1 and SMO; ref. 21, 22), we concluded that stromal Hh signaling may affect fibrosis in the setting of colitis. To address this question, we challenged mice with the chronic DSS colitis model (79). The Hh pathway was manipulated by either inhibiting it on the level of GLI1 (*Gli*^{LacZ} mice; experiment A) or enhancing the pathway's activity by genetically knocking out one *Ptch1* allele encoding for the inhibitory Hh receptor PTCH1 (experiment C). The latter experiment additionally included a cohort of mice that received the Hh antagonist Vismodegib, acting on the level of SMO (77).

After three cycles of DSS-induced chronic colitis, we did not observe significant differences in sonographically determined colon wall thickness or the histologically assessed thickness of the *lamina muscularis mucosae* in *Gli*^{LacZ} mice compared to controls. To rescue the genetically induced Hh pathway activation in *Col1a2;Ptch*$^{+/fl}$ mice subjected to iterated courses of DSS-induced colitis, we used Vismodegib, a clinically available inhibitor of Hh signaling. When comparing *Col1a2;Ptch*$^{+/fl}$ mice (with activated stromal Hh signaling) that received

pharmacological Hh inhibition (Vismodegib) with those that received vehicle treatment and with Tamoxifen-injected vehicle treated controls, no significant difference in the diameter of the colon wall or the thickness of the *lamina muscularis mucosae* was visible. Also, no effect of Vismodegib or vehicle treatment was seen in WT controls, which bore no genetically enhanced Hh signaling. In summary, neither genetic upregulation of stromal Hh signaling nor downregulation by inhibiting the Hh pathway on the level of SMO altered the parameters used as readout for fibrosis in a statistically significant manner. A previous study found an extensive fibrotic response in IHH (Hh ligand) deficient mice after they developed spontaneous inflammatory alterations in the gut (73). Since IHH is exclusively secreted by epithelial cells, the authors conclude that loss of epithelial Hh ligand triggers a fibrotic response by the recruitment of fibroblasts and macrophages (73). Interestingly, the inducible knockout construct of *Ihh* in that study involved Cre activation by β-naphthoflavone (73), a chemical agent that is able to attenuate colitis (124). A possible explanation for the differences seen in our experiment and the study using IHH deficient mice might be the activation of the Wnt (Wingless and Int) signaling pathway (125). Wnt signaling is known to be a driver of fibrosis in various organs (lung, kidney, liver) and also in systemic sclerosis (126). In intestinal fibrosis associated with IBD, Wnt signaling is perceived as a stimulator of fibrosis by increasing ECM proteins, regulating MMP and T-cell migration, and by crosstalk with TGF-β (127). Furthermore, patients suffering from fibrostenotic Crohn's disease show an upregulation of Wnt target genes in colon samples and Wnt drives EMT in *in vitro* studies; however, there is a lack of *in vivo* studies addressing the role of Wnt in intestinal fibrosis (128). Another aspect to be considered regarding the differences observed between our study and the one published previously (73) is the feedback mechanism of Hh signaling. The *Ptch1* gene is regulated by the expression levels of GLI transcription factors (3, 5, 11). Thus, activated Hh signaling by *Ptch1* knockout might dampen the pathway activity by a negative feedback loop.

Notably, it has to be considered that the Hh pathway can be activated independently of the canonical Hh factors (Hh ligand, GLI transcription factors or SMO; ref. 20, 129, 130). Indeed, *in vitro* studies suggest that this so-called non-canonical Hh signaling also appears in fibroblasts (130). Non-canonical Hh can be divided in pathways engaged by PTCH1 (type I) or SMO (type II) (20). Type I includes the induction of apoptosis by PTCH1, acting as a so-called dependence receptor, in the absence of Hh ligand, thus suggesting that the presence of the ligand is required for cell survival (20). Abrogation of ligand-secreting epithelial cells by colitis might therefore impair the survival of PTCH1 receptive cells in the stroma. Another GLI and SMO independent mechanism of Hh activation is cell cycle regulation by Cyclin B1 (20). Type II non-canonical Hh

signaling includes pathway regulation by small G-Proteins, affecting cytoskeletal organization and fibroblast migration (20). Fibroblast migration can also be induced by leukotrienes acting as a second messenger and in a GLI-independent manner (20). This may be especially important in the setting of IBD, since leukotrienes are a mediator on inflammation in colitis (131). Canonical Hh signaling requires the presence of primary cilia (16). Loss of the primary cilium occurs in fibroblasts in colitis (132), giving another indication that the role non-canonical Hh plays in colitis is not negligible. In the setting of liver fibrosis, it has been suggested that hepatic Hh responsive cells (hepatocytes, myofibroblasts) partly lack a primary cilium and that GLI activation therefore is executed by growth factors and chemokines, independent of Hh ligand, PTCH1 and SMO (133). Similar observations were made in pancreatic ductal adenocarcinoma, in which GLI transcription was regulated by TGF-β and KRAS (Kirsten rat sarcoma viral oncogene homolog) signaling, and not based on SHH, PTCH1 or SMO (134). Inhibition of Hh at the level of SMO (as with the Vismodegib used in this study) may therefore not be able to downregulate Hh signaling sufficiently, as downstream signaling may rely on non-canonical activating factors. To evaluate Hh signaling downstream of PTCH1 and SMO in colitis, we used Gli^{LacZ} mice in experiment A. In addition, pharmacological inhibitors acting on GLI, such as arsenic trioxide, GANT58, GANT61 or the anthelmintic drug Pyrvinium have been used (78). Type I non-canonical Hh, acting on PTCH1, should be impaired by the use of *Col1a2;*$Ptch^{+/fl}$ *mice,* as applied in experiments B and C of this study. Interestingly, the dual specificity tyrosine-phosphorylation-regulated kinase 1B (DYRK1B) is able to inhibit canonical- and promote non-canonical Hh (135), providing an interesting approach to further elucidate non-canonical signaling. The effect of a DYRK1B inhibitor has already been demonstrated in SMO inhibitor resistant cancer cell lines (136). To assess non-canonical Hh activity at the level of GLI transcription factors, a PCR assay, as used for *Gli1* mRNA in parts of this study, or a GLI-driven luciferase reporter assay has been applied (25). The intriguing partial loss of primary cilia in DSS colitis was evaluated in tissue samples from the different mouse strains used in this study by immunohistochemistry, since antibodies marking primary cilia (anti-ARL3B) are commercially available (132).

The fact that we did not see a significant effect of up- or downregulation of the Hh signaling pathway on fibrosis could at least in part also be due to the effect of other inflammation modifying pathways being differently regulated, e.g., NF-κB (137), c-Jun NH2-terminal Kinase (JNK, 138), JAK/STAT, TGF-β or Wnt (139). Furthermore, the role of TGF-β needs to be discussed. TGF-β is the best described pro-fibrotic cytokine in IBD, stimulating collagen synthesis by (myo)fibroblasts and smooth muscle cells (60). In murine and human colitis, TGF-β seems to act

as a suppressor of inflammation (58, 59), although pro-inflammatory properties have been attributed to TGF-β as well (44). In contrast to the proposed pro-fibrotic role of TGF-β, enhancing its activity (by knocking down the antagonist *Smad7*) led to reduced fibrosis in chronic (2 %, six cycles) DSS colitis (58). The authors of that study observed that these effects might be due to a reduction of inflammation (58). In skin and pancreas carcinomas, GLI1 can be induced by TGF-β, a process independent of the Hh ligand and not inhibited by SMO antagonists (140). Presumably, this is mediated by the inhibition of protein kinase-A by TGF-β, an enzyme that degrades GLI transcription factors (129, 140). TGF-β signaling might therefore, to some extent, circumvent the Hh downregulation by knocking out one *Gli1* allele (Gli^{LacZ} mice) or by utilizing the SMO antagonist Vismodegib, as used in parts of our study. Conversely, *Tgf-β2* is a target gene of Hh signaling, suggesting a self-sustaining effect of both pathways (140). This might play a particular role in our $Col1a2;Ptch^{+/fl}$ mice, bearing a disinhibition of Hh activity. In the PCR assay performed on samples of acute DSS colitis, we did not see a significant up- or downregulation of TGF-β signaling, albeit we only used primers for *Tgf-β1* mRNA, not targeting other genes involved in that pathway. Whether TGF-β exerts a pro- or anti-fibrotic effect in colitis, we cannot exclude it having a marked impact on the outcome of our experiments. Another prominent signaling pathway is Notch (neurogenic locus notch protein homolog). Notch signaling is upregulated in UC (141) and its inhibition dampens DSS colitis (142). Fibrosis of the kidney, lung and skin seems to be mediated by Notch signaling, by activating myofibroblasts and EMT (143). In cutaneous squamous cell carcinomas, Notch deficiency induces GLI transcription factors (140). Plenty of crosstalk between Hh and Notch signaling has been described, e.g., in organogenesis, stem cell regulation and the formation of intracranial tumors (140). Additionally, Notch mediates the trafficking of Hh pathway components into the primary cilium (140). Therefore, we cannot exclude that Notch impinged the fibrotic response in our experiments. In the case of NF-κB, an anti-inflammatory (82) as well as an Hh-stimulating (144) effect has been discussed. Inhibiting NF-κB signaling exacerbates DSS colitis in mice (82), but blockade of the pathway also reduces fibrosis in TNBS experimental colitis (145). The manifold crosstalk between the different signaling pathways, partly acting in an opposed or unknown fashion, may also influence the outcome of our experiments by not only affecting Hh signaling but also via a direct impact on inflammation or fibrosis.

5.4 Impact of upregulated Hh signaling on fibrosis in acute colitis

Fibrosis is mostly seen as a consequence of chronic inflammation (56). However, colectomy specimens from UC patients revealed a thickening of the *lamina muscularis mucosae* in longstanding (more than ten years duration) and acute (defined as less than two years) disease (146). The extent of collagen deposition did not differ significantly over time (146). Genes associated with fibrosis (e.g. *ACTA2*, *COL3A1*) were shown to be upregulated in healed mucosa (after treatment with the TNF-α blocker Infliximab) in endoscopic biopsies from UC patients, suggesting a persistent dysregulation of fibrosis markers after the acute inflammation has ceased (147). This is important because acute episodes can occur during the chronic course of IBD (32). There is an established protocol to induce acute colitis with DSS (79), also enabling the assessment of fibrosis in a more acute setting of IBD.

Col1a2;Ptch$^{+/fl}$ *mice*, in which Hh signaling is conditionally activated in stroma cells, did not differ from the controls either in the clinical parameters or in the diameter of the *lamina muscularis mucosae*. However, the colon length measured *post-mortem* was shorter in DSS-treated *Col1a2;Ptch*$^{+/fl}$ mice than in DSS-treated and non-DSS-treated controls. This finding is in contrast to a previously published report suggesting a colitis ameliorating effect of increased Hh signaling by heterozygous *Ptch1* knockout in acute colitis, in comparison with *Ptch1* WT mice (49). In contrast to our study, the mice used in these experiments carried a general knockout of the *Ptch1* allele (49), while we used a fibroblast-specific promoter and a conditional knockout. In the gut, our approach leads to activated Hh signaling only in *Col1a2* expressing cells of collagenous connective tissue, while *inter alia* enterocytes, smooth muscle cells or lymphocytes are not targeted (89). This means that in our experiments, Hh activation was limited to a fraction of stromal cells that are known for being both Hh responsive and a main mediator of intestinal fibrosis (21, 22, 56).

At the mRNA level, an upregulation of fibrogenic collagens *Col1a1* and *Col3a1* in *Col1a2;Ptch1*$^{+/fl}$ mice was shown. The increased expression of *Gli1* in *Col1a2;Ptch1*$^{+/fl}$ mice can be seen as a readout for a successful knockout of one *Ptch1* allele. It has been described that *Ptch1* is downregulated during acute colitis (49), which could explain why no significant changes in the expression level of *Ptch1* mRNA were noted. The lack of a significant increase in *α-SMA* mRNA levels could be due to the time point of tissue harvest, since it has been shown histologically that α-SMA positive myofibroblasts seem to appear between day 7 and 14 of DSS colitis (148).

Strikingly, no correlation between the expression of pro-fibrotic genes (namely *Col1a1* and *Col3a1*) and the thickness of the *lamina muscularis mucosae* or Sirius Red-positive collagen fiber deposition was found, but similar results were described in the setting of experimental chronic colitis (44). Taken together, these results suggest that Hh activation may lead to transient pro-fibrotic responses in the colon as occur in many other organs such as the liver, lung, and kidney. However, at least in the mouse model, this effect is not sufficient to maintain a pro-fibrotic reaction that would be amenable to pharmaceutical inhibition.

5.5 General aspects and limitations of the used model

DSS-induced colitis as a model for IBD is widely used, yet its histological and clinical aspects resemble UC more closely than Crohn's disease, e.g. transmural inflammation is absent in DSS-induced colitis (82). As a mouse model, DSS colitis cannot resemble human IBD in every aspect. The complexity of fibrogenesis in IBD involves nutritional factors and the intestinal microbiome, along with their influences on the various cell types that can produce components of the extracellular matrix (123). Research on colitis in a mouse model also depends on the selected mouse strain - for instance C57BL/6 mice, as used in this study, are more prone to develop (chronic) colitis than other mouse strains (82, 83). In addition to sex and age of the mice used, the composition of the intestinal microbiota, which depends on the animal facility in which the mice were raised or are used for an experiment, seems to play an important role (149). Furthermore, the responsiveness to DSS depends on the genetic background and can be influenced by chemical features of the DSS used (manufacturer, batch) and external factors, e.g. stress (150). Despite being an artificial model, DSS colitis is initially caused by chemical injury to mucosal enterocytes, thereby damaging the epithelial barrier and enabling an interaction between gut commensals and intestinal immune cells, a situation that is also seen as an important feature in the pathogenesis of human IBD (151). However, DSS colitis also occurs in immunodeficient mice lacking T- and B-cells, which is contrary to the assumed pathogenesis of human IBD involving lymphocytes (152). Basically, the immune system and response of mice and humans differs (153). For example, this affects the composition of white blood cells, T-cell development and signaling, secretion of cytokines and also the production of intestinal *defensins* (153). Those factors may contribute to a different inflammatory and fibrotic response in IBD between mice and humans. In addition, genome-wide expression analysis showed that only a fraction of genes are similarly up- or downregulated in DSS-treated mice and patients suffering from UC (139). Thus, despite being a widespread and robust model for human IBD, DSS-induced colitis has limitations and confirmative studies with other IBD models might be useful. Given the fact that DSS colitis is

more similar to UC than to Crohn's disease, a TBNS model could be used to further assess fibrosis. TBNS colitis is not only characterized by a transmural inflammation, driven by Th1- and Th17 cells (as typical for Crohn's disease), but it also provides a robust fibrotic response to intestinal inflammation with collagen deposition in the *lamina propria* (154, 155). Additionally, application of the SAMP1/Yit transgenic mouse strain would be a meaningful approach to study fibrosis in a more Crohn's disease-like setting, since these mice exhibit spontaneous, Th1-mediated inflammation of the terminal ileum, and also show "skip lesions", granulomas and fistulae in a later stage of disease (151, 154). Heterotopic transplantation (44) of inflamed colonic tissue might be another valuable, though somewhat artificial, tool to evaluate Hh's impact on colon fibrosis. The recent development of humanized mouse models for IBD research provides novel opportunities to assess fibrosis in colitis, especially because they involve immune cells derived from IBD patients, and the composition of human and murine inflammatory infiltrates differs (153, 156). A more generic approach to assess Hh's influence on fibrosis in intestinal inflammation is the chronic enteric *Salmonella* colitis model, marked by early and stable intestinal fibrotic response (157). The *Col1a2;Ptch1*$^{+/fl}$ mice used in this study only bear a monoallelic knockout of *Ptch1*. One could consider the usage of homozygous *Ptch1* knockout mice (in combination with DSS or another colitis model) to disinhibit Hh signaling to a greater extent. However, homozygous *Ptch1* knockout mice exhibit poor general health and also show premature enterocyte differentiation with crypt hypoplasia, even in the absence of inflammation (158), and thus the evaluation of colitis in those mice may be difficult.

A recent study (44), using chronic DSS-colitis, spontaneous colitis in IL-10 deficient mice and heterotopic transplantation showed a positive correlation among upregulated pro-fibrotic (*Col1a1*, *Col3a1*, *Tgf-β*, *Acta2*) as well as pro-inflammatory (*Il-1β*, *Il6*, *Tnf-α*, *Ifnγ*) mRNA. However, no significant correlation was determined between pro-inflammatory *Tnf-α* and the pro-fibrotic mRNA levels (with the exception of *Tgf-β,* which also exhibits a pro-inflammatory function) or between pro-fibrotic *Col1a1* and pro-inflammatory gene regulation (44). Since the intestinal collagen deposition (determined by Sirius Red and Elastica van Gieson stain) did not correlate with either *Tnf-α* or *Il-1β* mRNA levels, the authors question there being a link between the degree of inflammation and the progression of fibrosis (44). It was also shown that in the DSS colitis model, anti-fibrotic, collagen-degrading MMPs are upregulated and may account for comparatively weak collagen deposition (83).

The aim of this study was to reduce the use of research animals and follow the 3R's policy (replacement, reduction, refinement; ref. 84, 159). Refinement included, for example, the housing

of mice in enriched cages and the use of adequate anesthesia and analgesia (159). To reduce the number of animals, we used mice treated with AOM in addition to DSS in some experiments. Thereby, colitis was not only induced by DSS administration, but the cancerogenic agent AOM was also given to further elucidate colitis-associated tumor formation. Although it is known that neoplastic changes in the colon mucosa only occur focally and mucosal invasiveness is rare (95, 96), AOM administration might constitute a confounder. Since colorectal carcinoma histogenesis in the AOM/DSS model is sequential, beginning with the formation of distorted crypts that form microadenomas and are often infiltrated by lymphocytic cells (95), a distinction between nascent AOM-induced adenomas and inflamed mucosa with signs of crypt regeneration can prove difficult. Since numerous signaling pathways (e.g., JAK/STAT, NF-κB, TGF-β, Wnt) are regulated in AOM-induced carcinogenesis (95), and those pathways show interactions with Hh signaling (137, 139), we cannot completely exclude tumor-induced alterations in Hh signaling in the vicinity of AOM-induced (micro)adenomas. Additionally, it has been shown that AOM enhances fibrosis in murine liver tissue, but this seemed to be a secondary effect due to hepatic injury with hepatocyte apoptosis and the subsequent activation of stellate cells (160).

With regard to *Col1a2;Ptch1*$^{+/fl}$ mice which received Tamoxifen for Cre recombinase induction, it has been described that Tamoxifen itself can have an anti-fibrotic effect, e.g., in the porcine bile-duct (161) and the monotherapeutic treatment of human retroperitoneal fibrosis (162). Since Tamoxifen can affect fibrosis at least partially by influencing the level of TGF-β signaling (163), we cannot completely exclude anti-fibrotic effects due to Tamoxifen treatment, which might reduce the effects of Hh manipulation.

This study focused on stromal cell elements that are known to be Hh responsive (21, 22), but other cell types (e.g., bone marrow stem cells, fibrocytes, pericytes) and even components of the extracellular matrix can contribute to intestinal fibrosis (164), which might act independently of Hh signaling upon colitis induction. Whereas myeloid cells have been described as not Hh responsive during the course of DSS (22), other studies suggest myeloid cells as a target for Hh signaling, thereby modifying interleukin signaling (48), which might have a potential impact of fibrogenic processes as well.

While bowel ultrasound with the measurement of the colon wall is a common and reliable procedure to assess the course of colitis in rodents and humans (106, 108), conventional sonographic distinction between inflamed or fibrotic colon wall can be difficult (107). US measurements can be influenced by, for example, obesity, intestinal air and bowel movements

(106, 108). Additionally, the imaging quality depends on the frequency of the transducer, though a 40 MHz transducer, as used in this study, should deliver a highly sufficient imaging quality (108).

5.6 Outlook

Although our study did not show an impact of stromal Hh signaling on intestinal fibrosis, further investigations of Hh signaling in intestinal fibrosis may be of interest, considering the burden of fibrostenotic IBD and the potential of malignant transformation. Given the role of Hh signaling in EMT in the digestive system (74-76), the versatile crosstalk of Hh and other signaling pathways (notably TGF-β (129)), and the involvement of TGF-β in fistula formation and fibrotic lesion (61, 62), the impact of Hh on intestinal EMT might be of interest.

The expression profile of Hh components in samples from IBD patients is also still unclear, which could be attributed to the dynamics of the inflamed colon, patient selection and experimental procedures (50). Whereas some studies found a downregulation of Hh (25, 50), others reported the opposite findings (51). These inconclusive results on the expression of Hh in human IBD warrant closer evaluation.

Since we focused on two genetic (monoallelic *Gli1* knockout and upregulation of Hh by floxing-out the pathway inhibitor *Ptch1*) and one pharmacological (SMO inhibition) approach in targeting Hh signaling, the use of other genetic pathway modifications or inhibitors (e.g. the GLI1 inhibitor GANT61) is worth considering. Also, the SMO agonist SAG, acting as a pharmacological Hh activator (165), might deliver new insights in Hh related fibrosis.

Colon samples from patients suffering from non-IBD colitis (e.g., gastroenteritis, pseudomembranous colitis, amoebiasis or diverticulitis) showed a decreased expression level of Hh pathway components (25). Given that chronic infection with *Salmonella enterica* Serovar Typhimurium (a common pathogen causing infectious enteritis) leads to intestinal fibrosis in mice (157), and that amoebiasis (166) and diverticulitis (167) can present with fibrostenotic complications, murine models of, for instance, infectious colitis might give further insights into Hh's role in inflammation associated fibrosis.

In addition to changes in gene expression, epigenetic alterations can influence Hh signaling by changes in promoter methylation, histone modifications or via noncoding RNAs (168). Since fibrosis in various organs is also modified by epigenetic mechanisms (169), the interplay of epigenetic changes in Hh signaling and fibrosis could be a source for further interesting findings. For example, it was shown that epigenetic modification by microRNAs inhibits TGF-β signaling

and thereby decreases fibrosis in the liver (170), providing proof-of-principle that epigenetic pathway modification can alter fibrosis.

When treating patients with Hh inhibitors, it should be borne in mind that previous studies indicate that impaired Hh signaling favors the development of colorectal cancer in the context of colitis (27, 49). Furthermore, long-term treatment with Hh inhibitors such as Vismodegib causes gastrointestinal affections including diarrhea and weight loss in a number of patients, and experimental data suggest that Hh inhibition exacerbates experimental colitis (49). In contrast to the mouse, human enterocytes are considered as Hh responsive cell elements (in healthy and inflamed intestine), as determined by *PTCH1*/PTCH1 RNA *in situ* hybridization and immunohistochemistry (51). Hh modulating therapies in IBD patients might therefore also alter the epithelial cell function.

This study was aimed at further elucidating the potential role of stromal Hh signaling on colon fibrosis in a murine model of colitis. Although most of the performed experiments did not point towards a significant impact of altered Hh signaling on the extent of colonic fibrosis, further research is needed to gain deeper insights into IBD-associated fibrosis and the role of various signaling pathways and their interplay, which may eventually lead to novel therapeutic approaches to this important complication.

6. Literature

1. Nusslein-Volhard C, Wieschaus E. Mutations affecting segment number and polarity in Drosophila. Nature. 1980;287(5785):795-801.

2. Pereira J, Johnson WE, O'Brien SJ, Jarvis ED, Zhang G, Gilbert MT, Vasconcelos V, Antunes A. Evolutionary genomics and adaptive evolution of the Hedgehog gene family (Shh, Ihh and Dhh) in vertebrates. PLoS One. 2014;9(12):e74132.

3. Taipale J, Beachy PA. The Hedgehog and Wnt signalling pathways in cancer. Nature. 2001;411(6835):349-54.

4. Xavier GM, Seppala M, Barrell W, Birjandi AA, Geoghegan F, Cobourne MT. Hedgehog receptor function during craniofacial development. Dev Biol. 2016;415(2):198-215.

5. Petrova R, Joyner AL. Roles for Hedgehog signaling in adult organ homeostasis and repair. Development. 2014;141(18):3445-57.

6. Beachy PA, Karhadkar SS, Berman DM. Tissue repair and stem cell renewal in carcinogenesis. Nature. 2004;432(7015):324-31.

7. Dessinioti C, Antoniou C, Stratigos AJ. From basal cell morphogenesis to the alopecia induced by hedgehog inhibitors: connecting the dots. Br J Dermatol. 2017.

8. Tayyab M, Shahi MH, Farheen S, Mariyath MPM, Khanam N, Castresana JS, Hossain MM. Sonic hedgehog, Wnt, and brain-derived neurotrophic factor cell signaling pathway crosstalk: potential therapy for depression. J Neurosci Res. 2017.

9. Currier DG, Polk RC, Reeves RH. A Sonic hedgehog (Shh) response deficit in trisomic cells may be a common denominator for multiple features of Down syndrome. Prog Brain Res. 2012;197:223-36.

10. Li C, Heidt DG, Dalerba P, Burant CF, Zhang L, Adsay V, Wicha M, Clarke MF, Simeone DM. Identification of pancreatic cancer stem cells. Cancer Res. 2007;67(3):1030-7.

11. Armas-Lopez L, Zuniga J, Arrieta O, Avila-Moreno F. The Hedgehog-GLI pathway in embryonic development and cancer: implications for pulmonary oncology therapy. Oncotarget. 2017;8(36):60684-703.

12. Velcheti V. Hedgehog signaling is a potent regulator of angiogenesis in small cell lung cancer. Med Hypotheses. 2007;69(4):948-9.

13. Adolphe C, Hetherington R, Ellis T, Wainwright B. Patched1 functions as a gatekeeper by promoting cell cycle progression. Cancer Res. 2006;66(4):2081-8.

14. Athar M, Li C, Tang X, Chi S, Zhang X, Kim AL, Tyring SK, Kopelovich L, Hebert J, Epstein EH, Jr., Bickers DR, Xie J. Inhibition of smoothened signaling prevents ultraviolet B-

induced basal cell carcinomas through regulation of Fas expression and apoptosis. Cancer Res. 2004;64(20):7545-52.

15. Lin P, Pang Q, Wang P, Lv X, Liu L, Li A. The targeted regulation of Gli1 by miR-361 to inhibit epithelia-mesenchymal transition and invasion of esophageal carcinoma cells. Cancer Biomark. 2017.

16. Rohatgi R, Milenkovic L, Scott MP. Patched1 regulates hedgehog signaling at the primary cilium. Science. 2007;317(5836):372-6.

17. Philipp M, Caron MG. Hedgehog signaling: is Smo a G protein-coupled receptor? Curr Biol. 2009;19(3):R125-7.

18. Sabol M, Trnski D, Musani V, Ozretic P, Levanat S. Role of GLI Transcription Factors in Pathogenesis and Their Potential as New Therapeutic Targets. Int J Mol Sci. 2018;19(9).

19. Sasaki H, Nishizaki Y, Hui C, Nakafuku M, Kondoh H. Regulation of Gli2 and Gli3 activities by an amino-terminal repression domain: implication of Gli2 and Gli3 as primary mediators of Shh signaling. Development. 1999;126(17):3915-24.

20. Brennan D, Chen X, Cheng L, Mahoney M, Riobo NA. Noncanonical Hedgehog signaling. Vitam Horm. 2012;88:55-72.

21. Buller NV, Rosekrans SL, Westerlund J, van den Brink GR. Hedgehog signaling and maintenance of homeostasis in the intestinal epithelium. Physiology (Bethesda). 2012;27(3):148-55.

22. Westendorp BF, Buller N, Karpus ON, van Dop WA, Koster J, Versteeg R, Koelink PJ, Snel CY, Meisner S, Roelofs J, Uhmann A, Ver Loren van Themaat E, Heijmans J, Hahn H, Muncan V, Wildenberg ME, van den Brink GR. Indian Hedgehog Suppresses a Stromal Cell-Driven Intestinal Immune Response. Cell Mol Gastroenterol Hepatol. 2018;5(1):67-82 e1.

23. van den Brink GR. Hedgehog signaling in development and homeostasis of the gastrointestinal tract. Physiol Rev. 2007;87(4):1343-75.

24. Varnat F, Heggeler BB, Grisel P, Boucard N, Corthesy-Theulaz I, Wahli W, Desvergne B. PPARbeta/delta regulates paneth cell differentiation via controlling the hedgehog signaling pathway. Gastroenterology. 2006;131(2):538-53.

25. Lees CW, Zacharias WJ, Tremelling M, Noble CL, Nimmo ER, Tenesa A, Cornelius J, Torkvist L, Kao J, Farrington S, Drummond HE, Ho GT, Arnott ID, Appelman HD, Diehl L, Campbell H, Dunlop MG, Parkes M, Howie SE, Gumucio DL, Satsangi J. Analysis of germline GLI1 variation implicates hedgehog signalling in the regulation of intestinal inflammatory pathways. PLoS Med. 2008;5(12):e239.

26. Kolterud A, Grosse AS, Zacharias WJ, Walton KD, Kretovich KE, Madison BB, Waghray M, Ferris JE, Hu C, Merchant JL, Dlugosz AA, Kottmann AH, Gumucio DL. Paracrine Hedgehog signaling in stomach and intestine: new roles for hedgehog in gastrointestinal patterning. Gastroenterology. 2009;137(2):618-28.
27. Gerling M, Buller NV, Kirn LM, Joost S, Frings O, Englert B, Bergstrom A, Kuiper RV, Blaas L, Wielenga MC, Almer S, Kuhl AA, Fredlund E, van den Brink GR, Toftgard R. Stromal Hedgehog signalling is downregulated in colon cancer and its restoration restrains tumour growth. Nat Commun. 2016;7:12321.
28. Rimkus TK, Carpenter RL, Qasem S, Chan M, Lo HW. Targeting the Sonic Hedgehog Signaling Pathway: Review of Smoothened and GLI Inhibitors. Cancers (Basel). 2016;8(2).
29. Niyaz M, Khan MS, Mudassar S. Hedgehog Signaling: An Achilles' Heel in Cancer. Transl Oncol. 2019;12(10):1334-44.
30. Younis N, Zarif R, Mahfouz R. Inflammatory bowel disease: between genetics and microbiota. Mol Biol Rep. 2020;47(4):3053-63.
31. Burisch J, Jess T, Martinato M, Lakatos PL, EpiCom E. The burden of inflammatory bowel disease in Europe. J Crohns Colitis. 2013;7(4):322-37.
32. Nikolaus S, Schreiber S. Diagnostics of inflammatory bowel disease. Gastroenterology. 2007;133(5):1670-89.
33. Kaplan GG, Windsor JW. The four epidemiological stages in the global evolution of inflammatory bowel disease. Nat Rev Gastroenterol Hepatol. 2020.
34. Baumgart DC. The diagnosis and treatment of Crohn's disease and ulcerative colitis. Dtsch Arztebl Int. 2009;106(8):123-33.
35. Yantiss RK, Odze RD. Diagnostic difficulties in inflammatory bowel disease pathology. Histopathology. 2006;48(2):116-32.
36. Danese S, Semeraro S, Papa A, Roberto I, Scaldaferri F, Fedeli G, Gasbarrini G, Gasbarrini A. Extraintestinal manifestations in inflammatory bowel disease. World J Gastroenterol. 2005;11(46):7227-36.
37. Langner C, Magro F, Driessen A, Ensari A, Mantzaris GJ, Villanacci V, Becheanu G, Borralho Nunes P, Cathomas G, Fries W, Jouret-Mourin A, Mescoli C, de Petris G, Rubio CA, Shepherd NA, Vieth M, Eliakim R, Geboes K, European Society of P, European Cs, Colitis F. The histopathological approach to inflammatory bowel disease: a practice guide. Virchows Arch. 2014;464(5):511-27.
38. Baumgart DC, Carding SR. Inflammatory bowel disease: cause and immunobiology. Lancet. 2007;369(9573):1627-40.

39. Liu JZ, van Sommeren S, Huang H, Ng SC, Alberts R, Takahashi A, Ripke S, Lee JC, Jostins L, Shah T, Abedian S, Cheon JH, Cho J, Dayani NE, Franke L, Fuyuno Y, Hart A, Juyal RC, Juyal G, Kim WH, Morris AP, Poustchi H, Newman WG, Midha V, Orchard TR, Vahedi H, Sood A, Sung JY, Malekzadeh R, Westra HJ, Yamazaki K, Yang SK, International Multiple Sclerosis Genetics C, International IBDGC, Barrett JC, Alizadeh BZ, Parkes M, Bk T, Daly MJ, Kubo M, Anderson CA, Weersma RK. Association analyses identify 38 susceptibility loci for inflammatory bowel disease and highlight shared genetic risk across populations. Nat Genet. 2015;47(9):979-86.
40. Kostic AD, Xavier RJ, Gevers D. The microbiome in inflammatory bowel disease: current status and the future ahead. Gastroenterology. 2014;146(6):1489-99.
41. Wallace KL, Zheng LB, Kanazawa Y, Shih DQ. Immunopathology of inflammatory bowel disease. World J Gastroenterol. 2014;20(1):6-21.
42. Imam T, Park S, Kaplan MH, Olson MR. Effector T Helper Cell Subsets in Inflammatory Bowel Diseases. Front Immunol. 2018;9:1212.
43. Shih DQ, Targan SR. Immunopathogenesis of inflammatory bowel disease. World J Gastroenterol. 2008;14(3):390-400.
44. Hunerwadel A, Fagagnini S, Rogler G, Lutz C, Jaeger SU, Mamie C, Weder B, Ruiz PA, Hausmann M. Severity of local inflammation does not impact development of fibrosis in mouse models of intestinal fibrosis. Scientific Reports. 2018;8.
45. Abraham C, Cho JH. Inflammatory bowel disease. N Engl J Med. 2009;361(21):2066-78.
46. Noble CL, Abbas AR, Cornelius J, Lees CW, Ho GT, Toy K, Modrusan Z, Pal N, Zhong F, Chalasani S, Clark H, Arnott ID, Penman ID, Satsangi J, Diehl L. Regional variation in gene expression in the healthy colon is dysregulated in ulcerative colitis. Gut. 2008;57(10):1398-405.
47. Parkes M, Barmada MM, Satsangi J, Weeks DE, Jewell DP, Duerr RH. The IBD2 locus shows linkage heterogeneity between ulcerative colitis and Crohn disease. American Journal of Human Genetics. 2000;67(6):1605-10.
48. Zacharias WJ, Li X, Madison BB, Kretovich K, Kao JY, Merchant JL, Gumucio DL. Hedgehog Is an Anti-Inflammatory Epithelial Signal for the Intestinal Lamina Propria. Gastroenterology. 2010;138(7):2368-U226.
49. Lee JJ, Rothenberg ME, Seeley ES, Zimdahl B, Kawano S, Lu WJ, Shin K, Sakata-Kato T, Chen JK, Diehn M, Clarke MF, Beachy PA. Control of inflammation by stromal Hedgehog pathway activation restrains colitis. Proc Natl Acad Sci U S A. 2016;113(47):E7545-E53.
50. Buongusto F, Bernardazzi C, Yoshimoto AN, Nanini HF, Coutinho RL, Carneiro AJV, Castelo-Branco MT, de Souza HS. Disruption of the Hedgehog signaling pathway in

inflammatory bowel disease fosters chronic intestinal inflammation. Clinical and Experimental Medicine. 2017;17(3):351-69.
51. Nielsen CM, Williams J, van den Brink GR, Lauwers GY, Roberts DJ. Hh pathway expression in human gut tissues and in inflammatory gut diseases. Lab Invest. 2004;84(12):1631-42.
52. Rieder F, Zimmermann EM, Remzi FH, Sandborn WJ. Crohn's disease complicated by strictures: a systematic review. Gut. 2013;62(7):1072-84.
53. Cosnes J, Nion-Larmurier I, Beaugerie L, Afchain P, Tiret E, Gendre JP. Impact of the increasing use of immunosuppressants in Crohn's disease on the need for intestinal surgery. Gut. 2005;54(2):237-41.
54. Argollo M, Gilardi D, Roda G, Fiorino G, Peyrin-Biroulet L, Danese S. Anti-fibrotic drugs for Crohn's disease: Ready for prime time? Curr Pharm Des. 2019.
55. Gordon IO, Agrawal N, Goldblum JR, Fiocchi C, Rieder F. Fibrosis in ulcerative colitis: mechanisms, features, and consequences of a neglected problem. Inflamm Bowel Dis. 2014;20(11):2198-206.
56. Latella G, Di Gregorio J, Flati V, Rieder F, Lawrance IC. Mechanisms of initiation and progression of intestinal fibrosis in IBD. Scand J Gastroenterol. 2015;50(1):53-65.
57. Rieder F, Latella G, Magro F, Yuksel ES, Higgins PD, Di Sabatino A, de Bruyn JR, Rimola J, Brito J, Bettenworth D, van Assche G, Bemelman W, d'Hoore A, Pellino G, Dignass AU. European Crohn's and Colitis Organisation Topical Review on Prediction, Diagnosis and Management of Fibrostenosing Crohn's Disease. J Crohns Colitis. 2016;10(8):873-85.
58. Izzo R, Bevivino G, De Simone V, Sedda S, Monteleone I, Marafini I, Di Giovangiulio M, Rizzo A, Franze E, Colantoni A, Ortenzi A, Monteleone G. Knockdown of Smad7 With a Specific Antisense Oligonucleotide Attenuates Colitis and Colitis-Driven Colonic Fibrosis in Mice. Inflamm Bowel Dis. 2018;24(6):1213-24.
59. Monteleone G, Neurath MF, Ardizzone S, Di Sabatino A, Fantini MC, Castiglione F, Scribano ML, Armuzzi A, Caprioli F, Sturniolo GC, Rogai F, Vecchi M, Atreya R, Bossa F, Onali S, Fichera M, Corazza GR, Biancone L, Savarino V, Pica R, Orlando A, Pallone F. Mongersen, an oral SMAD7 antisense oligonucleotide, and Crohn's disease. N Engl J Med. 2015;372(12):1104-13.
60. Curciarello R, Docena GH, MacDonald TT. The Role of Cytokines in the Fibrotic Responses in Crohn's Disease. Front Med (Lausanne). 2017;4:126.

61. Scharl M, Bruckner RS, Rogler G. The two sides of the coin: Similarities and differences in the pathomechanisms of fistulas and stricture formations in irritable bowel disease. United European Gastroenterol J. 2016;4(4):506-14.
62. Corrigendum. United European Gastroenterol J. 2016;4(6):816.
63. Syn WK, Jung Y, Omenetti A, Abdelmalek M, Guy CD, Yang L, Wang J, Witek RP, Fearing CM, Pereira TA, Teaberry V, Choi SS, Conde-Vancells J, Karaca GF, Diehl AM. Hedgehog-mediated epithelial-to-mesenchymal transition and fibrogenic repair in nonalcoholic fatty liver disease. Gastroenterology. 2009;137(4):1478-88 e8.
64. Pereira Tde A, Witek RP, Syn WK, Choi SS, Bradrick S, Karaca GF, Agboola KM, Jung Y, Omenetti A, Moylan CA, Yang L, Fernandez-Zapico ME, Jhaveri R, Shah VH, Pereira FE, Diehl AM. Viral factors induce Hedgehog pathway activation in humans with viral hepatitis, cirrhosis, and hepatocellular carcinoma. Lab Invest. 2010;90(12):1690-703.
65. Choi SS, Omenetti A, Witek RP, Moylan CA, Syn WK, Jung Y, Yang L, Sudan DL, Sicklick JK, Michelotti GA, Rojkind M, Diehl AM. Hedgehog pathway activation and epithelial-to-mesenchymal transitions during myofibroblastic transformation of rat hepatic cells in culture and cirrhosis. Am J Physiol Gastrointest Liver Physiol. 2009;297(6):G1093-106.
66. Philips GM, Chan IS, Swiderska M, Schroder VT, Guy C, Karaca GF, Moylan C, Venkatraman T, Feuerlein S, Syn WK, Jung Y, Witek RP, Choi S, Michelotti GA, Rangwala F, Merkle E, Lascola C, Diehl AM. Hedgehog signaling antagonist promotes regression of both liver fibrosis and hepatocellular carcinoma in a murine model of primary liver cancer. PLoS One. 2011;6(9):e23943.
67. Ding H, Zhou D, Hao S, Zhou L, He W, Nie J, Hou FF, Liu Y. Sonic hedgehog signaling mediates epithelial-mesenchymal communication and promotes renal fibrosis. J Am Soc Nephrol. 2012;23(5):801-13.
68. Stewart GA, Hoyne GF, Ahmad SA, Jarman E, Wallace WA, Harrison DJ, Haslett C, Lamb JR, Howie SE. Expression of the developmental Sonic hedgehog (Shh) signalling pathway is up-regulated in chronic lung fibrosis and the Shh receptor patched 1 is present in circulating T lymphocytes. J Pathol. 2003;199(4):488-95.
69. Moshai EF, Wemeau-Stervinou L, Cigna N, Brayer S, Somme JM, Crestani B, Mailleux AA. Targeting the Hedgehog-Glioma-Associated Oncogene Homolog Pathway Inhibits Bleomycin-Induced Lung Fibrosis in Mice. American Journal of Respiratory Cell and Molecular Biology. 2014;51(1):11-25.
70. Horn A, Palumbo K, Cordazzo C, Dees C, Akhmetshina A, Tomcik M, Zerr P, Avouac J, Gusinde J, Zwerina J, Roudaut H, Traiffort E, Ruat M, Distler O, Schett G, Distler JH.

Hedgehog signaling controls fibroblast activation and tissue fibrosis in systemic sclerosis. Arthritis Rheum. 2012;64(8):2724-33.
71. Klieser E, Swierczynski S, Mayr C, Jager T, Schmidt J, Neureiter D, Kiesslich T, Illig R. Differential role of Hedgehog signaling in human pancreatic (patho-) physiology: An up to date review. World J Gastrointest Pathophysiol. 2016;7(2):199-210.
72. Kusano KF, Pola R, Murayama T, Curry C, Kawamoto A, Iwakura A, Shintani S, Ii M, Asai J, Tkebuchava T, Thorne T, Takenaka H, Aikawa R, Goukassian D, von Samson P, Hamada H, Yoon YS, Silver M, Eaton E, Ma H, Heyd L, Kearney M, Munger W, Porter JA, Kishore R, Losordo DW. Sonic hedgehog myocardial gene therapy: tissue repair through transient reconstitution of embryonic signaling. Nature Medicine. 2005;11(11):1197-204.
73. van Dop WA, Heijmans J, Buller NV, Snoek SA, Rosekrans SL, Wassenberg EA, van den Bergh Weerman MA, Lanske B, Clarke AR, Winton DJ, Wijgerde M, Offerhaus GJ, Hommes DW, Hardwick JC, de Jonge WJ, Biemond I, van den Brink GR. Loss of Indian Hedgehog activates multiple aspects of a wound healing response in the mouse intestine. Gastroenterology. 2010;139(5):1665-76, 76 e1-10.
74. Isohata N, Aoyagi K, Mabuchi T, Daiko H, Fukaya M, Ohta H, Ogawa K, Yoshida T, Sasaki H. Hedgehog and epithelial-mesenchymal transition signaling in normal and malignant epithelial cells of the esophagus. Int J Cancer. 2009;125(5):1212-21.
75. Wang F, Ma L, Zhang Z, Liu X, Gao H, Zhuang Y, Yang P, Kornmann M, Tian X, Yang Y. Hedgehog Signaling Regulates Epithelial-Mesenchymal Transition in Pancreatic Cancer Stem-Like Cells. J Cancer. 2016;7(4):408-17.
76. Omenetti A, Bass LM, Anders RA, Clemente MG, Francis H, Guy CD, McCall S, Choi SS, Alpini G, Schwarz KB, Diehl AM, Whitington PF. Hedgehog activity, epithelial-mesenchymal transitions, and biliary dysmorphogenesis in biliary atresia. Hepatology. 2011;53(4):1246-58.
77. Dlugosz A, Agrawal S, Kirkpatrick P. Vismodegib. Nat Rev Drug Discov. 2012;11(6):437-8.
78. Girardi D, Barrichello A, Fernandes G, Pereira A. Targeting the Hedgehog Pathway in Cancer: Current Evidence and Future Perspectives. Cells. 2019;8(2).
79. Eichele DD, Kharbanda KK. Dextran sodium sulfate colitis murine model: An indispensable tool for advancing our understanding of inflammatory bowel diseases pathogenesis. World Journal of Gastroenterology. 2017;23(33):6016-29.
80. Laroui H, Ingersoll SA, Liu HC, Baker MT, Ayyadurai S, Charania MA, Laroui F, Yan Y, Sitaraman SV, Merlin D. Dextran sodium sulfate (DSS) induces colitis in mice by forming

nano-lipocomplexes with medium-chain-length fatty acids in the colon. PLoS One. 2012;7(3):e32084.
81. Kim JJ, Shajib MS, Manocha MM, Khan WI. Investigating intestinal inflammation in DSS-induced model of IBD. J Vis Exp. 2012(60).
82. Chassaing B, Aitken JD, Malleshappa M, Vijay-Kumar M. Dextran sulfate sodium (DSS)-induced colitis in mice. Curr Protoc Immunol. 2014;104:Unit 15 25.
83. Suzuki K, Sun X, Nagata M, Kawase T, Yamaguchi H, Sukumaran V, Kawauchi Y, Kawachi H, Nishino T, Watanabe K, Yoneyama H, Asakura H. Analysis of intestinal fibrosis in chronic colitis in mice induced by dextran sulfate sodium. Pathol Int. 2011;61(4):228-38.
84. Balcombe J, Ferdowsian H, Briese L. Prolonged pain research in mice: trends in reference to the 3Rs. J Appl Anim Welf Sci. 2013;16(1):77-95.
85. Bai CB, Auerbach W, Lee JS, Stephen D, Joyner AL. Gli2, but not Gli1, is required for initial Shh signaling and ectopic activation of the Shh pathway. Development. 2002;129(20):4753-61.
86. Eames M, Kortemme T. Cost-benefit tradeoffs in engineered lac operons. Science. 2012;336(6083):911-5.
87. Trifonov S, Yamashita Y, Kase M, Maruyama M, Sugimoto T. Overview and assessment of the histochemical methods and reagents for the detection of beta-galactosidase activity in transgenic animals. Anat Sci Int. 2016;91(1):56-67.
88. Metzger D, Feil R. Engineering the mouse genome by site-specific recombination. Current Opinion in Biotechnology. 1999;10(5):470-6.
89. Zheng B, Zhang Z, Black CM, de Crombrugghe B, Denton CP. Ligand-dependent genetic recombination in fibroblasts : a potentially powerful technique for investigating gene function in fibrosis. Am J Pathol. 2002;160(5):1609-17.
90. Sauer B, Henderson N. Site-specific DNA recombination in mammalian cells by the Cre recombinase of bacteriophage P1. Proc Natl Acad Sci U S A. 1988;85(14):5166-70.
91. Metzger D, Clifford J, Chiba H, Chambon P. Conditional Site-Specific Recombination in Mammalian-Cells Using a Ligand-Dependent Chimeric Cre Recombinase. Proceedings of the National Academy of Sciences of the United States of America. 1995;92(15):6991-5.
92. Kasper M, Jaks V, Are A, Bergstrom A, Schwager A, Svard J, Teglund S, Barker N, Toftgard R. Wounding enhances epidermal tumorigenesis by recruiting hair follicle keratinocytes. Proc Natl Acad Sci U S A. 2011;108(10):4099-104.
93. Sonnylal S, Denton CP, Zheng B, Keene DR, He R, Adams HP, Vanpelt CS, Geng YJ, Deng JM, Behringer RR, de Crombrugghe B. Postnatal induction of transforming growth factor

beta signaling in fibroblasts of mice recapitulates clinical, histologic, and biochemical features of scleroderma. Arthritis Rheum. 2007;56(1):334-44.
94. Neufert C, Becker C, Neurath MF. An inducible mouse model of colon carcinogenesis for the analysis of sporadic and inflammation-driven tumor progression. Nat Protoc. 2007;2(8):1998-2004.
95. De Robertis M, Massi E, Poeta ML, Carotti S, Morini S, Cecchetelli L, Signori E, Fazio VM. The AOM/DSS murine model for the study of colon carcinogenesis: From pathways to diagnosis and therapy studies. J Carcinog. 2011;10:9.
96. Leon-Cabrera S, Vazquez-Sandoval A, Molina-Guzman E, Delgado-Ramirez Y, Delgado-Buenrostro NL, Callejas BE, Chirino YI, Perez-Plasencia C, Rodriguez-Sosa M, Olguin JE, Salinas C, Satoskar AR, Terrazas LI. Deficiency in STAT1 Signaling Predisposes Gut Inflammation and Prompts Colorectal Cancer Development. Cancers (Basel). 2018;10(9).
97. Fischer AH, Jacobson KA, Rose J, Zeller R. Hematoxylin and eosin staining of tissue and cell sections. CSH Protoc. 2008;2008:pdb prot4986.
98. Jaks V, Barker N, Kasper M, Van Es JH, Snippert HJ, Clevers H, Toftgard R. Lgr5 marks cycling, yet long-lived, hair follicle stem cells. Nature Genetics. 2008;40(11):1291-9.
99. Junqueira LCU, Bignolas G, Brentani RR. Picrosirius Staining Plus Polarization Microscopy, a Specific Method for Collagen Detection in Tissue-Sections. Histochemical Journal. 1979;11(4):447-55.
100. Montes GS, Junqueira LC. The use of the Picrosirius-polarization method for the study of the biopathology of collagen. Mem Inst Oswaldo Cruz. 1991;86 Suppl 3:1-11.
101. Hollenbach M, Thonig A, Pohl S, Ripoll C, Michel M, Zipprich A. Expression of glyoxalase-I is reduced in cirrhotic livers: A possible mechanism in the development of cirrhosis. Plos One. 2017;12(2).
102. Romano G, Reggi S, Kutryb-Zajac B, Facoetti A, Chisci E, Pettinato M, Giuffre MR, Vecchio F, Leoni S, De Giorgi M, Avezza F, Cadamuro M, Crippa L, Leone BE, Lavitrano M, Rivolta I, Barisani D, Smolenski RT, Giovannoni R. APOA-1Milano muteins, orally delivered via genetically modified rice, show anti-atherogenic and anti-inflammatory properties in vitro and in Apoe(-/-) atherosclerotic mice. Int J Cardiol. 2018;271:233-9.
103. Arunsan P, Ittiprasert W, Smout MJ, Cochran CJ, Mann VH, Chaiyadet S, Karinshak SE, Sripa B, Young ND, Sotillo J, Loukas A, Brindley PJ, Laha T. Programmed knockout mutation of liver fluke granulin attenuates virulence of infection-induced hepatobiliary morbidity. Elife. 2019;8.

104. Gerling M, Zhao Y, Nania S, Norberg KJ, Verbeke CS, Englert B, Kuiper RV, Bergstrom A, Hassan M, Neesse A, Lohr JM, Heuchel RL. Real-time assessment of tissue hypoxia in vivo with combined photoacoustics and high-frequency ultrasound. Theranostics. 2014;4(6):604-13.
105. Abdelrahman MA, Marston G, Hull MA, Markham AF, Jones PF, Evans JA, Coletta PL. High-Frequency Ultrasound for in Vivo Measurement of Colon Wall Thickness in Mice. Ultrasound in Medicine and Biology. 2012;38(3):432-42.
106. Bruckner M, Heidemann J, Nowacki TM, Cordes F, Stypmann J, Lenz P, Gohar F, Lugering A, Bettenworth D. Detection and characterization of murine colitis and carcinogenesis by molecularly targeted contrast-enhanced ultrasound. World J Gastroenterol. 2017;23(16):2899-911.
107. Stidham RW, Xu J, Johnson LA, Kim K, Moons DS, McKenna BJ, Rubin JM, Higgins PD. Ultrasound elasticity imaging for detecting intestinal fibrosis and inflammation in rats and humans with Crohn's disease. Gastroenterology. 2011;141(3):819-26 e1.
108. Lied GA, Milde AM, Nylund K, Mujic M, Grimstad T, Hausken T, Gilja OH. Increased wall thickness using ultrasonography is associated with inflammation in an animal model of experimental colitis. Clin Exp Gastroenterol. 2012;5:195-201.
109. Diaz-Granados N, Howe K, Lu J, McKay DM. Dextran sulfate sodium-induced colonic histopathology, but not altered epithelial ion transport, is reduced by inhibition of phosphodiesterase activity. Am J Pathol. 2000;156(6):2169-77.
110. Santella RM. Approaches to DNA/RNA Extraction and whole genome amplification. Cancer Epidemiol Biomarkers Prev. 2006;15(9):1585-7.
111. Kotewicz ML, D'Alessio JM, Driftmier KM, Blodgett KP, Gerard GF. Cloning and overexpression of Moloney murine leukemia virus reverse transcriptase in Escherichia coli. Gene. 1985;35(3):249-58.
112. Zipper H, Brunner H, Bernhagen J, Vitzthum F. Investigations on DNA intercalation and surface binding by SYBR Green I, its structure determination and methodological implications. Nucleic Acids Res. 2004;32(12):e103.
113. Jia Y. Chapter 3 - Real-Time PCR. In: Conn PM, editor. Methods in Cell Biology. 112: Academic Press; 2012. p. 55-68.
114. Ginzinger DG. Gene quantification using real-time quantitative PCR: An emerging technology hits the mainstream. Experimental Hematology. 2002;30(6):503-12.
115. Livak KJ, Schmittgen TD. Analysis of relative gene expression data using real-time quantitative PCR and the 2(T)(-Delta Delta C) method. Methods. 2001;25(4):402-8.

116. Mishra P, Singh U, Pandey CM, Mishra P, Pandey G. Application of student's t-test, analysis of variance, and covariance. Ann Card Anaesth. 2019;22(4):407-11.
117. Benjamini Y, Krieger AM, Yekutieli D. Adaptive linear step-up procedures that control the false discovery rate. Biometrika. 2006;93(3):491-507.
118. Pastille E, Bardini K, Fleissner D, Adamczyk A, Frede A, Wadwa M, von Smolinski D, Kasper S, Sparwasser T, Gruber AD, Schuler M, Sakaguchi S, Roers A, Muller W, Hansen W, Buer J, Westendorf AM. Transient ablation of regulatory T cells improves antitumor immunity in colitis-associated colon cancer. Cancer Res. 2014;74(16):4258-69.
119. Michel KD, Uhmann A, Dressel R, van den Brandt J, Hahn H, Reichardt HM. The hedgehog receptor patched1 in T cells is dispensable for adaptive immunity in mice. PLoS One. 2013;8(4):e61034.
120. Gravina AG, Dallio M, Masarone M, Rosato V, Aglitti A, Persico M, Loguercio C, Federico A. Vascular Endothelial Dysfunction in Inflammatory Bowel Diseases: Pharmacological and Nonpharmacological Targets. Oxid Med Cell Longev. 2018;2018:2568569.
121. Pola R, Ling LE, Silver M, Corbley MJ, Kearney M, Blake Pepinsky R, Shapiro R, Taylor FR, Baker DP, Asahara T, Isner JM. The morphogen Sonic hedgehog is an indirect angiogenic agent upregulating two families of angiogenic growth factors. Nat Med. 2001;7(6):706-11.
122. Alvarez JI, Dodelet-Devillers A, Kebir H, Ifergan I, Fabre PJ, Terouz S, Sabbagh M, Wosik K, Bourbonniere L, Bernard M, van Horssen J, de Vries HE, Charron F, Prat A. The Hedgehog pathway promotes blood-brain barrier integrity and CNS immune quiescence. Science. 2011;334(6063):1727-31.
123. Latella G, Rieder F. Intestinal fibrosis: ready to be reversed. Current Opinion in Gastroenterology. 2017;33(4):239-45.
124. Furumatsu K, Nishiumi S, Kawano Y, Ooi M, Yoshie T, Shiomi Y, Kutsumi H, Ashida H, Fujii-Kuriyama Y, Azuma T, Yoshida M. A role of the aryl hydrocarbon receptor in attenuation of colitis. Dig Dis Sci. 2011;56(9):2532-44.
125. Kosinski C, Stange DE, Xu C, Chan AS, Ho C, Yuen ST, Mifflin RC, Powell DW, Clevers H, Leung SY, Chen X. Indian hedgehog regulates intestinal stem cell fate through epithelial-mesenchymal interactions during development. Gastroenterology. 2010;139(3):893-903.
126. Akhmetshina A, Palumbo K, Dees C, Bergmann C, Venalis P, Zerr P, Horn A, Kireva T, Beyer C, Zwerina J, Schneider H, Sadowski A, Riener MO, MacDougald OA, Distler O, Schett

G, Distler JH. Activation of canonical Wnt signalling is required for TGF-beta-mediated fibrosis. Nat Commun. 2012;3:735.
127. Latella G, Rogler G, Bamias G, Breynaert C, Florholmen J, Pellino G, Reif S, Speca S, Lawrance IC. Results of the 4th scientific workshop of the ECCO (I): pathophysiology of intestinal fibrosis in IBD. J Crohns Colitis. 2014;8(10):1147-65.
128. Cosin-Roger J, Ortiz-Masia MD, Barrachina MD. Macrophages as an Emerging Source of Wnt Ligands: Relevance in Mucosal Integrity. Front Immunol. 2019;10:2297.
129. Javelaud D, Pierrat MJ, Mauviel A. Crosstalk between TGF-beta and hedgehog signaling in cancer. FEBS Lett. 2012;586(14):2016-25.
130. Faria AVS, Akyala AI, Parikh K, Bruggemann LW, Spek CA, Cao W, Bruno MJ, Bijlsma MF, Fuhler GM, Peppelenbosch MP. Smoothened-dependent and -independent pathways in mammalian noncanonical Hedgehog signaling. J Biol Chem. 2019;294(25):9787-98.
131. Sharon P, Stenson WF. Enhanced synthesis of leukotriene B4 by colonic mucosa in inflammatory bowel disease. Gastroenterology. 1984;86(3):453-60.
132. Tang R, Paul C, Lattanzio R, Eguether T, Tulari H, Bremond J, Maurizy C, Poupeau S, Turtoi A, Svrcek M, Seksik P, Castronovo V, Delvenne P, Lemmers B, Janke C, Pinet V, Hahne M. Partial loss of colonic primary cilia promotes inflammation and carcinogenesis. bioRxiv. 2019:2019.12.20.871772.
133. Grzelak CA, Martelotto LG, Sigglekow ND, Patkunanathan B, Ajami K, Calabro SR, Dwyer BJ, Tirnitz-Parker JE, Watkins DN, Warner FJ, Shackel NA, McCaughan GW. The intrahepatic signalling niche of hedgehog is defined by primary cilia positive cells during chronic liver injury. J Hepatol. 2014;60(1):143-51.
134. Nolan-Stevaux O, Lau J, Truitt ML, Chu GC, Hebrok M, Fernandez-Zapico ME, Hanahan D. GLI1 is regulated through Smoothened-independent mechanisms in neoplastic pancreatic ducts and mediates PDAC cell survival and transformation. Genes Dev. 2009;23(1):24-36.
135. Singh R, Dhanyamraju PK, Lauth M. DYRK1B blocks canonical and promotes non-canonical Hedgehog signaling through activation of the mTOR/AKT pathway. Oncotarget. 2017;8(1):833-45.
136. Gruber W, Hutzinger M, Elmer DP, Parigger T, Sternberg C, Cegielkowski L, Zaja M, Leban J, Michel S, Hamm S, Vitt D, Aberger F. DYRK1B as therapeutic target in Hedgehog/GLI-dependent cancer cells with Smoothened inhibitor resistance. Oncotarget. 2016;7(6):7134-48.

137. Marrero JA, Matkowskyj KA, Yung K, Hecht G, Benya RV. Dextran sulfate sodium-induced murine colitis activates NF-kappaB and increases galanin-1 receptor expression. Am J Physiol Gastrointest Liver Physiol. 2000;278(5):G797-804.
138. Roy PK, Rashid F, Bragg J, Ibdah JA. Role of the JNK signal transduction pathway in inflammatory bowel disease. World J Gastroenterol. 2008;14(2):200-2.
139. Fang K, Bruce M, Pattillo CB, Zhang S, Stone R, 2nd, Clifford J, Kevil CG. Temporal genomewide expression profiling of DSS colitis reveals novel inflammatory and angiogenesis genes similar to ulcerative colitis. Physiol Genomics. 2011;43(1):43-56.
140. Pelullo M, Zema S, Nardozza F, Checquolo S, Screpanti I, Bellavia D. Wnt, Notch, and TGF-beta Pathways Impinge on Hedgehog Signaling Complexity: An Open Window on Cancer. Front Genet. 2019;10:711.
141. Ghorbaninejad M, Heydari R, Mohammadi P, Shahrokh S, Haghazali M, Khanabadi B, Meyfour A. Contribution of NOTCH signaling pathway along with TNF-alpha in the intestinal inflammation of ulcerative colitis. Gastroenterol Hepatol Bed Bench. 2019;12(Suppl1):S80-S6.
142. Shinoda M, Shin-Ya M, Naito Y, Kishida T, Ito R, Suzuki N, Yasuda H, Sakagami J, Imanishi J, Kataoka K, Mazda O, Yoshikawa T. Early-stage blocking of Notch signaling inhibits the depletion of goblet cells in dextran sodium sulfate-induced colitis in mice. J Gastroenterol. 2010;45(6):608-17.
143. Hu B, Phan SH. Notch in fibrosis and as a target of anti-fibrotic therapy. Pharmacol Res. 2016;108:57-64.
144. Nakashima H, Nakamura M, Yamaguchi H, Yamanaka N, Akiyoshi T, Koga K, Yamaguchi K, Tsuneyoshi M, Tanaka M, Katano M. Nuclear factor-kappaB contributes to hedgehog signaling pathway activation through sonic hedgehog induction in pancreatic cancer. Cancer Res. 2006;66(14):7041-9.
145. Lawrance IC, Wu F, Leite AZ, Willis J, West GA, Fiocchi C, Chakravarti S. A murine model of chronic inflammation-induced intestinal fibrosis down-regulated by antisense NF-kappa B. Gastroenterology. 2003;125(6):1750-61.
146. de Bruyn JR, Meijer SL, Wildenberg ME, Bemelman WA, van den Brink GR, D'Haens GR. Development of Fibrosis in Acute and Longstanding Ulcerative Colitis. J Crohns Colitis. 2015;9(11):966-72.
147. Gundersen MD, Goll R, Fenton CG, Anderssen E, Sorbye SW, Florholmen JR, Paulssen RH. Fibrosis Mediators in the Colonic Mucosa of Acute and Healed Ulcerative Colitis. Clin Transl Gastroenterol. 2019;10(10):e00082.

148. Uehara H, Nakagawa T, Katsuno T, Sato T, Isono A, Noguchi Y, Saito Y. Emergence of fibrocytes showing morphological changes in the inflamed colonic mucosa. Dig Dis Sci. 2010;55(2):253-60.
149. Heimesaat MM, Dunay IR, Fuchs D, Trautmann D, Fischer A, Kuhl AA, Loddenkemper C, Siegmund B, Batra A, Bereswill S, Liesenfeld O. The distinct roles of MMP-2 and MMP-9 in acute DSS colitis. Eur J Microbiol Immunol (Bp). 2011;1(4):302-10.
150. Perse M, Cerar A. Dextran sodium sulphate colitis mouse model: traps and tricks. J Biomed Biotechnol. 2012;2012:718617.
151. Rieder F, Kessler S, Sans M, Fiocchi C. Animal models of intestinal fibrosis: new tools for the understanding of pathogenesis and therapy of human disease. Am J Physiol Gastrointest Liver Physiol. 2012;303(7):G786-801.
152. Dieleman LA, Ridwan BU, Tennyson GS, Beagley KW, Bucy RP, Elson CO. Dextran sulfate sodium-induced colitis occurs in severe combined immunodeficient mice. Gastroenterology. 1994;107(6):1643-52.
153. Mestas J, Hughes CC. Of mice and not men: differences between mouse and human immunology. J Immunol. 2004;172(5):2731-8.
154. Kiesler P, Fuss IJ, Strober W. Experimental Models of Inflammatory Bowel Diseases. Cell Mol Gastroenterol Hepatol. 2015;1(2):154-70.
155. Mizoguchi E, Low D, Ezaki Y, Okada T. Recent updates on the basic mechanisms and pathogenesis of inflammatory bowel diseases in experimental animal models. Intest Res. 2020;18(2):151-67.
156. Koboziev I, Jones-Hall Y, Valentine JF, Webb CR, Furr KL, Grisham MB. Use of Humanized Mice to Study the Pathogenesis of Autoimmune and Inflammatory Diseases. Inflamm Bowel Dis. 2015;21(7):1652-73.
157. Grassl GA, Valdez Y, Bergstrom KS, Vallance BA, Finlay BB. Chronic enteric salmonella infection in mice leads to severe and persistent intestinal fibrosis. Gastroenterology. 2008;134(3):768-80.
158. van Dop WA, Uhmann A, Wijgerde M, Sleddens-Linkels E, Heijmans J, Offerhaus GJ, van den Bergh Weerman MA, Boeckxstaens GE, Hommes DW, Hardwick JC, Hahn H, van den Brink GR. Depletion of the colonic epithelial precursor cell compartment upon conditional activation of the hedgehog pathway. Gastroenterology. 2009;136(7):2195-203 e1-7.
159. Taylor K. Reporting the implementation of the Three Rs in European primate and mouse research papers: are we making progress? Altern Lab Anim. 2010;38(6):495-517.

160. Khurana S, Jadeja R, Twaddell W, Cheng K, Rachakonda V, Saxena N, Raufman JP. Effects of modulating M3 muscarinic receptor activity on azoxymethane-induced liver injury in mice. Biochem Pharmacol. 2013;86(2):329-38.
161. Siqueira OHK, Oliveira KJ, Carvalho ACG, da Nobrega ACL, Medeiros RF, Felix-Patricio B, Ascoli FO, Olej B. Effect of tamoxifen on fibrosis, collagen content and transforming growth factor-beta1, -beta2 and -beta3 expression in common bile duct anastomosis of pigs. Int J Exp Pathol. 2017;98(5):269-77.
162. Brandt AS, Kamper L, Kukuk S, Haage P, Roth S. Tamoxifen monotherapy in the treatment of retroperitoneal fibrosis. Urol Int. 2014;93(3):320-5.
163. Ryu SH, Chung YH, Lee JK, Kim JA, Shin JW, Jang MK, Park NH, Lee HC, Lee YS, Suh DJ. Antifibrogenic effects of tamoxifen in a rat model of periportal hepatic fibrosis. Liver Int. 2009;29(2):308-14.
164. Rieder F, Fiocchi C. Intestinal fibrosis in IBD--a dynamic, multifactorial process. Nat Rev Gastroenterol Hepatol. 2009;6(4):228-35.
165. Lewis C, Krieg PA. Reagents for developmental regulation of Hedgehog signaling. Methods. 2014;66(3):390-7.
166. Grosse A. Diagnosis of colonic amebiasis and coexisting signet-ring cell carcinoma in intestinal biopsy. World J Gastroenterol. 2016;22(36):8234-41.
167. Weizman AV, Nguyen GC. Diverticular disease: epidemiology and management. Can J Gastroenterol. 2011;25(7):385-9.
168. Wils LJ, Bijlsma MF. Epigenetic regulation of the Hedgehog and Wnt pathways in cancer. Crit Rev Oncol Hematol. 2018;121:23-44.
169. Yao HW, Li J. Epigenetic modifications in fibrotic diseases: implications for pathogenesis and pharmacological targets. J Pharmacol Exp Ther. 2015;352(1):2-13.
170. Lakner AM, Steuerwald NM, Walling TL, Ghosh S, Li T, McKillop IH, Russo MW, Bonkovsky HL, Schrum LW. Inhibitory effects of microRNA 19b in hepatic stellate cell-mediated fibrogenesis. Hepatology. 2012;56(1):300-10.

7. Eidesstattliche Versicherung (statutory declaration)

„Ich, Benjamin Englert, versichere an Eides statt durch meine eigenhändige Unterschrift, dass ich die vorgelegte Dissertation mit dem Thema: The Role of Stromal Hedgehog Signaling in Intestinal Fibrosis of Mice (Die Rolle des stromalen Hedgehog Signalweges bei der intestinalen Fibrose der Maus) selbstständig und ohne nicht offengelegte Hilfe Dritter verfasst und keine anderen als die angegebenen Quellen und Hilfsmittel genutzt habe.
Alle Stellen, die wörtlich oder dem Sinne nach auf Publikationen oder Vorträgen anderer Autoren/innen beruhen, sind als solche in korrekter Zitierung kenntlich gemacht. Die Abschnitte zu Methodik (insbesondere praktische Arbeiten, Laborbestimmungen, statistische Aufarbeitung) und Resultaten (insbesondere Abbildungen, Graphiken und Tabellen) werden von mir verantwortet.

Ich versichere ferner, dass ich die in Zusammenarbeit mit anderen Personen generierten Daten, Datenauswertungen und Schlussfolgerungen korrekt gekennzeichnet und meinen eigenen Beitrag sowie die Beiträge anderer Personen korrekt kenntlich gemacht habe (siehe Anteilserklärung). Texte oder Textteile, die gemeinsam mit anderen erstellt oder verwendet wurden, habe ich korrekt kenntlich gemacht.

Meine Anteile an etwaigen Publikationen zu dieser Dissertation entsprechen denen, die in der untenstehenden gemeinsamen Erklärung mit dem/der Erstbetreuer/in, angegeben sind. Für sämtliche im Rahmen der Dissertation entstandenen Publikationen wurden die Richtlinien des ICMJE (International Committee of Medical Journal Editors; www.icmje.og) zur Autorenschaft eingehalten. Ich erkläre ferner, dass ich mich zur Einhaltung der Satzung der Charité – Universitätsmedizin Berlin zur Sicherung Guter Wissenschaftlicher Praxis verpflichte.

Weiterhin versichere ich, dass ich diese Dissertation weder in gleicher noch in ähnlicher Form bereits an einer anderen Fakultät eingereicht habe.

Die Bedeutung dieser eidesstattlichen Versicherung und die strafrechtlichen Folgen einer unwahren eidesstattlichen Versicherung (§§156, 161 des Strafgesetzbuches) sind mir bekannt und bewusst.“

Datum Unterschrift

8. Anteilserklärung an erfolgten Publikationen (contribution to published articles)

Benjamin Englert hatte folgenden Anteil an der folgenden Publikation:

Publikation 1: Gerling M, Buller NV, Kirn LM, Joost S, Frings O, **Englert B**, Bergstrom A, Kuiper RV, Blaas L, Wielenga MC, Almer S, Kuhl AA, Fredlund E, van den Brink GR, Toftgard R. Stromal Hedgehog signalling is downregulated in colon cancer and its restoration restrains tumour growth. Nature Communications, 2016;7:12321

Beitrag im Einzelnen:

- Mitarbeit bei den Tierexperimenten
  - Kontrolle des Gewichts und Gesundheitszustandes der untersuchten Mäuse, Verabreichung von AOM, DSS, Tamoxifen. Euthanasie einschließlich Nekropsie (Teile der Abbildungen 1, 3)
  - Färberische Aufarbeitung von Kolongewebe (X-Gal-Färbung, Immunfluoreszenz), hieraus sind Teile der Abbildungen 1 und 3 entstanden
- Korrekturlesen des Manuskripts

_____

Unterschrift, Datum und Stempel der erstbetreuenden Hochschullehrerin

_____

Unterschrift des Doktoranden/der Doktorandin

9. Lebenslauf (curriculum vitae)

Mein Lebenslauf wird aus datenschutzrechtlichen Gründen in der elektronischen Version meiner Arbeit nicht veröffentlicht.

10. Publikationsliste (list of publications)

- Gerling M, Zhao Y, Nania S, Norberg KJ, Verbeke CS, **Englert B**, Kuiper RV, Bergstrom A, Hassan M, Neesse A, Lohr JM, Heuchel RL. Real-time assessment of tissue hypoxia in vivo with combined photoacoustics and high-frequency ultrasound. Theranostics, 2014;4(6):604-13
- Gerling M, Buller NV, Kirn LM, Joost S, Frings O, **Englert B**, Bergstrom A, Kuiper RV, Blaas L, Wielenga MC, Almer S, Kuhl AA, Fredlund E, van den Brink GR, Toftgard R. Stromal Hedgehog signalling is downregulated in colon cancer and its restoration restrains tumour growth. Nature Communications, 2016;7:12321
- Dittmayer C, Stenzel W, Goebel HH, Krusche M, Schneider U, Uruha A, **Englert B**. Morphological characteristics of the transition from juvenile to adult dermatomyositis. Neuropatholy and Applied Neurobiology. 2020 Dec;46(7):790-794.
- Rocha ML, Dittmayer C, Uruha A, Korinth D, Chaoui R, Schlembach D, Rossi R, Pelin K, Suk EK, Schmid S, Goebel HH, Schuelke M, Stenzel W, **Englert B.** A novel mutation in NEB causing foetal nemaline myopathy with arthrogryposis during early gestation. Neuromuscular Disorders. 2021 Mar;31(3):239-245.

11. Danksagung (acknowledgment)

Mein besonderer Dank gilt meiner Doktormutter Frau Prof. Dr. Britta Siegmund für die Überlassung des Themas und die Möglichkeit, Teile der Experimente in Schweden absolvieren zu dürfen. Herrn PD Dr. Arend Koch danke ich für die Mitbetreuung meiner Arbeit und seinen Anregungen. Bei Herrn Prof. Rune Toftgård und seiner gesamten Arbeitsgruppe möchte ich mich für die herzliche Aufnahme und allzeitige Unterstützung sowie das Bereitstellen eines Laborarbeitsplatzes und der nötigen Geräte und Materialien bedanken. Hervorheben möchte ich Frau Agneta Andersson und Frau Åsa Bergström, deren Hilfsbereitschaft und *Know-how* mir halfen, einige Hürden zu überwinden. Herrn Leonard Kirn danke ich für seine Mitwirkung bei den PCR-Experimenten.

Dem Boehringer Ingelheim Fonds, Stiftung für medizinische Grundlagenforschung, Mainz danke ich für die finanzielle Unterstützung in Form eines MD Fellowships und die Aufnahme in das Stipendienprogramm.

Ganz besonders möchte ich mich bei Herrn Dr. Marco Gerling für seine exzellente Anleitung, Betreuung und Gesprächsbereitschaft bedanken.

Mein abschließender Dank gilt meinen Eltern für ihre immerwährende Unterstützung.

12. Bescheinigung eines akkreditierten Statistikers (certificate of statistical consulting)

CHARITÉ

CharitéCentrum für Human- und Gesundheitswissenschaften

Charité | Campus Charité Mitte | 10117 Berlin

Institut für Biometrie und Klinische Epidemiologie (iBikE)
Direktor: Prof. Dr. Geraldine Rauch
Postanschrift:
Charitéplatz 1 | 10117 Berlin
Besucheranschrift:
Reinhardtstr. 58 | 10117 Berlin
Tel. +49 (0)30 450 562171
geraldine.rauch@charite.de
https://biometrie.charite.de/

Name, Vorname: Englert, Benjamin

Emailadresse: benjamin.englert@charite.de

Matrikelnummer:

Promotionsbetreuerin: Prof. Britta Siegmund

Promotionsinstitution/Klinik: Medizinische Klinik m.S. Gastroenterologie, Infektiologie und Rheumatologie, CBF

Bescheinigung

Hiermit bescheinige ich, dass Herr Benjamin Englert innerhalb der Service Unit Biometrie des Instituts für Biometrie und Klinische Epidemiologie (iBikE) bei mir eine statistische Beratung zu einem Promotionsvorhaben wahrgenommen hat. Folgender Beratungstermin wurde wahrgenommen:

- 11.03.2019

Folgende wesentliche Ratschläge hinsichtlich einer sinnvollen Auswertung und Interpretation der Daten wurden während der Beratung erteilt:

- Konsistenz in der Entscheidung parametrische vs. nicht-parametrische Tests
- Fehlen von signifikanten Unterschieden kein Beweis für Äquivalenz, stattdessen gezielte Äquivalenztests verwenden, z.B. TOST

Diese Bescheinigung garantiert nicht die richtige Umsetzung der in der Beratung gemachten Vorschläge, die korrekte Durchführung der empfohlenen statistischen Verfahren und die richtige Darstellung und Interpretation der Ergebnisse. Die Verantwortung hierfür obliegt allein dem Promovierenden. Das Institut für Biometrie und Klinische Epidemiologie übernimmt hierfür keine Haftung.

Datum: 12.03.2019

Name des Beraters: Dario Zocholl

CHARITÉ
UNIVERSITÄTSMEDIZIN BERLIN
Institut für Biometrie und
Klinische Epidemiologie
Campus Charité Mitte
Charitéplatz 1 | D-10117 Berlin
Sitz: Reinhardtstr. 58

Unterschrift Beraterin, Institutsstempel